Resource Allocation and Performance Optimization in Wireless Networks

by

Wenxuan Guo

A Thesis
Submitted to the faculty of the

WORCESTER POLYTECHNIC INSTITUTE

In partial fulfillment of the requirements for the
Degree of Doctor of Engineering

in

Electrical and Computer Engineering

by

May 2011

APPROVED:

Professor Xinming Huang Thesis Advisor ECE Department WPI	Professor Wenjing Lou Thesis Committee ECE Department WPI	Professor Andrew G. Klein Thesis Committee ECE Department WPI
Professor Youjian Liu Thesis Committee ECE Department University of Colorado Boulder	Professor Donald R. Brown III Thesis Committee ECE Department WPI	

Abstract

As wireless networks continue streaking through more aspects of our lives, it is seriously constrained by limited network resources, in terms of time, frequency and power. In order to enhance performance for wireless networks, it is of great importance to allocate resources smartly based on the current network scenarios. The focus of this dissertation is to investigate radio resource management algorithms to optimize performance for different types of wireless networks.

Firstly, we investigate a joint optimization problem on relay node placement and route assignment for wireless sensor networks. A heuristic binary integer programming algorithm is proposed to maximize the total number of information packets received at the base station during the network lifetime. We then present an optimization algorithm based on binary integer programming for relay node assignment with the current node locations. Subsequently, a heuristic algorithm is applied to move the relay nodes to the locations iteratively to better serve their associated edge nodes.

Secondly, as traditional goal of maximizing the total throughput can result in unbalanced use of network resources, we study a joint problem of power control and channel assignment within a wireless mesh network such that the minimal capacity of all links is maximized. This is essentially a fairness problem. We develop an upper bound for the objective by relaxing the integer variables and linearization. Subsequently, we put forward a heuristic approach to approximate the optimal solution, which tries to increase the minimal capacity of all links via setting tighter constraint and solving a binary integer programming problem. Simulation results show that solutions obtained by this algorithm are very close to the upper bounds

obtained via relaxation, thus suggesting that the solution produced by the algorithm is near-optimal.

Thirdly, we study the topology control of disaster area wireless networks to facilitate mobile nodes communications by deploying a minimum number of relay nodes dynamically. We first put forward a novel mobility model for mobile nodes that describes the movement of first responders within a large disaster area. Secondly, we formulate the square disk cover problem and propose three algorithms to solve it, including the two-vertex square covering algorithm, the circle covering algorithm and the binary integer programming algorithm.

Fourthly, we explore the joint problem of power control and channel assignment to maximize cognitive radio network throughput. It is assumed that an overlaid cognitive radio network (CRN) co-exists with a primary network. We model the opportunistic spectrum access for cognitive radio network and formulate the cross-layer optimization problem under the interference constraints imposed by the existing primary network. A distributed greedy algorithm is proposed to seek for larger network throughput. Cross-layer optimization for CRN is often implemented in centralized manner to avoid co-channel interference. The distributed algorithm coordinates the channel assignment with local channel usage information. Thus the computation complexity is greatly reduced.

Finally, we study the network throughput optimization problem for a multi-hop wireless network by considering interference alignment at physical layer. We first transform the problem of dividing a set of links into multiple maximal concurrent link sets to the problem of finding the maximal cliques of a graph. Then each concurrent link set is further divided into one or several interference channel networks, on which interference alignment is implemented to guarantee simultaneous transmission. The network throughput optimization problem is then formulated as a

non-convex nonlinear programming problem, which is NP-hard generally. Thus we resort to developing a branch-and-bound framework, which guarantees an achievable performance bound.

Acknowledgements

I would like to express my deepest gratitude for my advisor, Professor Xinming Huang for his guidance through my Ph.D study. There have been many times that I feel frustrated and helpless when I was engaged with some research project. It was his numerous suggestions, inspiring ideas, patience and support that have helped me conquer obstacles and finally made this dissertation possible.

I am also indebted to Professor Donald R. Brown III, Professor Andrew G. Klein, Professor Wenjing Lou, Professor Youjian Liu for their valuable comments as my thesis committee and many professors in WPI from whom I have learned greatly.

I am grateful to my fellow graduate students in the Embedded Computing Lab, Cao Liang, Kai Zhang, Yanjie Peng, Chen Shen and Hongkui Zhu for their friendship and support.

Last but not least, I would like to thank my parents Bingtang Guo and Xuefei Wang, my wife Liyan Luo for their love, support and encouragement.

Contents

List of Figures

List of Tables

Chapter 1

Introduction

This chapter discusses the motivation and describes context for the problems considered in this dissertation in Section 1.1. A description of related works is provided in Section 1.2. The organization of this dissertation is presented in Section 1.3, followed by a summary of the main contributions in Section 1.4.

1.1 Motivation

The past decade has witnessed a tremendous proliferation of the use of wireless networks, driven by the rapid growth of portable computing, communication and embedded devices. Accompanying this trend is the revolutionary advances in the wireless communication technologies, which enables the realization of a wide range of heterogenous wireless systems, such as cellular networks, wireless local area networks, wireless sensor networks, etc. This technological development is further inspiring the researchers to envision many new scenarios, such as wireless regional area networks, disaster area wireless networks, vehicular ad hoc networks, etc. However, as wireless networks continue streaking through more aspects of our lives, it is seriously constrained by limited network resources, in terms of time, frequency

and power. In order to enhance performance for wireless networks, it is of great importance to allocate resources smartly based on the specific network applications.

Resource allocation for wireless networks is the process of deciding how a set of network resources are used. In this dissertation, scenarios of wireless systems contain resources in terms of time, frequency, and power. Allocating time resources can be mainly exemplified by link scheduling. In particular, resource allocation is the process of selecting which link(s) to be active during a specific time slot. The same time slot can be assigned to multiple links as long as they are not generating interference to any other link. Resources in terms of frequency is limited as any wireless system is always constrained by bandwidth. Each active link necessitates a certain amount of bandwidth to be able to send data. Frequency resources require careful allocation because two mutually interfered links can not be active within the same bandwidth simultaneously. Power resource allocation is mainly referred as setting transmit power in this dissertation. Transmit power levels of nodes largely determine the performance of wireless systems. In particular, the transmitter's power determines the capacity of a wireless link, which further influences the throughput the whole network. On the other hand, setting larger transmit power levels would result in more interference collisions, thus decrease the performance of the wireless network.

Based on different network scenarios, smart resource allocation leads to optimization of different performance objectives. In this thesis, we consider various performance objectives according to specific models. For example, throughput is the objective that is always desirable for most kinds of wireless networks. For wireless sensor networks, the network lifetime is regarded important. Coverage is critical to disaster area wireless networks.

This dissertation is motivated by the desire to explore advanced resource al-

location techniques designated for modern wireless networks. Although resource allocation has been a extensive research topic for decades, there are still many unresolved issues regarding emerging types of wireless networks, such as disaster area wireless networks, wireless regional area networks, etc. This thesis tackles significant unresolved resource allocation problems to optimize for various performance objectives. The research challenges are summarized as follows.

1.1.1 Relay Management for Wireless Sensor Networks

Many recent research efforts are focused on maximizing the lifetime of wireless sensor networks [87, 42, 58, 82, 34], while others try to address the problem of maximizing the capacity or throughput in wireless local area networks (WLANs) [74]. The strategies they adopt consist of power control, relay node placement, channel assignment, link scheduling, etc. However, few studies available in the literature investigate approaches to maximize the absolute amount of information packets received during the network lifetime. As placing relay nodes between sensor nodes and base stations can increase packet reception rate, we propose to deploy a fixed number of energy-constrained relay nodes to help uplink data transmission. Instead of studying solely network lifetime elongation or network throughput optimization, we propose to investigate the joint problem of both on how to maximize the network data reception within the network lifetime, which is defined as the time period from start till all relay nodes die. As a result, the proposed approach can be applied to many other task-oriented data-collection wireless networks. For instance, in a burning forest, the amount of temperature information from widely distributed sensors matters as much as the extent to which firefighters can control the fire; farmers can well adjust the environmental parameters if they obtain much feedback information from greenhouse sensors.

1.1.2 Capacity Fairness for Wireless Mesh Networks

Fairness of network throughput among users is another important issue. The reason is that the traditional goal of maximizing the summation of throughput on all links could result in unbalanced use of network resources. More importantly, emphasizing on fairness can satisfy more network users and thus generate more revenue for service providers. Few research efforts truly address the max-min fairness problem of general wireless mesh networks via channel assignment and power control. We study a joint problem of channel assignment and power control such that the minimal capacity of all links is maximized. We develop an upper bound of the max-min performance and propose a heuristic approach to increase the minimal capacity of all links via setting tighter constraints.

1.1.3 Dynamic Resource Allocation for Disaster Area Wireless Networks

Public safety organizations increasingly rely on wireless technology to provide effective communications during emergency and disaster response operations. However, any previously installed wireless network infrastructure may be damaged or completely destroyed in a major disaster event, such as earthquake, hurricane, tsunami, etc. It is necessary to develop wireless networks that can be quickly deployed to build a replacement communication system to connect all first responders. Considering the first responders as mobile nodes (MNs), the communication range of each MN is often limited by its power constraint. Mobile relay nodes (RNs) can be introduced to relay the communications between MNs and the far-away base stations. The RNs installed on wheeled vehicles can be deployed at places where the first responders are actively working in the field. As mobile nodes have different locations

at time goes, RNs need to be relocated dynamically within the disaster area to cover mobile nodes. We study the dynamic resource allocation problem to place RNs such that most number of mobile nodes can be covered within the disaster area wireless networks (DAWN).

1.1.4 Distributed Optimization for Cognitive Radio Networks

Traditional spectrum allocation can be very inefficient due to fixed assignment and exclusive use. Emerging cognitive radio technology becomes a promising approach to exploit the under-utilized spectrum [3]. In a cognitive radio network, unlicensed wireless users (secondary users (SUs)) are allowed to dynamically access the licensed bands, as long as the licensed wireless users (primary users (PUs)) in those particular bands are not interfered. Wireless devices equipped with cognitive radios are implemented with flexibility, including frequency agility, transmit power control, access coordination etc., which render more efficient use of available spectrum.

Cognitive radio networks (CRN) may operate in infrastructure-based systems. As a practical application, IEEE 802.22 wireless regional area networks (WRAN) dynamically allocates TV spectrum to SUs [16] while keep provisioning service to PUs. The TV bands are selected because they feature very favorable propagation characteristics and are scarcely used due to popularity of cable and satellite TV services. We investigate the joint problem of power control and channel assignment to maximize WRAN-based cognitive radio network throughput. As WRAN are spreading out in rural area, an omniscient central entity to operate the whole network is impractical. Therefore, it is highly desirable to introduce a distributed method which only entails local knowledge but optimize WRAN in terms of overall performance.

1.1.5 Interference Alignment for Multi-hop Wireless Networks

Interference has been considered harmful for throughput performance of wireless networks. However, the emergence of the idea of interference alignment provides a new perspective to achieve higher throughput by allowing concurrent transmissions. Initially introduced in [14], interference alignment allows a transmitter to align its interference to unused directions of other links, generating no harmful interference at the receiver ends. Consequently, the implementation of interference alignment can greatly improve the network throughput. The canonical example of interference alignment is a communication scenario where every user is able to achieve one half of the capacity that could be achieved in the absence of all interference.

Recent works on interference alignment mainly focus on multi-user interference channel networks [14] and multi-input multi-output networks [24], our study of optimizing end-to-end throughput of multi-hop wireless networks is among one of the first research efforts to employ interference alignment on multi-hop networking.

1.2 Related Works

1.2.1 Relay Node Placement in Wireless Networks

There are many researches focusing on the RN placement problem for sensor wireless networks. In [42], a joint problem of energy provisioning and relay node placement for wireless sensor network is considered to maximize the network lifetime. In [58], the authors seek to deploy a minimum number of relay nodes such that all the network nodes are connected, when sensor nodes and relay nodes have different communication ranges. In [82], the problem to deploy a minimum number of relay

nodes to guarantee connectivity of sensor nodes and the base station is studied. The network modelling also considers communication range of sensors and relay nodes. In [57], the relay node placement problem in two-tiered wireless sensor network is considered. The objective is to place minimum number of relay nodes to forward packets from sensor nodes to the sink. Likewise, communication ranges for sensor nodes and relay nodes are also considered in the network modelling. Few papers focus on the amount of data reception at the BS during the network lifetime. Concerning techniques utilized in RN placement in wireless networks, many researches have done significant achievements that motivate us to pursue our goal. In [52], the optimal power is calculated for peer to peer communication with respect to fixed Signal-to-Noise ratio. Besides, many heuristic and iterative approaches are employed to solve the RN placement problems with different objectives. For example, A heuristic algorithm is presented in [5] for energy provisioning and RN placement in wireless sensor networks. In [74], an integer programming optimization formulation and an iterative approach are proposed to compute the best placement of a fixed number of RNs. In [84], a novel BIP formulation of the BS placement problem is proposed to find the optimal BS position in an interference-limited indoor wireless system. Not only in sensor network area, RNs have also been used in cellular networks and WLAN. In [85], the iCAR architecture is introduced to use RNs to redirect the cellular communication traffic from congested cell to its neighboring cells. Another aspect of relay network applications is wireless LAN. Relay points [74] with access to power supply are strategically placed to improve the throughput of wireless LAN. In [27], we studied the optimal relay association problem to maximize the data reception during the network lifetime. The RNs in the network scenario have fixed positions. Based on the previous work, we investigate the RN placement problem by iteratively moving the RNs to "better" locations based on the optimal

relay routing assignment of the current network scenario.

1.2.2 Power Control

Power control schemes has been extensively studied to enhance wireless network performance. Sun et. al propose that increasing nodal transmit power can lessen the interference caused by hidden node problem, and thus the network throughput could be increased [76]. Behzad and Rubin analyze and investigate the effect of nodal transmit power on the maximum level of the source-destination throughput [10]. It adopts a different system model: the network nodes are accessing the channel based on time-division-multiple-access (TDMA) scheme to transmit packets. Tang et. al study joint link scheduling and power control in a TDMA-based multihop wireless network with the objective of maximizing network throughput [79]. The successful transmission is guaranteed only when the SINR is above a certain threshold value. Narayanaswamy et. al propose that within a heterogeneous ad hoc network, all the network nodes choose identical transmit power can maximize traffic carrying throughput, extend battery life as well as reduce contention at MAC layer. The so-called COMPOW protocol selects a common minimum transmit power for all nodes such that network connectivity is preserved [61]. Kawadia and Kumar consider the power control problem when nodes are non-homogeneously dispersed, and proposes three solutions, CLUSTERPOW, tunnelled CLUSTERPOW, and MINPOW for joint clustering and power control problem [46]. All above-mentioned works are assuming that network nodes are sharing a common transmit channel, thus are different from our network model. In [66], Qiao et. al analyze the relationship among different radio ranges and transmit power's effects on the interference in 802.11a/h systems, and proposes several frame-based intelligent power control mechanisms, which employs the best combination of the physical layer mode and transmit power

level. The objective is different from ours: it pursues the minimization of communication energy consumption in 802.11 systems. In [35], Ho and Liew point out that the minimum transmit power scheme[61] can create hidden node problems, thus decrease network performance. However, most of the power control schemes are implemented in a scenario with one common shared channel.

1.2.3 Channel Assignment

A number of channel assignment schemes has been proposed in recent years. In [17], Chin et. al address the problem of dynamically assigning channels in ad-hoc wireless networks via power control in order to satisfy their minimum QoS requirements. The objective then is to maximize the number of co-channel links subject to some stability conditions. In [62], a cluster-based multipath topology control and channel assignment scheme is proposed, which explicitly creates a separation between the channel assignment and topology control functions, thus minimizes flow disruptions. In [68], Raniwala et. al propose a greedy load-aware channel assignment scheme when network nodes are with multiple radios. The goal of channel assignment is to bind each network interface to a radio channel in such a way that the available bandwidth on each link is proportional to its expected load. In [4], Alicherry et. al mathematically formulate the joint channel assignment and routing problem, taking into account the interference constraints, the number of channels in the network and the number of radios available at each mesh router. A centralized algorithm is developed to solve the problem to yield the optimized network throughput. The channel assignment algorithm is used to adjust the flow on the flow graph to keep the increase of interference for each channel to a minimum. In [67], Ramachandran et. al propose an interference-aware channel assignment algorithm and protocol for multi-radio wireless mesh networks. The proposed solution intelligently assigns channels

to radios to minimize interference and thus enhance network performance. Few research efforts have addressed the problem of utilizing power control mechanism to influence the interference as well as channel gains between network nodes and further determine the optimal channel assignment.

1.2.4 Fairness for Wireless Networks

In the area of Operations Research, the max-min problem has been extensively studied. In [78], Tang develops a nonsimplex-based algorithm that finds an optimal solution to a max-min allocation problem with nonnegative integer variables. Fairness has been well studied in both network layer and MAC layer. Recently, in [41], Hou et. al develop an elegant polynomial time algorithm to calculate the rate allocation under a network lifetime constraint with respect to a two-tiered wireless sensor network. In [79], a Linear Programming (LP) formulation is provided to solve the max-min guaranteed maximum throughput bandwidth allocation problem. In addition, the Lexicographical Max-Min Bandwidth Allocation (LMMBA) problem is solved by a polynomial time optimal algorithm. In [56], Liang et. al investigate resource allocation for fading relay channels under separate power constraints, which falls into max-min problems. However, it is studied within a context of three-terminal networks.

1.2.5 Disaster Area Wireless Networks

[22] describes the use of radio frequency spectrum dedicated for public safety communications in the United States. Regarding research efforts focusing on first responder networks, [70, 20, 7] discuss incorporating public safety communication wireless technologies into commercial wireless networks, which provides public safety communication terminals with unified network resources to satisfy tactical require-

ments. [59] examines two hierarchical network solutions which allow the delivery of mission-critical multimedia data between rescue teams and headquarters over extremely long distances using a combination of wireless network technologies and multimedia software applications to meet the requirements of disaster rescue communication scenarios. However, the mobility model assumes that mobile nodes move randomly within the large disaster area that is supposed to be covered, which does not apply practically in reality. Ad hoc network has also been applied to scenarios such as disaster area [77] and battle field [81]. However, the topology of ad hoc network is static or very slow in motion, otherwise it would be difficult to maintain the connectivity of all network nodes. According to DAWN, all the MNs (We will use our terminology to describe related works) are randomly moving within busy square. [64] introduces a sensor network designed for disaster area relief operations. However, the sensors distributed over the disaster area are fixed and are used by survivors to contact first responders. Such kind of network can not be adopted either, because first responders can not use fixed sensors to contact each other as they are moving all over the disaster area.

1.2.6 Mobility Model

In recent years, a lot of different mobility models have been proposed and used for performance evaluation of networks. Models like the abstract Random-Waypoint-Mobility-Model[45] or Gauss-Markov-Mobility-Model [55] describe random-based movement and distribute the nodes over the complete simulation area. However, a distribution and movement of the nodes over the complete simulation area does not fit into the characteristics of DAWN. To study more realistic non-equally distributed movement, [11] proposes a mobility model in which the probability that a node selects an attraction point or a point in an attraction area as next destination is larger

than the choice of other points. Thus, some nodes visit several spots within the simulation area more frequently than others. This mobility model does not apply to large scale disaster area as the disaster intensity is measured in large areas. [48] divides the simulation area into pixels similar to the squares in our proposed scenario. However, the mobility pattern of MNs within the area follows moving from pixel to pixel according to probabilities. Such a moving pattern do not exactly match the needs for relieving a disaster area as our mobility model does. The Reference Point Group Mobility Model [39] considers the movement of groups and relative movement inside groups. Disaster area relief might favor such a group-based movement pattern, since first responders work in groups identified by each square. However, the concepts of splitting up and reassembling fail to be introduced to help cover the whole simulation area. Thus this model does not apply to our large scale disaster area. [12, 26] divides the whole simulation area into small subareas and a different mobility model is utilized in each subarea. Therefore, nodes moving between different subareas are subject to changes of moving pattern. Since in a large scale disaster area, usually different small subareas are similar except CI values, thus various kinds of mobility models would only increase the complexity of the model. Furthermore, there are two approaches [6, 63] that describe two event-driven role-based mobility model for disaster area relief applications. However, these two models only apply in small area with specific disaster sites instead of large-sized disaster area.

1.2.7 Coverage in Wireless Networks

There have been many research efforts dedicated to covering targets using RNs while maintaining connectivity of RNs. In [19], a similar problem named as Connected Dominating Set is studied. However, it abides by that the transmission range of MNs and RNs are the same and RNs can only be deployed at the positions of the

MNs. In DAWN, the placement of RNs does not have this constraint. In[31],the Connected Sensor Cover problem is studied, which involves placing the minimum number of RNs such that they form a connected network, while still covering a specified area. According to DAWN, as MNs are randomly moving within each busy square, we aim to place RNs in a way that each busy square has to be fully covered by at least one RN to ensure all MNs can access the backbone network. Therefore, the target covering area is divided into several small squares that needs to be covered by RNs respectively. There are plenty of work done to study covering a set of specified target points ([79, 75, 33, 44, 23]). All of these research efforts differ with ours in the goal that is pursued: Given the transmission range of MNs, their aim is to cover those specified target points, while RNs are deployed to cover several squares in our work. Furthermore, different from many of researches done on the RN placement in wireless networks, the connection between RNs is not a issue in our scenario, as the transmission range of RNs are very large compared to the simulation area.

1.2.8 Channel Assignment and Power Control for Cognitive Radio Networks

Regarding channel assignment and power control for cognitive radio networks, our work is related with [36, 37, 86, 21, 73, 9]. In [36], Hoang and Liang consider the joint problem of downlink channel assignment and power control for CRN. Our problem is different from that, because our objective is to achieve the maximum network throughput instead of supporting the most number of SUs. In [37], the problem is studied to maximize the throughput for a cognitive radio network while not affecting the performance of primary users. In [86], the problem of selecting the maximum subset of SUs to maximize the total secondary revenue of the cognitive

radio network is investigated, while the Quality of Service (QoS) requirements for both PUs and admitted SUs should be guaranteed. In [21], a joint problem of optimizing power control and channel assignment is considered for cognitive radio networks. However, only one base station is introduced to control and support a set of SUs at fixed locations for all the works above. In our network model, multiple base stations are jointly considered to support the secondary users, which results in inter-cell interference and thus leads to a more complex problem to deal with. In [73], Shi et. al study the problem of channel allocation, power control and routing assignment for multi-hop cognitive radio networks and a distributed algorithm is proposed. The difference with our work mainly lies in the fact that traffic flows from a set of BSs to a unknown subset of user nodes in our network model, while the destination nodes are pre-specified in [73]. In [9], a distributed cross-layer optimization scheme is proposed, which incorporates scheduling, power control and channel assignment. However, interference constraint is not considered in the problem formulation due to the assumption that the time-sharing sub-intervals are non-overlapping across all users. Regarding cross-layer design for cognitive radio networks, our work is related with [80, 40]. In [80], Tang et. al study joint spectrum allocation and scheduling problems in cognitive radio wireless networks with the objective of achieving fair spectrum sharing. In [40], a joint problem of spectrum sharing, scheduling and routing assignment is investigated for cognitive radio network. Compared with these two papers, our main contribution is on the computation of power control and the distributed implementation of the proposed approach.

1.2.9 Distributed Optimization of Wireless Networks

There have been extensive research efforts on distributed optimization for wireless networks. Some of these algorithms focus on channel assignment problem [15] or

power control problem [2], without addressing cross-layer optimization. Research efforts addressing cross-layer optimization problems in distributed fashion include [9, 73, 32]. In [9], scheduling, power control and channel assignment are considered within one problem and a distributed optimization algorithms is proposed. The authors assume that time-sharing sub-intervals are non-overlapping, thus no interference exists. In [73], a cross-layer optimization problem for cognitive radio networks is studied, with joint consideration of power control, scheduling and routing. In [32], a distributive non-cooperative game is proposed to perform channel assignment, adaptive modulation and power control for multi-cell multi-user OFDMA networks. Compared with these two works, our main contribution is the protection of PUs.

1.2.10 Capacity of Multihop Wireless Networks

Jain et. al study a routing problem between a pair of nodes to calculate the throughput bounds for a multi-hop wireless network, adding wireless interference constraints into the maximum flow formulations [47]. Zhai and Fang study the path capacity of traditional routing in a multi-rate scenario [89]. Zeng et. al propose a method to compute the end-to-end throughput bounds of opportunistic routing for a multi-hop wireless network [88]. Distinguished from the previous works, we solve a throughput maximization problem for a multi-hop wireless network by assuming interference alignment at the physical layer, which can bring fundamental changes to wireless networking problem formulation and can substantially improve the performance.

1.2.11 Interference Alignment

Investigations on Degrees of Freedom (DoF) on the two-user interference channel leads to the later discovery of interference alignment. In [60], an elegant coding

scheme is proposed for two-user interference channel, which achieved $\lfloor \frac{4}{3}M \rfloor$ DoF when all nodes are equipped with M antennas. According to the scheme, the use of iterative optimization of transmit precoding and receive combining vectors is a implicit implementation of interference alignment. The idea of interference alignment was first coined in [14], where it is proved that every user in a wireless interference network is able to achieve one half of the capacity that he could achieve in the absence of all interference. Following that work, Gomadam et. al propose an iterative algorithms that utilize the reciprocity of wireless networks to achieve interference alignment with only local channel knowledge at each node [25]. The algorithms also provide numerical insights into the feasibility of interference alignment. Different from the early works, this chapter focuses on cross-layer optimization of multiple layers, incorporating assignment of DoF in physical layer, scheduling in MAC layer and routing in network layer.

1.3 Organization

This dissertation is organized based on research studies of resource allocation schemes for different kinds of wireless networks. We first address a relay placement and route assignment problem for wireless sensor networks. Secondly, we study a joint problem of power control and channel assignment for a wireless mesh network. Thirdly, we investigate a dynamic resource allocation problem for a disaster area wireless network. We then present a study on throughput maximization for WRAN-based cognitive radio networks. At last, we consider the network throughput optimization problem for a multi-hop wireless network by considering interference alignment at physical layer. The contents of each chapter are described as follows.

Chapter 2 presents a two-tiered wireless network architecture in which relay

nodes are temporarily added to overcome the long distance communications between the edge nodes and the base station. Then, a joint-optimization problem is defined and analyzed for relay node placement and assignment. Subsequently, an elegant yet practical solution is proposed using binary integer programming and weighted clustering techniques.

Chapter 3 addresses a joint problem of power control and channel assignment within a wireless mesh network. A wireless mesh network is made up of two kinds of nodes: mesh routers and user nodes. The mesh routers form a backbone network, while user nodes receive data from the backbone network by connecting to the mesh routers via one hop. This chapter aims to find the optimal joint solution of power control and channel assignment of the wireless mesh networks such that the minimum capacity of all links is maximized. We develop an upper bound for the objective by relaxing the integer variables and linearization. Subsequently, we put forward a heuristic approach to approximate the optimal solution, which tries to increase the minimal capacity of all links via setting tighter constraint and solving a binary integer programming problem.

Chapter 4 investigates the disaster area communication system using relay-assisted wireless network for first responders as mobile nodes. At first, a novel mobility model is proposed to describe the movement pattern of mobile nodes within a large disaster area. Secondly, we study the relay management of finding a minimum number of Relay Nodes and their dynamic locations to cover all the mobile nodes within the disaster area. A Square Disk Cover (SDC) problem is formulated and three different algorithms, including the Two-Vertex Square Covering (TVSC) algorithm, the Circle Covering algorithm and the optimal algorithm, are proposed to solve the SDC problem.

Chapter 5 presents an investigation on an overlaid cognitive radio network with

existing primary network. We model the opportunistic spectrum access for cognitive radio networks and formulate the cross-layer optimization problem under the interference constraint imposed by the existing primary network. Then we propose a distributed greedy algorithm to approximate the optimal network throughput.

Chapter 6 studies the network throughput optimization problem for a multi-hop wireless network by considering interference alignment at physical layer. We first transform the problem of dividing the set of links into multiple maximal concurrent link sets into finding all maximal cliques of a graph. Then each concurrent link set is further divided into one or several multi-access interference networks, on which interference alignment is implemented to guarantee simultaneous interference-free transmission. The network throughput optimization problem is then formulated as a non-convex nonlinear programming problem, which is NP-hard generally. Thus we resort to developing a branch-and-bound framework, which guarantees an achievable performance bound.

1.4 Contributions

This thesis has made outstanding contributions in the research field of resource allocation for wireless networks. In system modelling aspect, we have brought up quite a lot of networking models to fit into different wireless network scenarios. For instance, we advocated two-tiered model for data transmission from wireless sensor nodes to the data center [27]. To study disaster area wireless networks, we put forward a macroscopic mobility model to analyze moving patterns of first responders [28]. In addition, we also proposed a distributed scheme to model the procedure to implement optimization of wireless regional area networks as in Chapter 5. Last but not least, we incorporate interference alignment into modelling of multi-hop wireless

networks to improve the capacity performance [30]. In theoretic aspect, we explore many optimization algorithms to be applied to various resource allocation problems. We sought heuristic algorithms to approximate the optimal solution which is of very high complexity or non-obtainable. As an example, for nonlinear problems, we can approximate the optimal solution by iteratively doing linear computation [29]. We can also divide the conquer by splitting the task into subtasks and assign them to multiple entities as in Chapter 5. The main contributions of this dissertation can be summarized as follows:

- Chapter 2

  — We study an optimization problem to maximize the total number of information packets received at the base station during the network lifetime.

  — We demonstrate a solution to obtain the optimal transmit power for a relay node such that it can send the maximum number of packets to the base station during the network lifetime.

  — The proposed weighted clustering algorithm is a heuristic approach to move relay nodes to better locations iteratively to better serve edge nodes in terms of received packets. The proposed scheme demonstrates better performance than other methods.

- Chapter 3

  — The key obstacle lies in the nonlinearity of the objective function. We successfully transform the max-min objective to a more solvable linear objective with additional constraints in compromise of optimality. In particular, we propose a heuristic approach to iteratively increase the minimal throughput of all links tightening the constraint that the capacity of each link is larger than a threshold value.

—We prove that when the sum rate of all links are maximized and each link share the same capacity, it is guaranteed that max-min performance is optimized. Then the upper bound of max-min fairness problem can be easily acquired by solving a linear programming problem. The upper bound offers a benchmark to measure the quality of the feasible solution obtained from the heuristic approach.

- Chapter 4

  — We propose a novel and practical mobility model for mobile nodes in disaster area. We describe typical movement pattern of first responders in a disaster area. Since the movement pattern for all the first responders is not random within the disaster area as in the Waypoint model[45], and they basically are heading deep into the disaster area from the boundary, we put forward our mobility model for mobile nodes (MNs) by combining these two traits together. The disaster area are divided into many small square regions (we call them squares in this chapter later), each square with a Catastrophic Intensity (CI) to show how severe the disaster is in that area. The larger the CI value is, the more time and first responders are required to relieve that square. At the beginning, first responders are disseminated into several arbitrarily chosen starting squares on the boundary of the disaster area, and then each time after they finish relieving one region, the first responders in that square are divided into 3 groups, entering the 3 adjacent squares based on their CI values. Therefore, we actually observe the mobility pattern of MNs as a square based moving behavior. Then what is the moving pattern for MNs within each square? We model it by using the Waypoint model that gives MNs freedom to displace themselves within the square, which can be justified

by our ignorance of the situation in each square.

— We strive to place minimum number of relay nodes such that each mobile nodes can connect to at least one relay node. We formulate the square disk cover problem and propose three algorithms to solve it, including the Two-Vertex Square Covering (TVSC) algorithm, the Circle Covering algorithm and the binary integer programming algorithm. We also investigate carefully into the performance comparison between the TVSC algorithm, the Circle Covering algorithm, and the binary integer programming algorithm. As the optimal approach, the BIP algorithm yields the deployment of the least number of RNs, while having the largest computational complexity $O(N^3)$; the TVSC algorithm yields the deployment of the second least number of RNs, and consuming much less computational resources in $O(N^2)$; the Circle Covering algorithm yields the deployment of the most number of RNs, but consuming the least computation resources only in $O(N)$. In practice, the TVSC algorithm and Circle Covering algorithm might be more preferable because they require much less computational complexity, but yield only a small number of the RNs deployed more than the BIP algorithm does.

- Chapter 5

  — An overlaid CRN is constructed with existing primary network. We model the opportunistic spectrum access for CRN formulate the cross-layer optimization problem under the interference constraint imposed by the existing primary network.

  — A distributed greedy algorithm is proposed to approximate the optimal network throughput. Cross-layer optimization for CRN is often implemented in centralized manner to avoid co-channel interference. The distributed al-

gorithm coordinates the channel assignment with local channel usage information. Thus the computation complexity is greatly reduced. In particular, we compare the distributed algorithm with 4 other algorithms, the optimal algorithm, two-phased algorithm and dynamic interference graph allocation and power-based algorithm. The computation complexity of the distributed algorithm is $O(N^4)$ and the optimal algorithm is of $O(2^N)$. Simulation results show that the distributed algorithm outperforms 3 other algorithms and perform close to the optimal.

- Chapter 6

  — We study the network throughput optimization problem for a multi-hop wireless network by considering interference alignment at physical layer. We first transform the problem of dividing the set of links into multiple maximal concurrent link sets into finding all maximal cliques of a graph.

  —Each concurrent link set is further divided into one or several multi-access interference networks, on which interference alignment is implemented to guarantee simultaneous interference-free transmission. The network throughput optimization problem is then formulated as a non-convex nonlinear programming (NLP) problem, which is NP-hard generally.

  — We resort to developing a branch-and-bound framework, which guarantees an achievable performance bound. We use numerical results to validate the efficacy of the algorithm and to offer insights on the throughput enhancement brought by interference alignment.

1.5 Discussions

In this dissertation, we solve problems stemmed from various kinds of wireless networks. Once the network model is specified and optimization objective determined, a mathematical problem can be formulated and solved accordingly. Some of the problems are NP-hard to solve for the optimal solution, thus suboptimal solutions are sought with algorithms of much smaller complexity. Fig . 1.1 demonstrates the procedure of researching a resource allocation problem within a wireless network scenario.

Although the resource allocation problems we study are formulated out of different network scenarios, they do share some similarities. For instance, some problems have the same constraints stemmed from different wireless networks, such as one channel per base station can support at most one node, and one node can access at most one channel. Interference constraint is often set as two geographically close links can not be active on the same channel simultaneously. Performance objectives also have the same terms. For example, the capacity of one link is often calculated using the shannon formula. Some problems study the same objects, such as channel assignment, power control, etc.

We also employ some technique as part of the solution procedure for many problems. For instance, since many problems can be transformed into mixed-integer linear programs, we resort to the traditional branch-and-bound algorithm for the optimal solution. As the optimal solutions are often of high complexity, the heuristic approaches, which are based on specific problems, are needful to render low-complexity implementation.

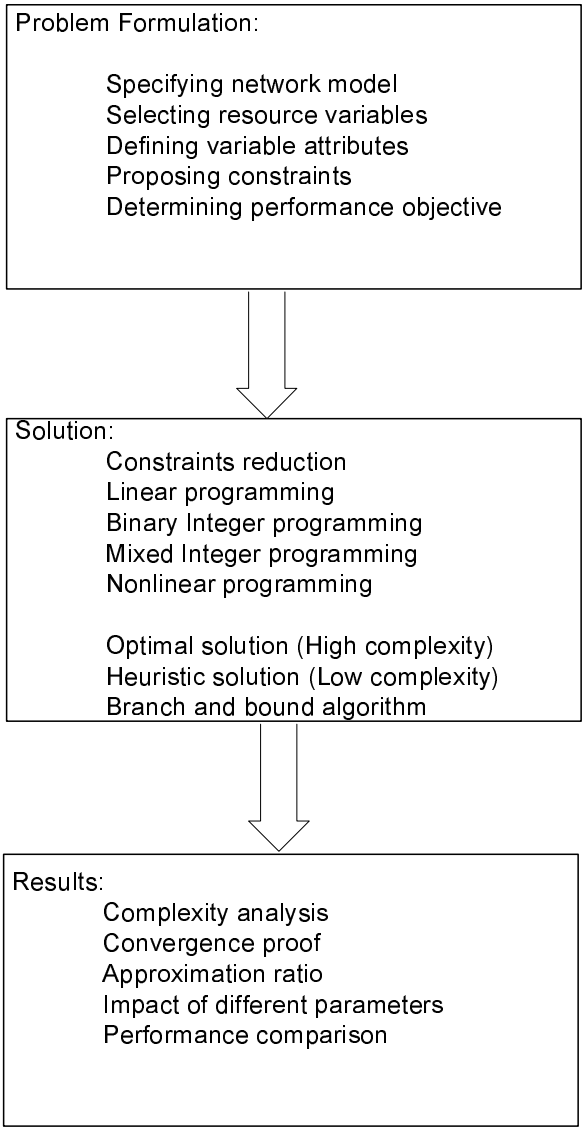

Figure 1.1: Procedure of researching a resource allocation problem within a wireless network scenario.

Chapter 2

Relay Management for Wireless Sensor Networks

Wireless sensor networks have been used in a wide range of applications. As one example of disaster communications, spatially distributed temperature sensors in an ablaze forest can provide critical information about fire distribution, which helps to control the fire diffuse. Another example can be found on the farms. Farmers use transducers to gather information about environmental parameters in their greenhouses. In both scenarios, Edge Nodes (ENs), such as sensors and transducers, are deployed at strategic positions with fixed sensing and transmit power, thus they can sustain a fixed length of lifetime. In addition to the deployment of ENs, a Base Station (BS) is needful to collect data from the sensing field. However, due to geographic reasons, sometimes the BS could only be established far away from the sensing field, resulting in very low data reception rate if there is any. To address this problem, a small number of Relay Nodes (RNs), as energy-limited as ENs, can be placed between the sensing field and the BS to forward data packets. Here we only consider two-hop relay routing from ENs to the BS. It is assumed that the power of

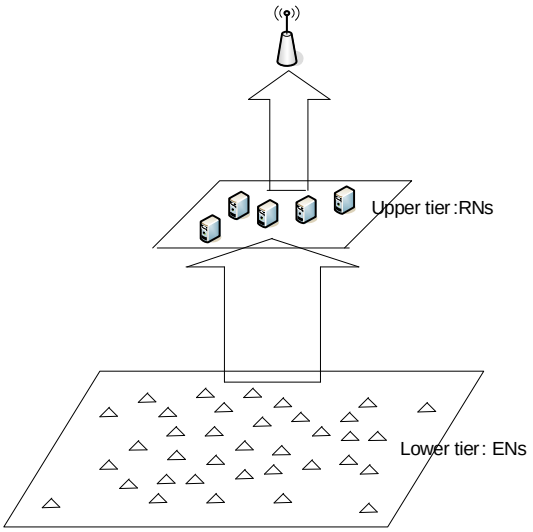

Figure 2.1: A two-tiered wireless network

RNs can be adjusted to amplify the faded signals received from ENs and forward it to the BS. Therefore, the ENs, RNs, and BS build up a two-tiered wireless network in such applications.

To define relayed network designations, we have to specify the RN placement and the corresponding dynamic mapping from ENs to RNs. These two issues are highly interdependent. Directly applying the optimization techniques to solve the joint problem is unrealistic due to a large number of varying parameters. Therefore, we resort to develop an efficient iterative algorithm, called Weighted Clustering with Binary Integer Programming (WCBIP). It is a three-step iterative process: (1) based on the current locations of RNs, calculate the optimal power for each RN to maximize its capability to transmit data, then compute the network lifetime; (2) determine the optimal relay routing table using Binary Integer Programming (BIP), which provides the dynamic mapping from ENs to RNs; (3) update each RN's position using weighted clustering method based on the current routing table. These three procedures are executed recursively until the algorithm converges.

The main contributions are as follows: first, we present a two-tiered wireless

network architecture in which RNs are temporarily added to overcome the long distance communications between the ENs and the BS and the RNs are energy constrained; secondly, a joint-optimization problem is defined and analyzed for relay node placement and assignment; thirdly, an elegant yet practical solution is proposed using BIP and weighted clustering techniques; finally, the simulation results are presented to demonstrate that the WCBIP algorithm outperforms other relay placement schemes.

In Section 2.1, we describe the network model and formulate the RN placement problem. In Section 2.2, we present the BIP scheme together with its implementation to figure out the optimal association between ENs and RNs. In Section 2.3, we present the WCBIP algorithm to solve the RN placement problem. The simulation results are demonstrated in Section 2.4.

2.1 Network Modeling and Problem Formulation

2.1.1 Network Architecture

We focus on a two-tiered architecture for wireless sensor networks. As shown in Figure 2.1, there are three types of nodes in the network: ENs, RNs and the BS. ENs, constituting the lower tier of the network, are portable or quasi-stationary user terminals that are usually battery powered and are equipped with wireless transceivers. They could also be low-bandwidth application-specific sensor devices. As ENs are responsible for collecting local task-based information, we assume that ENs are pre-deployed in the field at strategic positions. The operation mode for ENs is very simple: Once triggered by an event, each EN sends an F-bit packet directly to a relay node in one hop per time period using a constant transmit power. Each EN may select a different path to BS by choosing a different RN from time to time.

Therefore, the ENs associated with each relay may change over time. Since RNs are supposed to be energy constraint, we assume that ENs keep alive before all the RNs die. It should also be noted here that because ENs are very close to each other and the BS is far away from ENs, multi-hop routing among ENs is not necessary as it will not bring any distinct benefits to the data transmission.

The upper tier of a network is made up of RNs. During each period, each RN simply forwards all packets received from ENs to the BS. RNs share equivalent receiving power, but differ with each other in the aspect of transmit power. Since RNs are deployed between ENs and the BS, and are associated with different ENs during the network lifetime, their optimal locations are subject to the distribution of ENs and location of the BS to yield the best performance. Suppose their initial energy levels are the same, RNs may deplete their energy at different time because of different traffic load and transmit power. When one RN runs out its energy, the ENs associated with this RN in the previous period may switch to another RN to send packets in the next period. Here we also disregard multi-hop data transmission among RNs, because the transmit power of RNs are adjustable to amplify the signals to reach the BS. Moreover, as it is easily understood that more RNs would achieve a larger amount of packets received at the BS, a fixed and moderate number of RNs are introduced in this network model.

The data sink in a two-tiered wireless network is the BS. As the BS collects all information packets forwarded by the RNs from the ENs, it is assumed that the BS has sufficient energy provided by a large or constantly-reprovisioned battery source. It is also assumed that the BS has a fixed position as an information gathering center.

2.1.2 Joint Problem of RN Placement and Assignment

As an ultimate goal, RNs should be placed in locations resulting in the largest amount of data reception at the BS within the network lifetime. For a two-tiered wireless network with every node placed at certain fixed position, the optimal association between ENs and RNs needs to be computed such that the amount of correct packets received at the BS is maximized. It is obvious that different network topologies could yield different maximized amount of data reception. Then for a network with a BS, a group of ENs, and a given number of RNs waiting to be deployed, the question becomes: where should we place these RNs and what are the optimal associations between ENs and RNs, such that the total amount of correct packets received at the BS during the network lifetime is maximized?

From the above analysis, we can see that the two issues of RN placement and the corresponding dynamic mapping from ENs to RNs are highly interdependent. As we are desirous of finding the optimal RN placement, we should also consider the corresponding association between ENs and RNs for the node locations as well as the maximized amount of data received at the BS.

In the definition of system objective and constraint functions, Table 2.1 contains all adopted conventions.

Since packets are transmitted through a two-hop transmission, the total number of correct packets received at the BS would be (2.1)

$$\sum_{i=1}^{n}\sum_{j=1}^{m}\sum_{t=1}^{T} PRR(e_i, r_j)PRR(r_j, BS)x_{ij}^{t} \tag{2.1}$$

The RNA problem is defined as follows: For a two-tiered network, $e = e_1, e_2, ..., e_n$ are placed at $e_i x, y (i = 1, 2, ..., n)$; $r = r_1, r_2, ..., r_m$ are placed at $r_j x, y (j = 1, 2, ..., m)$; the BS is placed at $s(x, y)$;

Table 2.1: Notation of relay management of wireless sensor networks

Symbol	Definition
$\{e_1, e_2, ..., e_n\}$	the set of ENs
$e_i(x, y)$	the XY location of e_i
$\{r_1, r_2, ..., r_m\}$	the set of RNs
$r_j x, y$	the XY location of r_j
$s(x, y)$	the XY location of BS
PRR	packet reception rate (PRR)
T	network lifetime in periods
X_{ij}	number of times that e_i sends packets to r_j during T periods
x_{ij}^t	if e_i sends data to r_j in the t-th period, $x_{ij}^t = 1$; else $x_{ij}^t = 0$
$buffer(j)$	number of packets that r_j can transmit;
Pt_j	transmit power of r_j;
N_{total}	total number of packets received within network lifetime

$$max \sum_{i=1}^{n} \sum_{j=1}^{m} \sum_{t=1}^{T} PRR(e_i, r_j) PRR(r_j, BS) x_{ij}^t \tag{2.2}$$

$$\sum_{j=1}^{m} x_{ij}^t = 1 \tag{2.3}$$

$$\sum_{i=1}^{n} \sum_{t=1}^{T} x_{ij}^t \leq buffer(j) \tag{2.4}$$

RNP problem: Given a deployment of ENs and one BS, find the positions for a fixed number of RNs, such that the maximum number of correct packets from ENs can be received at the BS.

2.2 Technical Approach for RNA

In this section, we present a BIP method based on power control for RNA problem. Given a two-tiered topology with known locations of all nodes, we can calculate the optimal power for all the RNs and compute the network lifetime. Then we can obtain two constraints and adopt the BIP method with the constraints to find a

solution for RNA problem under current network deployment.

2.2.1 Optimal Power Control for RNs

Path Loss Model

The RNA solution depends heavily on the relationship between transmit power and packet error rate, which can be modeled using path loss channel model in physical layer. The following path loss model is used.

$$P_a d_a^{\alpha} = P_b d_b^{\alpha} \tag{2.5}$$

P_a and P_b are the signal power measured at d_a and d_b meters away from the transmitter respectively. α denotes the path loss exponent. If we set d_a to be 1 meter, thus P_a is the reference signal power measured at 1 meter away from the transmitter. Then (5.1) is simplified as (2.6).

$$P_b = \frac{P_a d_a^{\alpha}}{d_b^{\alpha}} \tag{2.6}$$

P_a can be calculated using the free space propagation model as (2.9).

$$P_a = G_t G_r (\frac{\lambda}{4\pi})^2 \times P_t \tag{2.7}$$

P_t denotes the transmit power, G_t and G_r are the transmitter and receiver antenna gains respectively. $\lambda = \frac{c}{f}$ is the wavelength of the transmitted signal, and c is the velocity of radio-wave propagation in free space, which is equal to the speed of light. The received power P_r at a distance d meters away from the transmitter can be calculated as (2.8).

$$P_r = \frac{G_t G_r (\frac{\lambda}{4\pi})^2 \times P_t}{d^\alpha} \tag{2.8}$$

Suppose P_{noise} denotes the power of noise, then the signal-to-noise ratio (SNR) at the receiver end is:

$$SNR = \frac{P_r}{P_noise} \tag{2.9}$$

The bit error rate can be determined by the SNR based on the error probability model. For illustration purpose, we take BPSK [65] as the modulation scheme and the bit error rate is given by:

$$P_b = \frac{1}{2} e^{-\frac{1}{2} SNR} \tag{2.10}$$

Assuming bit error rate occurs independently, the packet reception rate (PRR) is:

$$PRR = (1 - P_b)^F = (1 - \frac{1}{2} e^{-\frac{1}{2} SNR})^F \tag{2.11}$$

Optimal Power Control

Considering a peer-to-peer communication between a relay r_i and the BS, there is a certain distance d_i between r_i and the BS. We assume r_i uses transmit power Pt_i, and it relays z_i^t packets to the BS in time period t, or there are z_i^t ENs sending packets to r_i in the tth period. Using above-mentioned error probability model, the

total number of packets that the BS receives from r_i is:

$$M_i = \sum_{t=1}^{T} z_i^t (1 - \frac{1}{2} e^{-\rho \frac{Pt_i}{d_i^\alpha}})^F \tag{2.12}$$

$\rho = \frac{1}{2} G_t G_r (\frac{c}{4\pi f})^2 \frac{1}{P_{noise}}$ and T is the overall number of periods, also referred as the relay network lifetime. The total number of packets that can be transmitted by r_i is restricted by its energy. Then we have:

$$\sum_{t=1}^{T} z_i^t = \frac{Ev}{Pt_i + P_{elec}F} \tag{2.13}$$

E denotes the total energy each RN holds, v is the transmission bit rate, P_{elec} denotes the electronic power consumed by receiving one packet. Combining (2.12) and (2.13) yields:

$$M_i = \frac{Ev}{Pt_i + P_{elec}F} (1 - \frac{1}{2} e^{-\rho \frac{Pt_i}{d_i^\alpha}})^F \tag{2.14}$$

To maximize M_i, we need to find the optimal power Pt_i. Take a derivative of M_i with respect to Pt_i, and set the derivative to zero, we get the following characteristic equation from convex theory:

$$\frac{1}{2}(Pt_i + P_{elec}) F e^{-\rho \frac{Pt_i}{d_i^\alpha}} \frac{\rho}{d_i^\alpha} + \frac{1}{2} e^{-\rho \frac{Pt_i}{d_i^\alpha}} - 1 = 0 \tag{2.15}$$

Let us set Ω to be the collection of all solutions to (2.15). By optimizing theory, the optimal point Pt_i^* maximizing the function $M_i Pt_i$ must lie in the union of the

set Ω and the boundary points of Pt_i. Note that (2.15) is transcendental and may not have closed form solutions. Numerical solutions for an experimental setup will be provided in Section 2.4.

2.2.2 Fixed Relay Network Lifetime

Based on the analysis in Section 2.2.1, each RN has an optimal transmit power Pt_i^* setup for best energy efficiency. Given the total energy constraint E, the total number of packets r_i can relay is:

$$buffer(i) = \frac{Ev}{(Pt_i^* + P_{elec})F} \tag{2.16}$$

Relay network lifetime is defined as the total number of network operating periods, represented by T. The total number of packets received from ENs equals to the total number of packets forwarded by all RNs. Thus,

$$T = \frac{1}{n}\sum_{i=1}^{m} \frac{Ev}{(Pt_i^* + P_{elec})F} \tag{2.17}$$

m denotes the number of RNs and n denotes the number of ENs. For r_i with fixed location in a two-tiered wireless network, Pt_i^* can be determined from (2.15). Therefore, the relay network lifetime T is fixed if the energy levels of RNs are known.

2.2.3 Binary Integer Programming Optimization

Binary integer programming is a linear programming (LP)-based branch-and-bound algorithm. The algorithm searches for an optimal solution to the BIP problem by solving a series of LP-relaxation problems. The branch-and-bound method is described briefly below. More details can be referred to [83].

The algorithm creates a search tree by repeatedly adding constraints to the problem, called "branching". At a branching step, the algorithm chooses a variable x_j whose current value is not an integer and adds the constraint $x_j = 0$ to form one branch and the constraint $x_j = 1$ to form the other branch. This process can be represented by a binary tree, in which the nodes represent the added constraints.

At each node, the algorithm solves the LP-relaxation problem using the constraints at that node and decides whether to branch or to move to another node depending on the outcome. There are three possibilities: (1) If the LP-relaxation problem at the current node is infeasible or its optimal value is greater than that of the best integer point, the algorithm removes the node from the tree, after which it does not search any branches below that node. The algorithm then moves to a new node according to the pre-specified method. (2) If the algorithm finds a new feasible integer point with lower objective value than that of the best integer point, it updates the current best integer point and moves to the next node. (3) If the LP-relaxation problem's optimal value is not an integer and the optimal objective value of the LP relaxation problem is less than the best integer point, the algorithm branches below this node.

As the algorithm could potentially search all 2^n binary integer vectors, the running time for binary integer programming is $O(2^n)$. n is the number of variables that need to be specified. As future work, we can transform the Binary Integer Programming problem into a linear optimal distribution problem [54] by generating a directed graph, to reduce the computation complexity to only $O(n^3)$.

2.3 WCBIP: an Iterative Approach for RNP

In this section, we first provide an analysis on how to maximize the amount of correct data reception with respect to different relay node placements. Then the analysis results are used to bring forward an efficient algorithm called WCBIP.

2.3.1 Analysis on RNP Problem

Section 2.2 gives a detailed description on how to assign ENs to RNs within a fixed scenario, such that the amount of correct data received at the BS can be maximized. As can be seen, the result of assigning every edge node to the relay node in each transmission period is illustrated as (2.1). Each relay node functions as a cluster head to forward packets from its cluster members. As we observe this two-tiered network system in this cluster view, maximizing the total number of correct packets received at the BS is tantamount to maximizing performance of each cluster. Because within the current network scenario, the edge nodes are immobile while the relay nodes are temporarily placed, intuitively, we construct the clustering function for relay node r_j as:

$$f_j = \sum_{i=1}^{n} \frac{X_{ij}}{buffer(j)} R_{ij} R_j = \sum_{i=1}^{n} \frac{X_{ij}}{buffer(j)} (1 - \frac{1}{2} e^{-\rho \frac{Pt_{edge}}{d_{ij}^2}})^F (1 - \frac{1}{2} e^{-\rho \frac{Pt_i}{d_{ij}^2}})^F \quad (2.18)$$

Pt_{edge} denotes the constant transmit power of edge nodes. d_{ij} represents the distance between edge node e_i and relay node r_j. f_j is a function of the x-y location of r_j. The weighted factor $\frac{X_{ij}}{buffer(j)}$ denotes the contribution each edge node makes to the overall cluster performance. As we move r_j, we can search for the position where the clustering function reaches its maximal value.

2.3.2 Implementation of WCBIP

Based on the relay placement analysis, we propose an iterative procedure to search for the optimal positions of all RNs so that the maximum amount of correct data can be received at the BS.

- Step 1: According to the EN deployment, RNs are evenly distributed within the coverage area;
- Step 2: Calculate optimal power for each RN and compute the network lifetime;
- Step 3: With respect to current node locations (the positions of ENs, RNs and the BS), BIP is applied to obtain the relay's assignment result $\mathcal{X}$ and the total number of correct packets received at the BS at this optimal point is N_{total}.
- Step 4: According to the assignment result, for each relay node r_j, construct the clustering function f_j, as a function of $r_j x, y$. Search for the maximal value of f_j, move r_j to the new position.
- Step 5: The algorithm terminates when any one of the following conditions is true: (1) Predefined number of iterations are completed. (2) N_{total} has not increased for C_{th} consecutive times. Otherwise, the procedure goes back to Step 2.

2.4 Simulation Results

2.4.1 Experimental Study on RNA Problem

For experimental setup, we establish the network scenario as follows: 10 edge nodes are randomly distributed on one sixth of circles with their center located at (0, 0),

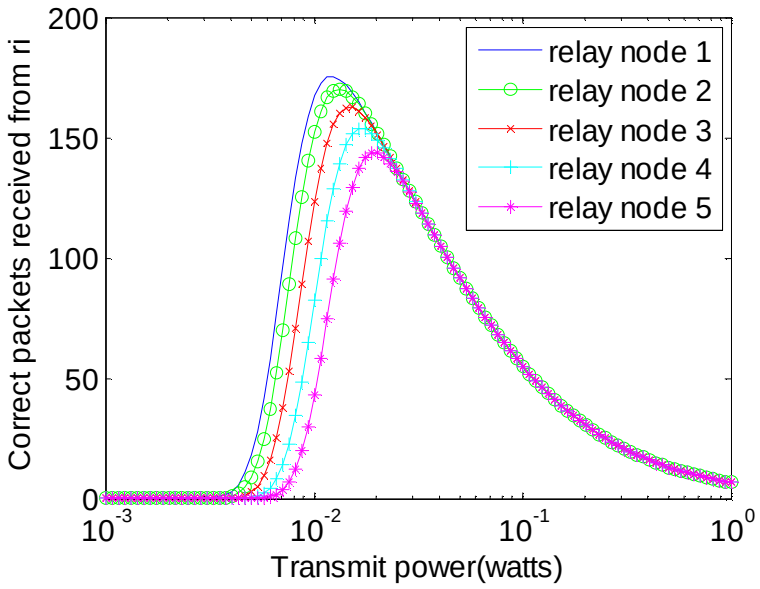

Figure 2.2: Total number of packets correctly received at the BS from relays using different transmit power

and radius varying between [40, 50]; the relay nodes, with the equal radians between each other, are also placed on the same set of concentric circles with their radius at 30. The BS is placed at XY coordinate [10, 0]. The assumptions and experimental parameters are: unit gain of both the transmitter and receiving antenna; the frequency of the electromagnetic signal is 2.4GHz; the noise power is 2.15×10^{-8}Watts, the electronic power for forwarding one packet is 2.53×10^{-2} Watts; the size of one packet is 80 bits; the edge nodes each use a constant transmit power of 10^{-2} Watts; the bit rate that the relay nodes send data is 11Mb/s [5]; the total energy for one relay node is 5×10^{-5} Joule. (We render the energy of relay nodes such small for simulation purpose.)

Given the fixed position of the relay nodes and the BS, we can draw the number of packets that r_i is able to forward with different transmit power based on (2.15). Transmission at the optimal power provides the best energy efficiency for the relay nodes.

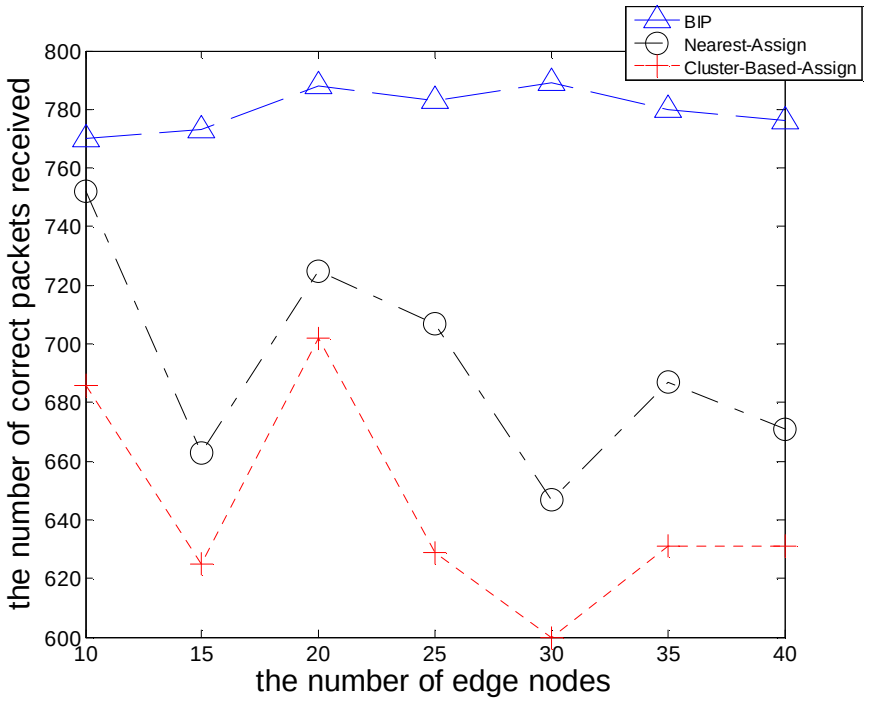

Figure 2.3: The number of correct packets received using 3 different assignment schemes.

As shown in Fig. 2.2, for each relay node, the optimal transmit power can be obtained at the peak point. It can also be observed that the optimal transmit power is larger if the relay is further away from the BS.

To demonstrate the advantages of the proposed method, we compare it with two other assignment schemes under the current network topology. One scheme is called the nearest relay assignment method [69], namely that every edge node sends its packets to the nearest active relay node. The other scheme requires that all RNs manage their members(ENs) as the cluster heads [42]. The RNs are assigned ENs according to their capacity. Technically, the number of edge nodes assigned to is in inverse proportion to based on the energy constraint as in (2.14). Fig. 2.3 shows the performance of these three methods for the cases the number of edge nodes varies from 10 to 40.

For each experimental setup, the locations of edge nodes are placed almost ran-

domly. Therefore, the PRR from edge nodes to relay nodes changes. The number of packets correctly received at BS varies. But for any given experimental cases, Fig. 2.3 clearly shows that the BIP method results significantly more information packets received at the BS than the other two techniques.

2.4.2 Experimental study on WCBIP for RNP problem

The BIP method can be used to find the fixed relay scheme to maximize the number of correct packets received at the BS. As prescribed in Figure 4, the WCBIP method incorporates the BIP for each relay as part of iteration, and in every iteration searches for a "better" location to improve the value of each clustering function. The search function we choose is the simplex search method [51], as one kind of unconstrained nonlinear optimization. In our simulations, we adopt the fminsearch function in Matlab to implement this optimization method.

We change the energy level for RN to 2×10^{-5}. The total number of correct packets received at each iteration is demonstrated in Fig. 2.4. To demonstrate its advantage, we also adopt the other two methods, called as weighted clustering nearest assign and weighted clustering cluster-based assign. As they are named, these methods updates the placement of RNs similarly as WCBIP, but based on their own association table. For WCBIP, the number of correct packets received increases greatly after the first iteration, followed by small improvement in the next a few iterations. This is because the first iteration has already moved each relay node close to its optimal place. As shown in Fig. 2.4, WCBIP algorithm has the advantage of quick convergence with significant performance improvement. In contrary, results for the other two methods remain much lower.

We also consider the impact that the range of ENs in radian has on the data reception performance. From Fig. 2.5, we can see the total number of packets

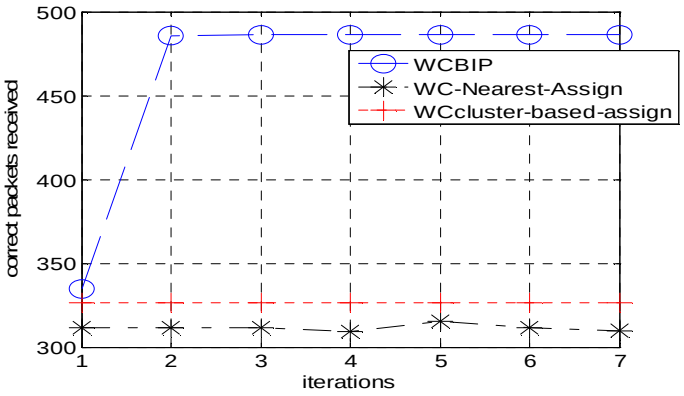

Figure 2.4: Iterations vs. Total number of received packets for 3 weighted clustering-based methods.

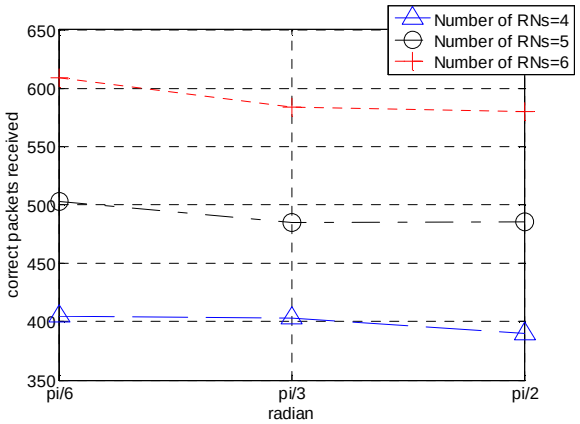

Figure 2.5: Number of received packets with respect to different Range of ENs in radian and number of RNs.

received increases as the number of RNs increases. This is because more RNs induces more energy to transmit data. Besides, as the radian of range increases, the number of packets received at the BS decreases slightly. The reason is that with a larger range, every packet would travel longer distances thus decreases its own reception rate.

To demonstrate the relationship between EN's locations and the number of packets received, we set up another network scenario as follows: 20 edge nodes are evenly distributed on one sixth of a circle with its center located at (0, 0), and radius changing. The BS is placed at XY coordinate [0, 0]. We employ the WCBIP method to

Table 2.2: RN placement with respect to different EN locations

EN locations	r1	r2	r3	r4	r5
35	(4.9, 1.2)	(6.4, 0.8)	(5.8, 3.6)	(3.4, 3.0)	(4.7, 5.2)
40	(8.4, 0.6)	(8.1, 2.4)	(7.3, 4.0)	(6.6, 5.6)	(5.1, 6.6)
45	(12.2, 3.6)	(12.4, 1.0)	(11.1, 6.0)	(9.6, 8.2)	(7.5, 10.0)
50	(17.0, 1.4)	(16.5, 4.9)	(15.2, 8.1)	(13.1, 11.1)	(10.5, 13.6)
55	(21.8, 1.7)	(21.1, 6.3)	(19.4, 10.6)	(16.6, 14.2)	(13.3, 17.2)
60	(26.7, 2.1)	(25.9, 7.6)	(23.4, 12.6)	(20.3, 17.4)	(16.4, 21.3)
65	(31.6, 2.5)	(30.7, 9.1)	(28.0, 15.1)	(24.5, 20.8)	(19.4, 25.1)
70	(37.0, 2.8)	(35.5, 10.5)	(32.5, 17.7)	(28.1, 24.0)	(22.7, 29.6)

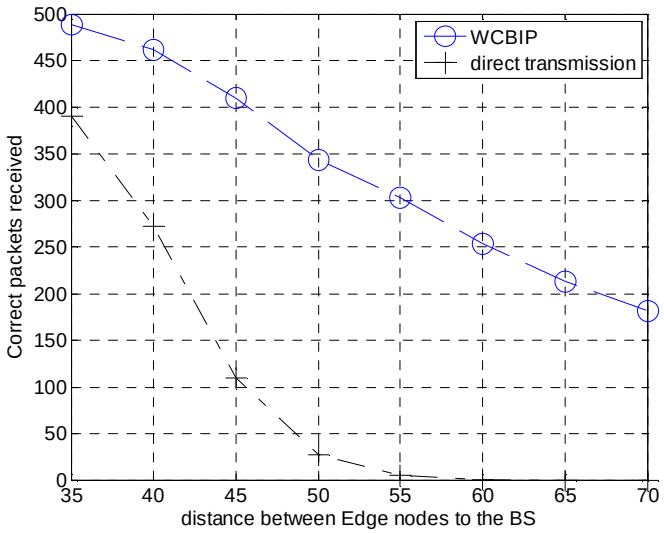

Figure 2.6: Number of received packets with respect to different Range of ENs in radian and number of RNs.

place 5 RNs between the BS and ENs. The placement results are shown in Table 2.2. Each of the dual numbers represents the XY-location of the corresponding RN when ENs are placed at the corresponding distance away from the BS. As can be seen from the table, the RN placements become further away from the BS as the ENs are placed at a larger distance away.

Fig.2.6 depicts the number of correct packets received with respect to WCBIP and direct transmission from ENs to the BS without data relay when ENs are placed at different distances from the BS. From the figure, it can be seen that introducing a

tire of relay nodes brings much benefits in increasing the number of packets received. Although results for both methods decreases as the ENs are placed further away from the BS, packets received through direct transmission goes down much more rapidly than the case that RNs are placed with WCBIP to help forward packets from ENs.

2.5 Conclusion

In this chapter, we investigate the joint problem of RNA and RNP for two-tiered wireless sensor networks. Since these two problems are highly interdependent, we developed an efficient iterative algorithm, called as WCBIP to find the optimal the RN placement to maximize the data received at the BS within a network lifetime. This approach firstly derives the optimal transmit power for each RN as well as the fixed relay network lifetime. Subsequently, we determine the dynamic optimal RNA in every period using BIP such that the BS receives the maximum number of effective information packets. Then we update each RN's position by optimizing their data transmission performance under current assignment results using a weighted clustering method. These three steps are executed iteratively until the algorithm converges. Experimental results show that within a fixed network scenario, the proposed BIP method yields much better performance than the other two schemes, nearest relay assignment and cluster-based assignment. The simulation results demonstrate that RNs can send the most information packets when taking the optimal transmit power. Moreover, we observe that WCBIP converges within a few steps, yielding better results than other two weighted clustering methods and direct data transmission from ENs to the BS. Finally, we quantify the effects of EN locations, with respect to angle and distance from the BS, on RNP and the maximum number of information packets received.

Chapter 3

Capacity Fairness for Wireless Mesh Networks

Recently fairness of network throughput of channels has been placed with great importance. The reason is that the traditional goal of maximizing the summation of throughput on all links could result in unbalanced use of network resources. In this chapter, we consider a two-tiered wireless mesh network that consists of a number of user nodes (UNs) and multiple Mesh Routers (MRs). UNs are deployed at strategic positions, transmitting and receiving information to/from the nearby MR via a single hop (see Fig. 3.1). We aim to enhance the fairness of network throughput by maximizing the minimal capacity of all users. In our proposed two-tiered wireless network model, one main issue is to deal with an increasing number of UNs while using orthogonal frequency-division multiple access (OFDMA) as a multiple access mechanism. Obviously, the fairness of network throughput is highly dependent on the channel assignment as well as power control of each MR. Transmissions on the same channel could seriously depreciate each other's capacity due to interference. Therefore, in this chapter, we aim to exploit channel reuse to maximize the minimal

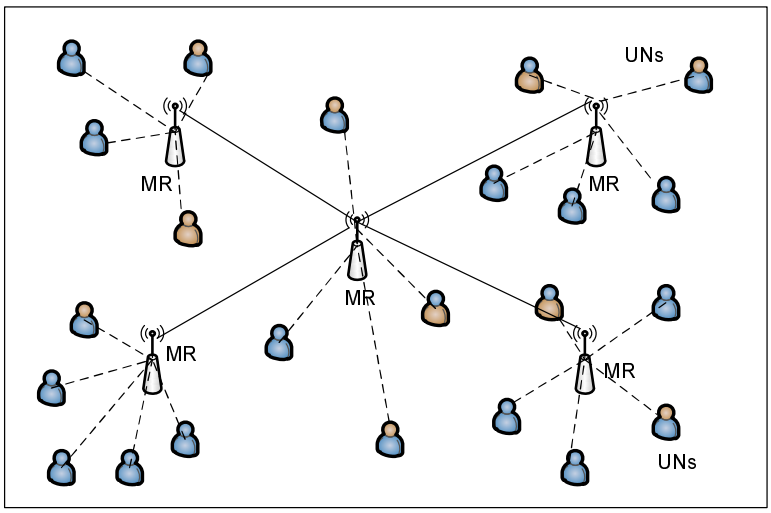

Figure 3.1: Reference architecture for a two-tiered wireless mesh network. The dashed line represents the link connection between network UNs and MRs. The solid line represents the links between MRs.

capacity of all assigned links.

Jointly studying power control on physical layer and channel assignment on MAC layer falls into cross-layer design problems. It would be natural to consider the power control parameter as a continuous variable and the channel assignment parameter as a binary integer variable. As a result, the fairness problem formulation falls into mixed integer non-linear programming (MINLP), which is NP-hard in general. Thus we resort to approximating the problem by setting the power control parameter as a discrete variable, e.g. a finite number of equally-spaced power levels. Subsequently, we put forward a heuristic approach: Binary Integer Programming-based Algorithm with fairness constraint (BIPA) to achieve suboptimal result when the power of MRs can only be set as discrete variables. In particular, the channel assignment and power control results are updated via solving a binary integer programming problem at each iteration when the fairness constraints are set tighter. In order to measure the quality of the suboptimal results obtained by BIPA, we develop an upper bound of the fairness objective by relaxing the integer variables and linearization. Simulation

results show that the results obtained by BIPA are very close to the upper bound, thus suggest that (1) the upper bound is very tight; and (2) the solution obtained by BIPA is near-optimal.

The rest of this chapter is organized as follows. In Section 3.1, we describe the network and interference model. In Section 3.2, we formulate the channel assignment and power control problem to maximize the minimal capacity of all assigned links. In Section 3.3, we propose BIPA as the heuristic approach followed by the method to obtain the upper bound solution presented in Section 3.4. In Section 3.5, simulation results are presented to compare the solutions obtained by BIPA and the upper bound. Section 3.6 concludes this chapter.

3.1 Network Modelling

In this section, we present an example of cross-layer optimization problem for a wireless mesh network. We first address some technical aspects of this mesh network in terms of network architecture, path loss model as well as interference model. Then we set out to formulate the cross-layer optimization problem. We list the notation in this chapter in Table 3.1.

3.1.1 Network architecture

We focus on a two-tiered wireless mesh networks. There are two types of nodes in a mesh network: UNs and MRs. All nodes are placed at fixed locations. Each UN can connect to only one MR by establishing a channel with an adjustable transmit power. Since the mesh network uses OFDM for multiple access, we assume each MR can support the same limited number of channels. As for typical mesh network, the downlink data traffic is much more than uplink data traffic, thus we only consider

Table 3.1: Notation of capacity fairness of wireless mesh networks

Symbol	*Definitions*
d_0	An amount of distance.
d_1	An amount of distance.
P_0	Signal power measured at d_0 meters from transmitter.
P_1	Signal power measured at d_1 meters from transmitter.
P_t	General transmit power.
G_t	Transmitter antenna gain.
G_r	Receiver antenna gain.
λ	Wavelength of the transmitted signal.
c	Velocity of radio-wave propagation in free space.
P_r	General received power.
P_{noise}	Noise Power.
A	General Capacity of a channel.
W	Bandwidth of the channel.
d	Distance between the transmitter and receiver.
N	Number of UNs.
M	Number of MRs.
$\mathcal{U}$	Set of UNs.
$\mathcal{R}$	Set of MRs.
u_i	The ith UN.
r_i	The ith MR.
P_{max}	Maximum transmit power.
Q	Number of power levels.
l	Index of a power level
Pr_{ij}^{lk}	Received power at u_j when the transmitter power of r_i is set as $\frac{l}{Q}P_{max}$ on channel k
t_I	Interference threshold.
t_R	Receiving threshold.
$\mathcal{A}$	Channel capacity matrix A.
Pr_{ij}	Power of the received signal at u_j from r_i .
ρ_{ij}^{lk}	Binary assignment variable indicating the assignment of the kth channel of r_i to u_j at the transmit power of $\frac{l}{Q}P_{max}(1 \leq l \leq Q)$
ζ	Minimum capacity of all assigned links
τ	Obtained second smallest capacity of all assigned links.
$\mathcal{X}$	A general set of continuous variables.
x_i	A general variable within the set $\mathcal{X}$.
σ	Optimal max-min value of $\mathcal{X}$.
η	Summation of all variables $\mathcal{X}$.
n	Number of variables in $\mathcal{X}$.
μ	Value of variables in $\mathcal{X}$, when $x_1 = x_2 = ... = x_n$.

the downlink case. It is also assumed that MRs can connect to each other without distance and interference constraints. At least one of the MRs can access to the backbone network.

3.1.2 Path loss model

The network throughput depends heavily on the packet reception rate, which can be modelled using path loss channel model in physical layer. In this chapter, the following path loss model (3.1) is being used.

$$P_0 d_0^{\alpha} = P_1 d_1^{\alpha} \tag{3.1}$$

P_0 and P_1 are the signal power measured at d_0 and d_1 meters away from the transmitter, respectively. α denotes the path loss exponent. If we set d_0 to be 1 meter, thus P_0 is the reference signal power measured at 1 meter away from the transmitter. Then (3.1) is simplified as $P_1 = \frac{P_0}{d_1^{\alpha}}$. P_0 can be calculated using the free space propagation model [8] as (3.2).

$$P_0 = P_t G_t G_r (\tfrac{\lambda}{4\pi})^2 \tag{3.2}$$

P_t is the transmit power. G_t and G_r are the transmitter and receiver antenna gains respectively. $\lambda = c/f$ is the wavelength of the transmitted signal. c is the velocity of radio-wave propagation in free space, which is equal to the speed of light. Then the received power P_r at a distance d meters away from the transmitter can be calculated as (3.3).

$$P_r = \frac{P_t G_t G_r (\frac{\lambda}{4\pi})^2}{d^{\alpha}} \tag{3.3}$$

Let P_{noise} denote the noise power, then the signal-to-noise ratio (SNR) at the

receiver end as (3.4).

$$SNR = \frac{P_r}{P_{noise}} \tag{3.4}$$

Based on Shannon formula [71], the capacity of the channel of a link can be expressed as (3.5).

$$A = W \times log_2(1 + \frac{P_t G_t G_r (\lambda/4\pi)^2}{d^\alpha P_{noise}}) \tag{3.5}$$

where A denotes the capacity of the channel, W denotes the bandwidth of the channel, d denotes the distance between the transmitter and receiver of the link.

3.2 Problem Formulation

First of all, we need to provide some notation. Let the number of UNs be N, the number of MRs be M and the number of OFDM channels be C. Denote the set of UNs as $\mathcal{U} = \{u_1, u_2, ..., u_N\}$, the set of MRs as $\mathcal{R} = \{r_1, r_2, ..., r_M\}$. Denote the maximum transmit power as P_{max}. We then introduce an integer parameter Q that represents the total number of power levels to which a transmitter can be adjusted, i.e. $\frac{1}{Q}P_{max}, \frac{2}{Q}P_{max}, ..., P_{max}$. If the transmitter power of r_i is set as $\frac{l}{Q}P_{max}(1 \leq l \leq Q)$ on channel k, the received power at u_j is denoted as Pr_{ij}^{lk}. Secondly, receiving constraint is considered regarding a successful transmission. Suppose there is a transmission from r_i to u_j, then the received power at u_j should be no less than the receiving constraint, denoted as t_R. Then we can define a channel capacity matrix $\mathcal{A}$ as (3.6).

$$\mathcal{A}_{ij}^{lk} = \begin{cases} W \times log_2(1 + \frac{Pr_{ij}^{lk}}{P_{noise}}) & : \quad if \;\; Pr_{ij}^{lk} \geq t_R; \\ 0 & : \quad otherwise; \end{cases} \tag{3.6}$$

Let us denote the ρ_{ij}^{lk} as the binary assignment variable with $\rho_{ij}^{lk} = 1$ indicating the assignment of the kth channel of r_i to u_j at the transmit power of $\frac{l}{Q}P_{max}$; $\rho_{ij}^{lk} = 0$ means the kth channel at power level l is not assigned between r_i and u_j. Then we consider constraint on interference. Suppose there is a transmission from r_i to u_j on the kth channel, then there is a limitation on the transmission powers of all other concurrent transmissions on the same channel. Specifically, we consider the interference power on u_j due to all other concurrent transmissions on the same channel is negligible if the overall received interference power is less than a threshold t_I ($t_I \leq t_R$), as shown by (3.7).

$$\sum_{a=1}^{M}\sum_{b=1}^{N}\sum_{l=1}^{Q}\rho_{ab}^{lk} \times Pr_{aj}^{lk} \leq t_I \tag{3.7}$$

Note that (3.7) only holds when u_j receive signals on the kth channel. Therefore, it is necessary to develop (3.7) into a more general form as shown in (3.8).

$$\sum_{a=1}^{M}\sum_{b=1}^{N}\sum_{l=1}^{Q}\rho_{ab}^{lk} \times Pr_{aj}^{lk} + (\epsilon - t_I) \times \sum_{i=1}^{M}\sum_{l=1}^{Q}\rho_{ij}^{lk} \leq \epsilon \tag{3.8}$$

where ϵ is a large value such that $\forall\ j\ (1 \leq j \leq N)$, $\sum_{a=1}^{M}\sum_{b=1}^{N}\sum_{l=1}^{Q}\rho_{ab}^{lk} \times Pr_{aj}^{lk} \leq \epsilon$ always holds. In (3.8), the term $\sum_{i=1}^{M}\sum_{l=1}^{Q}\rho_{ij}^{lk}$ accurately indicates if u_j is working on the jth channel.

Using the channel capacity matrix (3.6) and the interference constraint as (3.8), our fairness problem can be formulated as (3.9).

Fairness Problem :(Optimal channel assignment and power control problem)

$$
\begin{aligned}
&\textit{maximize} \quad \zeta \\
&s.t. \quad \rho_{ij}^{lk} \in \{0,1\} \\
&\quad \textstyle\sum_{i=1}^{M}\sum_{k=1}^{C}\sum_{l=1}^{Q}\rho_{ij}^{lk} = 1 \\
&\quad \textstyle\sum_{a=1}^{M}\sum_{b=1}^{N}\sum_{l=1}^{Q}\rho_{ab}^{lk} \times Pr_{aj}^{lk} + (\epsilon - t_I) \times \sum_{i=1}^{M}\sum_{l=1}^{Q}\rho_{ij}^{lk} \leq \epsilon \\
&\quad \textstyle\sum_{i=1}^{M}\sum_{k=1}^{C}\sum_{l=1}^{Q}\rho_{ij}^{lk} \times \mathcal{A}_{ij}^{lk} \geq \zeta \\
&\quad \forall r_i, u_j, 1 \leq k \leq C, 1 \leq l \leq Q
\end{aligned}
\tag{3.9}
$$

The objective our optimization problem is to maximize the minimal capacity of all assigned links, which is denoted as ζ in (6.2). The second constraint is to guarantee that each UN can only be assigned to one channel linked to an MR. The third constraint is to ensure each transmission is interference free from other transmissions on the same channel, as the interference constraint (3.8).

3.3 BIPA: Binary Integer Programming based Algorithm with Fairness Constraint

We now take a closer look at the fairness problem as formulated in (3.9) in Section 3.2. Observe that the objective is not a linear function of the set of variables ρ_{ij}^{lk}, which obstructs many classic algorithms from being applicable. In other words, the key obstacle in solving this fairness problem lies in the transformation of the objective function, while still maintaining the motive of the $max - min$ problem: the minimal capacity of all assigned links are maximized. To this end, it comes down very naturally that the sum of the capacity of all assigned links could be recognized as the simplest linear function. Based on the foregoing discussion, the newly generated problem is described as (3.10).

suboptimal fairness problem:

$$
\begin{aligned}
max \quad & \textstyle\sum_{j=1}^{N}\sum_{i=1}^{M}\sum_{k=1}^{C}\sum_{l=1}^{Q}\rho_{ij}^{lk}\times\mathcal{A}_{ij}^{lk} \\
s.t. \quad & \rho_{ij}^{lk}\in\{0,1\} \\
& \textstyle\sum_{i=1}^{M}\sum_{k=1}^{C}\sum_{l=1}^{Q}\rho_{ij}^{lk}=1 \\
& \textstyle\sum_{a=1}^{M}\sum_{b=1}^{N}\sum_{l=1}^{Q}\rho_{ab}^{lk}\times Pr_{aj}^{lk}+(\epsilon-t_I)\times\sum_{i=1}^{M}\sum_{l=1}^{Q}\rho_{ij}^{lk}\leq\epsilon \\
& \textstyle\sum_{i=1}^{M}\sum_{k=1}^{C}\sum_{l=1}^{Q}\rho_{ij}^{lk}\times\mathcal{A}_{ij}^{lk}\geq\zeta \\
& \forall r_i,u_j,1\leq k\leq C,1\leq l\leq Q
\end{aligned}
\tag{3.10}
$$

In (3.10), the second constraint is to guarantee that each UN can only be assigned to one channel with one MR. The third constraint is to ensure each transmission is interference free from other transmissions on the same channel, as the interference constraint (8). We notice that the fourth constraint demands that each of the assigned links have a capacity larger than ζ. It is obvious that if ζ is set the same as the maximized value of the minimal capacity of all assigned links, the optimal solution of the fairness problem can be yielded. Naturally, the key to obtain the optimal result to the fairness problem resides in adjusting the value of ζ. The value of ζ is very subtle to the extent that the suboptimal fairness problem would be infeasible with very high value of ζ while we would end up obtaining a solution that is far from the optimal when ζ is set too low. Then the intuition would be to reach the maximal value of ζ such that the suboptimal fairness problem is feasible. It would seem quite straightforward to update the value of ζ after each iteration with the minimal value of all assigned links. However, a closer examination would repel this idea due to the fact that the updated constraint would not alter the results in following iterations since the current solution is already optimized. But since possibilities still remain that the minimal capacity could be increased if the constraint is set tighter, we choose to take the risk that the suboptimal fairness

problem be infeasible by updating ζ with the second smallest capacity of all assigned links yielded by the previous iteration. Since transmit power on all assigned links has been maximized (otherwise there is still space for the summation of all assigned links to increase, which violates the objective of the suboptimal fairness problem), it would also be justifiable to point out that setting ζ as the second smallest capacity could break the current assignment: eliminating the link with smallest capacity and assigning that corresponding UN a "better" link. Since the cases that the two smallest capacities are equal are very rare due to different distances among all UN-MR pairs, this iterative procedure terminates as soon as it can not reach a feasible problem.

We also need to justify the validity of the transformation of the objective function from maximizing the minimal capacity to maximizing the summation of the capacity of all assigned links. Given a value of ζ, the objective of the suboptimal fairness problem should help produce solutions with higher minimal capacity of all assigned links. Based on this consideration, the objective of maximizing the summation of capacity on all assigned links has the following two merits: 1) it is the most simplified form of linear functions; 2) it pushes the minimal capacity of all assigned links higher.

To solve the suboptimal fairness problem, we use a linear programming (LP)-based branch-and-bound algorithm [83]. The algorithm creates a search tree by repeatedly adding constraints to the problem, called Branching. At a branching step, the algorithm chooses a variable x_j whose current value is not an integer and adds the constraint $x_j = 0$ to form one branch and the constraint $x_j = 1$ to form the other branch. This process can be represented by a binary tree, in which the nodes represent the added constraints. At each node, the algorithm solves the LP-relaxation problem using the constraints at that node and decides whether to

branch or to move to another node depending on the outcome. There are three possibilities: (1) If the LP relaxation problem at the current node is infeasible or its optimal value is greater than that of the best integer point, the algorithm removes the node from the tree, after which it does not search any branches below that node. The algorithm then moves to a new node according to the pre-specified method. (2) If the algorithm finds a new feasible integer point with lower objective value than that of the best integer point, it updates the current best integer point and moves to the next node. (3) If the LP-relaxation problem's optimal value is not an integer and the optimal objective value of the LP relaxation problem is less than the best integer point, the algorithm branches below this node.

From the foregoing, we propose BIPA algorithm as the following.

- step 1: Set $\zeta = 0$;
- step 2: Solve the suboptimal fairness problem as (3.10);
- step 3: Obtain the second smallest value τ of all assigned links based on the channel assignment solution obtained from step 2;
- step 4: Update ζ with τ, repeat step 2 and 3 until no feasible solution exists.

3.4 Upper Bound

In Section 3.3, we propose a heuristic approach to aggressively approximate the maximized minimal value by iteratively tightening the constraint that the capacity of each link is larger than a threshold value ζ. In this section, we develop an upper bound for the objective function. First of all, we claim Theorem 1 and give the proof subsequently.

Theorem 1 **(Equivalent Conditions for Max-min Objective)**: Given a set of continuous variables $\mathcal{X} = \{x_1, x_2, ..., x_n\}$, $max - min\ \mathcal{X}$ is achieved iff

- $\sum \mathcal{X}$ is maximized;
- $x_1 = x_2 = ... = x_n$.

Proof : Suppose $x_i = \sigma$ denotes the optimal max-min value. Since $x_j \geq x_i$ ($\forall\ j \neq i$), then we can reduce the value of x_j ($j \neq i$) to the point that $x_1 = x_2 = ... = x_n$. Because max-min value σ can not be increased with respect to the set $\mathcal{X}$, then $\sum \mathcal{X} = n \times \sigma$ is maximized. Thus the necessary condition is validated.

We will validate the sufficient condition based on contradiction. Assume $\sum \mathcal{X} = \eta$ is maximized, $x_1 = x_2 = ... = x_n$, and the optimal max-min value $\mu \geq \frac{\sum \mathcal{X}}{n}$. Then we can set $x_1 = x_2 = ... = x_n = \mu$, obviously $n \times \mu \geq \eta$, which violates the assumption that $\sum \mathcal{X}$ is maximized. Therefore the sufficient condition is proved to be true. $\square$

$$
\begin{aligned}
& max\ \textstyle\sum_{i=1}^{M}\sum_{j=1}^{N}\sum_{k=1}^{C}\sum_{l=1}^{Q}\rho_{ij}^{lk}\times\mathcal{A}_{ij}^{lk} \\
& s.t.\quad \rho_{ij}^{lk}\in[0,1] \\
& \quad \textstyle\sum_{i=1}^{M}\sum_{k=1}^{C}\sum_{l=1}^{Q}\rho_{ij}^{lk}=1 \\
& \quad \textstyle\sum_{a=1}^{M}\sum_{b=1}^{N}\sum_{l=1}^{Q}\rho_{ab}^{lk}\times Pr_{aj}^{lk}+(\epsilon-t_I)\times\sum_{i=1}^{M}\sum_{l=1}^{Q}\rho_{ij}^{lk}\leq\epsilon \\
& \quad \textstyle\sum_{i=1}^{M}\sum_{k=1}^{C}\sum_{l=1}^{Q}\rho_{i1}^{lk}\times\mathcal{A}_{i1}^{lk} \\
& \quad =\textstyle\sum_{i=1}^{M}\sum_{k=1}^{C}\sum_{l=1}^{Q}\rho_{i2}^{lk}\times\mathcal{A}_{i2}^{lk} \\
& \quad =... \\
& \quad =\textstyle\sum_{i=1}^{M}\sum_{k=1}^{C}\sum_{l=1}^{Q}\rho_{iN}^{lk}\times\mathcal{A}_{iN}^{lk} \\
& \quad \forall r_i, u_j, 1\leq k\leq C, 1\leq l\leq Q
\end{aligned}
\tag{3.11}
$$

Inspired by Theorem 1, we figure out that the optimal max-min capacity of all

assigned links can be achieved iff the overall network capacity is maximized and all assigned links have the same capacity. Now we reexamine the fairness problem in (3.9). Since the capacity values are discrete due to a finite number of power levels, it is hardly possible to reach a point that the same capacity is achieved on all links with different distances of MR-UN pairs. To render the capacity values continuous, we can relax the binary integer requirement on ρ_{ij}^{lk} by setting $0 \leq \rho_{ij}^{lk} \leq 1$. In this way, we can pursue an upper bound for the objective when the throughput of each assigned link is equal to each other. Such relaxation enables us to formulate the $max - min$ problem as (3.11).

In (3.11), the second constraint is to guarantee that each UN can only be assigned to one channel with one MR. The third constraint is to ensure each transmission is interference free from other transmissions on the same channel. The fourth constraint demands the capacity values of all links are the same. This new (relaxed) formulation falls into a standard linear programming (LP) problem. We can obtain the solution in polynomial time. Due to the relaxation, the solution to this LP problem corresponds to an upper bound to the objective of the original problem in (3.9). There may not exist a feasible solution to achieve this upper bound. Nevertheless, this upper bound offers a benchmark to measure the quality of the feasible solution obtained from BIPA proposed in Section 3.3.

3.5 Simulation Results

In this section, we present simulation results on max-min capacity values yielded by BIPA and the corresponding upper bound. In particular, we compare the fairness performance yielded by BIPA and the upper bound by proposing a new evaluation metric named **performance ratio**. We produce performance ratios under different

parameter sets to investigate the impact of different factors on the fairness performance, such as the number of channels, the number of power levels and the interference threshold.

3.5.1 Simulation Setup

A set of UNs are randomly distributed in a square region ($\{(x, y)|0 \leq x \leq 100, 0 \leq y \leq 100\}$, (x, y) denotes the Cartesian coordinate of a point). Totally 4 MRs are placed within the area at coordinates (25 25),(25 75),(75 75), (75 25) respectively. The bandwidth of each channel is set as 1 MHz. The transmitter and receiver antenna gains are both set as 100. The path loss exponent $\alpha = 2$. The wavelength λ is set as $\frac{3\times10^8}{2.4\times10^9}$ meters, which corresponds to the center frequency of 2.4GHz. The noise power is set as 1×10^{-6} watt. For each set of system parameters, we generate 20 instances of the network scenarios with randomly distributed UNs to obtain the average performance.

Intuitively, the following parameters may have significant impact on system performance: the number of users (N), the total number of channels (C), the number of power levels (Q) and the interference threshold (t_I). To obtain extensive results, we vary the values of three parameters: Q, C and t_I. To construct different network topologies, we randomly place 10 UNs in the given region at the first trial and 15 UNs at the second trial.

3.5.2 Evaluation Metric

To evaluate the performance of BIPA, we propose a metric named as performance ratio, as the main evaluation measure for the simulation results. The performance ratio is defined as the ratio of the suboptimal solution yielded by BIPA to the upper bound. As the suboptimal solution is always less than the upper bound, BIPA yields

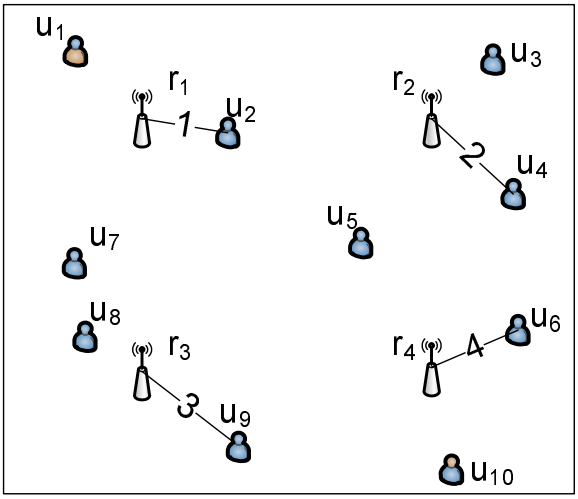

Figure 3.2: An example showing channel assignment with respect to our simulation scenario without power control. The number on the line between a UN-MR pair shows the index of channel assigned for the link.

better solutions when performance ratios are closer to 1.

3.5.3 Impact of Power Control

Power control exerts a pivotal influence on results of channel assignment for a wireless mesh network. In Fig. 3.2 and 3.3, we show an example of channel assignment with respect to our simulation area. From Fig. 3.2, it can be seen that to avoid interference, only four UNs can be assigned channels. Any other assigned channel would be seriously interfered by one of the four channels as all the MRs are transmitting signal at their maximum power. In contrast, Fig. 3.3 shows that all UNs can be assigned channels when power control can be realized at MRs. This is due to the fact each MR can automatically adjust its transmit power to avoid causing interference to other transmissions, and thus channels can be assigned at each MR to accommodate a lot more UNs.

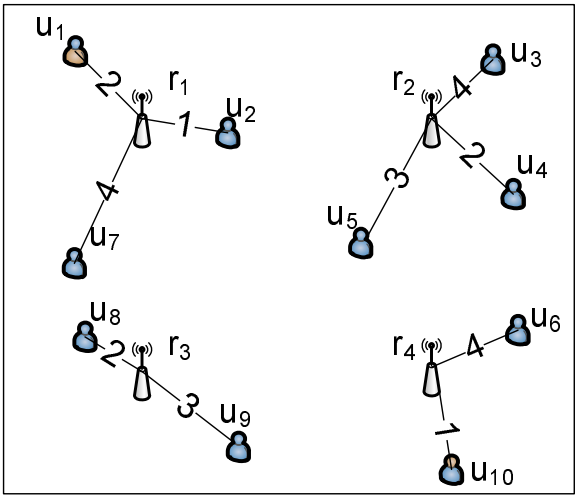

Figure 3.3: An example showing channel assignment with respect to our simulation scenario with power control. The number on the line between a UN-MR pair shows the index of channel assigned for the link.

3.5.4 Impact of Number of Channels

In this subsection, we evaluate the impact of number of channels on the performance ratios in 10-UN and 15-UN network scenarios. The performance ratios are calculated using the minimal capacity yielded by BIPA and the upper bound computed from (3.11).

First of all, it can be seen from Fig. 3.4 that most performance ratios are very close to 1, which shows that the gap between solutions yielded by BIPA and the upper bound is very narrow. In addition, since the unknown optimal solution is between the solution obtained by BIPA algorithm and the upper bound, the upper bound is very tight, and BIPA yields near-optimal solutions.

Secondly, from Fig. 3.4, it is obvious that as we enlarge C from 5 to 9 regarding the same 20 10-UN scenarios, the points of performance ratios are positioned higher and the majority of the points are equal to 1 when $C = 9$. The reason is that with more channels, the interference constraint would be less tight and some MRs can increase its transmit power on certain channels. Thus the UN associated with

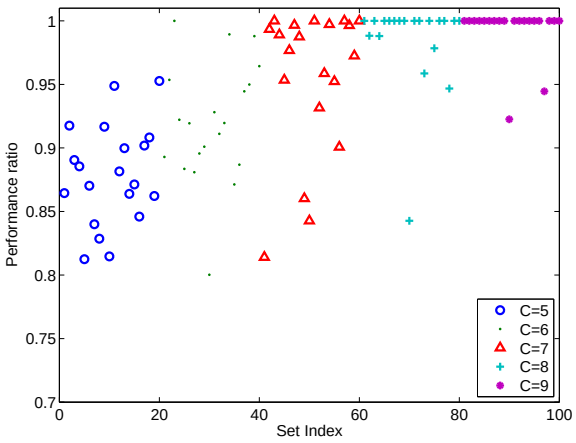

Figure 3.4: Performance ratios when C changes for 10-UN scnenario. $P_{max} = 5$ watt. $t_R = 10^{-3}$ watt. $Q = 10$. $t_I = 4 \times 10^{-4}$ watt.

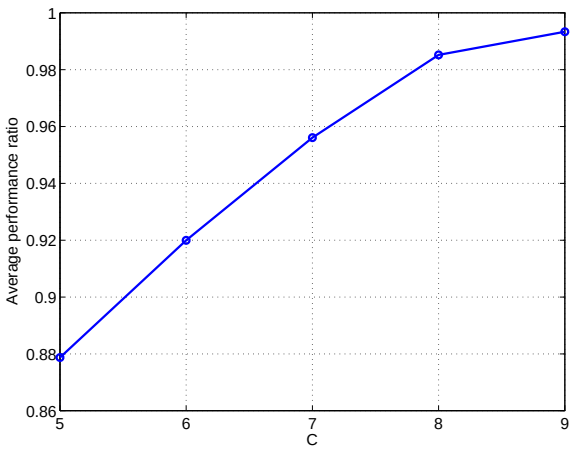

Figure 3.5: Average performance ratios when C changes for 10-UN scenario. $P_{max} = 5$ watt. $t_R = 10^{-3}$ watt. $Q = 10$. $t_I = 4 \times 10^{-4}$ watt.

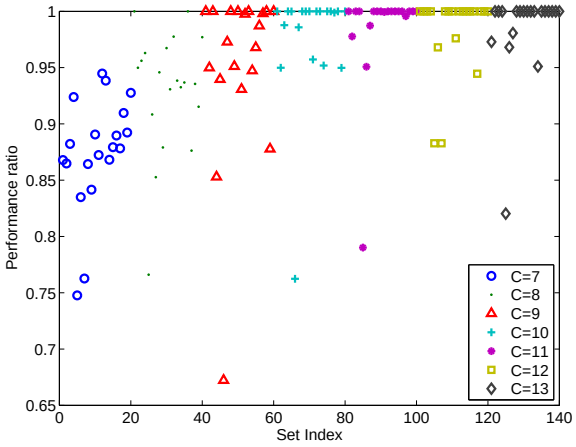

Figure 3.6: Performance ratios when C changes for 15-UN scenario. $P_{max} = 2.5$ watt. $t_R = 10^{-3}$ watt. $Q = 3$. $t_I = 4 \times 10^{-4}$ watt.

the minimal capacity link would have the chance to be assigned a link with higher capacity.

Accordingly, the same phenomenon is witnessed in Fig. 3.5 where each point represents the average value of the performance ratios of the 20 10-UN scenarios corresponding with the same parameter set.

In addition, for 15-UN network scenarios, similar trend can be witnessed as C is increased from 7 to 13 in Fig. 3.6 and Fig. 3.7.

3.5.5 Impact of Number of Power levels

In this subsection, we evaluate the impact of number of power levels on the performance ratios in 10-UN and 15-UN network scenarios. The performance ratios are calculated using the minimal capacity yielded by BIPA and the upper bound computed from (3.11).

First of all, it can be seen from Fig. 3.8 and Fig. 3.9 that most performance ratios are near 1, which shows that solutions yielded by BIPA is close to the upper bound. Therefore BIPA yields near-optimal solutions. Secondly, from Fig. 3.8, the

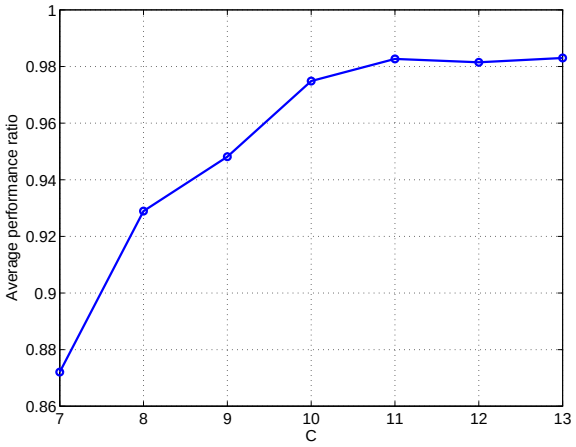

Figure 3.7: Average performance ratios when C changes. $P_{max} = 2.5$ watt. $t_R = 10^{-3}$ watt. $Q = 3$. $t_I = 4 \times 10^{-4}$ watt.

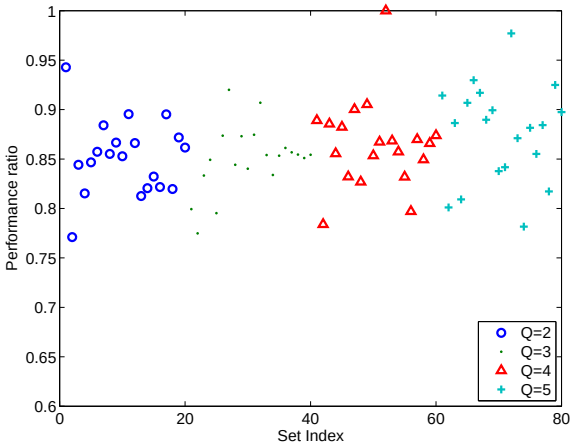

Figure 3.8: Performance ratios when Q changes for 10-UN scenario. $P_{max} = 5$ watt. $t_R = 10^{-3}$ watt. $C = 5$. $Q = 10$.

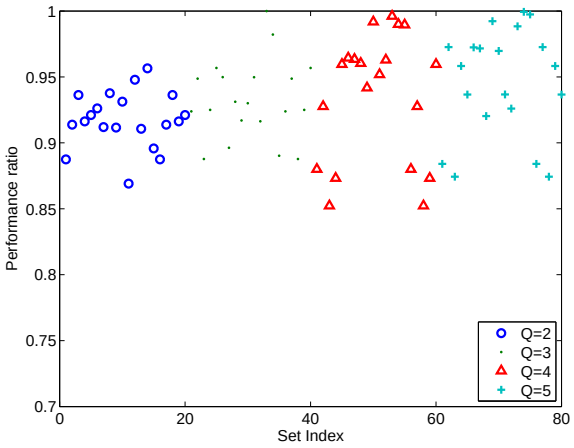

Figure 3.9: Performance ratios when Q changes for 15-UN scenario. $P_{max} = 2.5$ watt. $t_R = 10^{-3}$ watt. $C = 7$. $t_I = 4 \times 10^{-4}$ watt.

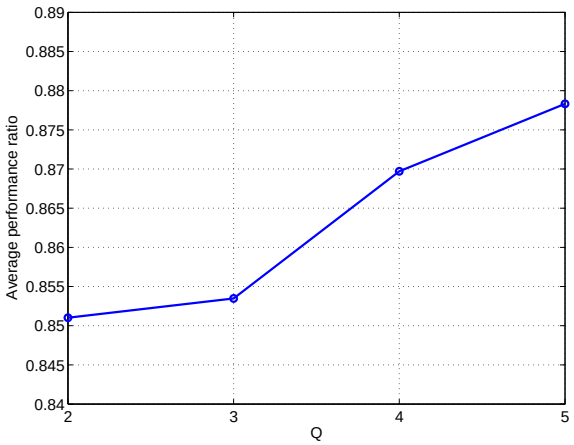

Figure 3.10: Average performance ratios when Q changes for 10-UN scenario. $P_{max} = 5$ watt. $t_R = 10^{-3}$ watt. $C = 5$. $t_I = 4 \times 10^{-4}$ watt.

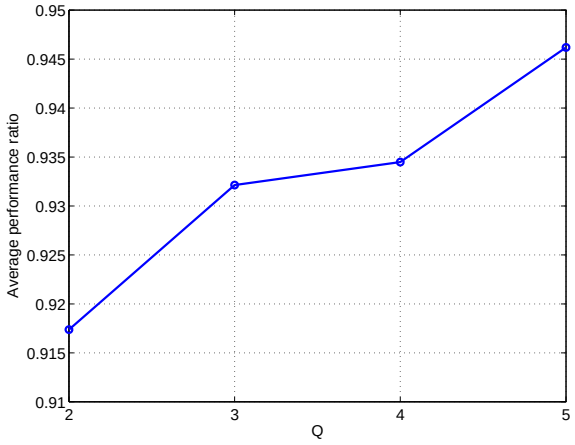

Figure 3.11: Average performance ratios when Q changes for 15-UN scenario.$P_{max} = 2.5$ watt. $t_R = 10^{-3}$ watt. $C = 7$. $t_I = 4 \times 10^{-4}$ watt.

points of performance ratios do not get obvious higher positions as Q is increased from 2 to 5.

However, as we can see from Fig. 3.10, the average value of each set of 20 performance ratios does increase when Q is larger. This is because the larger number of power levels increases the tunability of the power control, and as a result, the fairness performance gets closer to the optimal.

Again, for 15-UN network scenarios, although obvious performance enhancement can not be easily observed in Fig.3.9, the change in average performance ratios in Fig. 3.11 does suggest that the increase of power levels works in the fairness performance's favor. However, it should also be noted that the fairness performance can not be increased dramatically by more power levels. Due to the exponentially increased complexity induced by larger Q, it would not be recommended to pursue better fairness performance by rendering Q a large number.

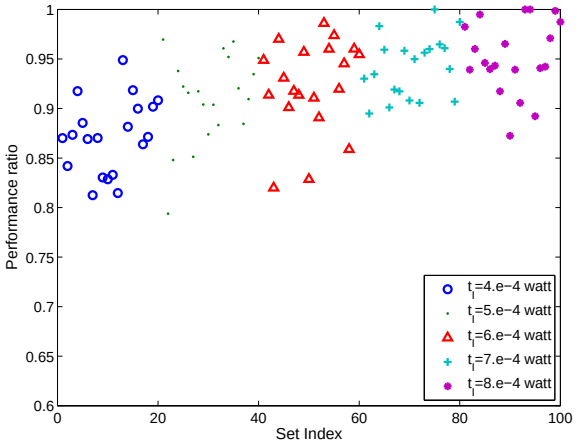

Figure 3.12: Performance ratios when t_I changes for 10-UN scenario. $P_{max} = 5$ watt. $t_R = 10^{-3}$ watt. $C = 5$. $Q = 10$.

3.5.6 Impact of Interference Threshold

In this subsection, we evaluate the impact of interference threshold on the performance ratios in 10-UN and 15-UN network scenarios. The performance ratios are calculated using the minimal capacity yielded by BIPA and the upper bound computed from (3.11).

It can be seen from Fig. 3.12 and Fig. 3.13 that most performance ratios are very close to 1, which shows that the solutions yielded by BIPA is very close to the upper bound, and thus near the unknown optimal solution. It can also be implied that the upper bound is very tight. As can be seen from Fig. 3.12 and Fig. 3.14, the max-min performance is enhanced as t_I grows from $4 \times 10^{-4} watt$ to $8 \times 10^{-4} watt$. The rationale behind is that when the value of t_I is larger, MRs can transmit at higher power levels without violating the interference constraints, causing the general link capacities to increase. Therefore the minimal capacity is increased accordingly. Similar trend is also witnessed in Fig. 3.13 and Fig. 3.15 for 15-UN scenarios.

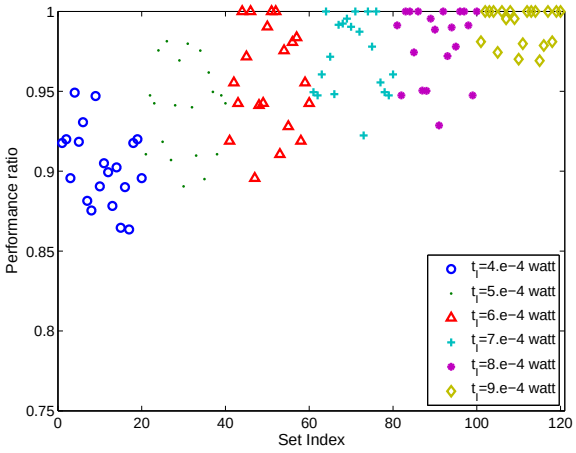

Figure 3.13: Performance ratios when t_I changes for 15-UN scenario. $P_{max} = 2.5$ watt. $t_R = 10^{-3}$ watt. $C = 7$. $Q = 3$.

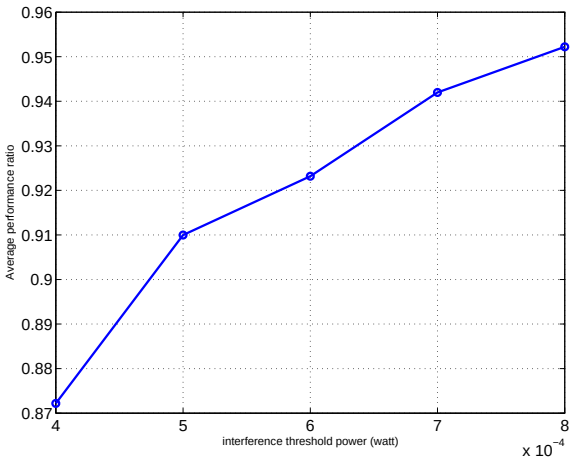

Figure 3.14: Average performance ratios when t_I changes for 10-UN scenario. $P_{max} = 5$ watt. $t_R = 10^{-3}$ watt. $C = 5$. $Q = 10$.

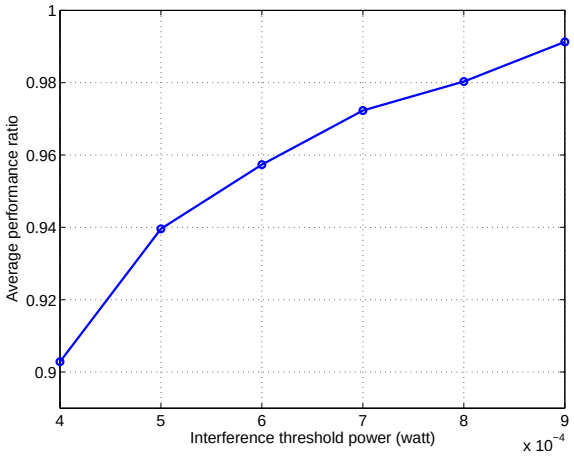

Figure 3.15: Average performance ratios when t_I changes for 15-UN scenario. $P_{max} = 2.5$ watt. $t_R = 10^{-3}$ watt. $C = 7$. $Q = 3$.

3.6 Conclusion

This chapter addresses fairness problem on the throughput of all links for a two-tiered wireless mesh network. The fairness problem is formulated with cross-layer behaviors and constraints, i.e. channel assignment on MAC layer and power control on physical layer. We successfully transform the max-min objective to more solvable linear objective with additional constraints in compromise of optimality. In particular, we propose a heuristic approach BIPA to maximize the minimal capacity of all links by optimally assigning channels as well as setting transmit powers for each link. To measure the quality of solutions yielded by BIPA, we develop an upper bound to estimate the objective function subsequently. Simulation results show that solutionis yielded by BIPA are very close to the upper bound, which suggests that they are near-optimal.

Chapter 4

Dynamic Resource Allocation for Disaster area wireless networks

Public safety organizations increasingly rely on wireless technology to provide effective communications during emergency and disaster response operations. However, any previously installed wireless network infrastructure may be damaged or completely destroyed in a major disaster event, as occurred during Hurricane Katrina, it is necessary to develop wireless networks that can be quickly deployed to build a replacement communication system to connect all first responders. Considering the first responders as mobile nodes (MNs), the communication range of each MN is often limited by its power constraint. Mobile relay nodes (RNs) can be introduced to relay the communications between MNs and the base stations. The RNs installed on wheeled vehicles can be dynamically relocated to places where the first responders are actively working in the field. We term such a dynamic communication system as disaster area wireless networks (DAWN).

When maintaining the functionality of DAWN, understanding the mobility model of the MNs is an important task because the network topology highly depends on the

model used. Traditional assumptions are: MNs are allowed to move over the whole disaster area; MNs are connected to the backbone network all the time. However, such assumptions do not always apply in reality. First of all, the assumption that MNs can choose any destination within the disaster area is not valid. For instance, a firefighter walking across a burning forest would endanger his life. Then, does it always apply that the MNs can connect to the backbone network? Again, the answer would be negative in most occasions because MNs have limited transmission range. As rescue teams move further away from the base station, they risk losing connections with the backbone network.

Connectivity is of the greatest importance to MNs in DAWN. The frequent lost connection to the backbone network could decrease disaster relief efficiency, disorder rescue efforts and even jeopardize first responders' lives. As we can picture, first responders can not start their work deep within the disaster area, but at certain places on the boundary and then proceed into the diaster area. As the transmission range for MNs is often small, to facilitate their communication to the outside of the disaster area, we ought to place RNs near the MNs to establish the wireless network. Note that at different periods, when the locations of first responders are different, a new network topology is formed with different placement of RNs. To justify this assumption, we can exemplify the movable RNs as vehicles with powerful antennas or even satellites, with very long transmission range that communications between RNs are absolutely positive.

In this chapter, we mainly fulfill two tasks: (1) proposing a novel and practical mobility model for MNs in disaster area; (2) placing minimum number of RNs such that the each MN following the mobility model can connect to the backbone network. Then we need to place a number of mobile RNs, such that each of the target squares can be fully covered by at least one RN under limited transmission

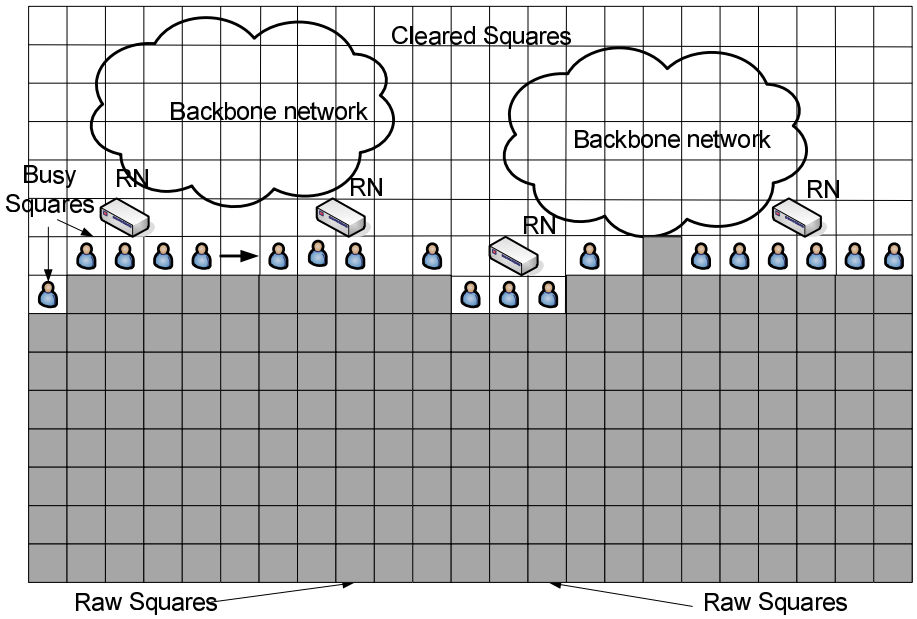

Figure 4.1: A realistic scenario of DAWN in the middle of the disaster area relief process. The squares with head portraits denote busy squares. White squares denote cleared squares. Shaded squares denote raw squares. The MNs are mainly heading downward.

range, which is called as Square Disk Cover (SDC) problem. We bring forward three algorithms in this chapter, the Two-Vertex Square Covering (TVSC) algorithm, the Circle Covering algorithm and the Binary Integer Programming (BIP) algorithm. An example of DAWN is described in Fig.4.1.

The rest of this chapter is organized as follows. In Section 4.1, we describe the mobility model of MNs. Section 4.2 formulates the SDC problem, followed by the algorithms presented in Section 4.3. Complexity analysis and simulation results are given in Sections 4.4 and 4.5 respectively. Finally Section 4.6 concludes this chapter.

4.1 The Disaster Area Mobility Model

In this section, we first describe the characteristics of movements in a large disaster area. Secondly, we propose the disaster area mobility model which represents these

characteristics. The notation utilized in this section are provided as follows. t denotes the time counter that records the current time; $\mathcal{CI}_t$ denotes the CI values of squares within the disaster area at time t; $\mathcal{MN}_t$ denotes the distribution of MNs over the disaster area at time t; $\triangle$ denotes the change of MNs over the disaster area at the next time unit; $s_{i,j}$ denotes the square of the ith row and jth column; $MN_{i,j,t}$ denotes the number of MNs in $s_{i,j}$ at time t; $CI_{i,j,t}$ denotes the CI value of $s_{i,j}$ at time t; ξ denotes the time needed for one MN to reduce one unit of CI; $MN^d_{i,j,t}$ denotes the number of MNs move downward at time t from $s_{i,j}$; $MN^l_{i,j,t}$ denotes the number of MNs move leftward at time t from $s_{i,j}$; $MN^r_{i,j,t}$ denotes the number of MNs move rightward at time t from $s_{i,j}$; T denotes the time required to clear three adjacent squares. Table 4.1 lists the notation in this chapter.

4.1.1 Movements Within a Large Disaster Area

In catastrophic situations, the users that need reliable communication are civil protection forces, such as troops, fire brigades, rescue teams, etc. Faced with a mission of relieving a large scale disaster area, first responders ought to start from a few squares on the boundary of the disaster area. There are two reasons for not to begin relieving the disaster in the middle of the disaster area. Firstly, it seems unnecessary and practically difficult to build a passage for first responders to move to the middle of the disaster area. Secondly, it is dangerous for first responders to be encompassed by severe unrelieved surroundings, such as fire and toxicant dissemination, etc.

After justifying the initialization of first responders to relieve the disaster area, herein we describe how they proceed exploring the disaster area. We first divide the whole disaster area into small squares, each square with a CI value to show how severe the disaster is in it. The squares that have never been relieved are called raw

Table 4.1: Notation of dynamic resource allocation for disaster area wireless networks

Symbol	*Definitions*
t	Time counter to record the current time
$\mathcal{CI}_t$	CI values of squares within the disaster area at time t;
$\mathcal{MN}_t$	Distribution of MNs over the disaster area at time t
MN_i	The $i$the MN
$\triangle$	Change of MNs over the disaster area at the next time unit;
$s_{i,j}$	Square of the ith row and jth column
$MN_{i,j,t}$	Number of MNs in $s_{i,j}$ at time t
$CI_{i,j,t}$	The CI value of $s_{i,j}$ at time t
ξ	How much CI value one MN can reduce with one unit of time
$MN^d_{i,j,t}$	Number of MNs move downward at time t from $s_{i,j}$
$MN^l_{i,j,t}$	Number of MNs move leftward at time t from $s_{i,j}$
$MN^r_{i,j,t}$	Number of MNs move rightward at time t from $s_{i,j}$
T	Time required to clear three adjacent squares
r	Transmission range of MNs
$V_{i,j}$	Four vertices of the square $s_{i,j}$
$d(a,b)$	Distance between node/point a and b
$e(a,b)$	Edge connecting node/point a and b
RN_i	The ith RN
C_k	Circle centering at RN_k with a radius r
$\mathcal{U}$	Set of all busy squares
G	A polygon
E	Set of all edges of the polygon G
V	Set of all vertices of the polygon G
v_i	The $i$the vertex of the polygon G
C_{v_i,v_j}	Circle with node/point v_i and v_j on its border
CR	Set of all circle regions
N	Number of positions that RNs can be placed
$\mathcal{A}$	Set of all possible positions for placing RNs
$\mathcal{C}$	A position for placing RN(s)
$\mathcal{S}$	A subset of $\mathcal{A}$
$\mathcal{S}_\mathcal{C}$	The set of squares that are covered by the RN placed at $\mathcal{C}$
CR_i	The ith circle region
r_i	The row index of the ith busy square
c_i	The column index of the ith busy square
$\|\mathcal{B}\|$	The cardinality of the set $\mathcal{B}$
x_n	Binary assignment variable indicating whether to select the nth position to place one RN

squares. ξ denotes how much CI value one MN can reduce within one unit of time. Then $\xi MN_{i,j,t}$ denotes how much CI value can be reduced for the square $s_{i,j}$ from time t to $t+1$. However, if the current CI value of the square at time t is less than ξ times the number of MNs in that square at time t, the CI value will be 0 at time $t+1$, as shown in (4.1). Such squares are named as busy squares. Obviously, raw squares and busy squares are uncleared squares. A square is said to be cleared if the CI value is reduced to zero. No first responder in the square will stop working until the square is cleared. When first responders finish clearing one square, they split up and enter the adjacent uncleared squares. Specifically, the larger number of first responders working in the square and less the CI value of the square is, the fewer first responders are entering that square. In this way, from several beginning squares, the first responders can finally clear the whole disaster area as they go deeper and wider.

$$CI_{i,j,t+1} = \begin{cases} CI_{i,j,t} - \xi MN_{i,j,t} & : \quad CI_{i,j,t} > \xi MN_{i,j,t} \\ 0 & : \quad CI_{i,j,t} \leq \xi MN_{i,j,t} \end{cases} \tag{4.1}$$

Now we describe the square-based movement pattern for the MNs, then what about their mobility pattern within each square? As we are unknown about the differences between the situations in each square, we presume first responders are moving according to the Waypoint model[45] for simplicity concerns: each picks up a random destination within the square and then heads for it. The proposition of MNs' random movement within a small square would render this mobility model easily extended to other kinds of disaster area scenarios.

Table 4.2: Mobility Model for MNs

```
1  Divide disaster area into squares;
2  while CI_t ≠ zero /* Uncleared square(s) still exist*/
3  △ ← 0;
4   for each busy square s_{i,j}
5    if CI_{i,j,t} > ξMN_{i,j,t} /* s_{i,j} can not be cleared now*/
6       CI_{i,j,t+1}=CI_{i,j,t}-ξMN_{i,j,t};
7    else
8       △ = Regroup(△, MN_t, s_{i,j}, CI_t);
     /* MN_{i,j,t} split up and enter into neighbors of s_{i,j} */
9       CI_{i,j,t+1}=0;
10   end if
11  end for
12  MN_{t+1} = MN_t + △;
13  t=t+1;
14 end while
```

4.1.2 Mobility Model for First Responders

In Section 4.1.1, we discussed the movements of first responders to relieve a large scale disaster area and provide intuition behind. In this section we formalize the mobility model of MNs as in Table 4.2.

From Table 4.2, the function *Regroup* is adopted to compute how the MNs split up and enter adjacent squares after they clear a square. The procedure of the function *Regroup* goes as follows: First obtain the CI values and number of MNs of the 3 squares adjacent to $s_{i,j}$, which are $CI_{i,(j-1),t}$, $CI_{i,(j+1),t}$, $CI_{i+1,j,t}$ and $MN_{i,j-1,t}$, $MN_{i,j+1,t}$, $MN_{i+1,j,t}$ (without loss of generality, we assume that the MNs enter the disaster area from the top boundary and explore downward, leftward and rightward). The number of MNs moving towards an square plus the number of MNs in that destination square should be in inverse proportion to the CI value of the square, such that the three adjacent neighboring squares can be cleared at the same time, illustrated as (4.2).

$$\frac{CI_{i,j+1,t}}{MN_{i,j+1,t}+MN^r_{i,j,t}} = \frac{CI_{i,j+1,t}}{MN_{i,j-1,t}+MN^l_{i,j,t}} = \frac{CI_{i+1,j,t}}{MN_{i+1,j,t}+MN^d_{i,j,t}} \tag{4.2}$$

In this case, the time required to clear the 3 adjacent squares would be as (4.3).

$$T = \frac{CI_{i,j+1,t}+CI_{i,j-1,t}+CI_{i+1,j,t}}{\xi\times(MN_{i,j+1,t}+MN_{i,j-1,t}+MN_{i+1,j,t}+MN_{i,j,t})} \tag{4.3}$$

Then we compute the change of the number of MNs in these squares after the *Regroup* function is executed at $s_{i,j}$, and add the change into the record matrix $\triangle$.

Note that $MN^r_{t,i,j}+MN^l_{t,i,j}+MN^d_{t,i,j}=MN_{t,i,j}$. However, there are several exceptions when MNs do not move as above:

- *Ignore Zero-CI squares*: When an adjacent square is cleared or is about to be cleared at the next time, the first responders will not enter it after one unit of time.

- *Small CI or Many MNs*: There are already many MNs working in an adjacent square or the CI value of the adjacent square is small, then this square actually lose some MNs based on (4.2). Such a condition would be illustrated as (4.4). (we assume the square considered is the neighbor on the right without loss of generality);

$$\frac{CI_{i,j+1,t}+CI_{i,j-1,t}+CI_{i+1,j,t}}{\xi\times(MN_{i,j+1,t}+MN_{i,j-1,t}+MN_{i+1,j,t}+MN_{i,j,t})} > \frac{CI_{i,j+1,t}}{\xi\times MN_{i,j+1,t}} \tag{4.4}$$

  then only the neighboring squares on the left and beneath are considered in the *Regroup* function.

- *Boundary Case*: When the square that has been just cleared is on the boundary of the diaster area, then the number of adjacent squares would be less

than 3.

4.2 Problem Formulation

We consider a set of MNs moving within the disaster area following the mobility model mentioned above and assume that a set of RNs has to be deployed near MNs to keep all the MNs connected with the backbone network. We assume that all the MNs have small transmission range r, while the transmission range of RNs is large, and RNs can communicate with each other wherever their positions are. The transmission circle of an MN is defined as the boundary of the area of all points having a distance of no larger than r from the MN. An MN MN_i can communicate bi-directionally with an RN RN_j if the distance between them $d(MN_i, RN_j) \leq r$. In other words, the MN MN_i is said to be covered by RN_j if RN_j is within the transmission range of MN_i.

We also assume that the number of RNs is not bounded, which means more RNs will be deployed if required. However, we will try to minimize the number of RNs to be deployed at different time, due to the movement of MNs, causing different distribution of busy squares. At last, it is also assumed that some command center, which controls the placement of RNs, has full knowledge of the distribution of busy squares at each time. We shall define our RN Placement problem within the disaster area as follows.

RN placement problem: Given a set of MNs moving according to the proposed mobility model, place the smallest number of RNs such that:

- At all times, $\forall$ MN MN_i, $\exists$ RN RN_j such that $d(MN_i, RN_j) \leq r$. (Problem SDC);

4.3 Placing RNs for SDC Problem

In this section, we introduced three algorithms, Two-Vertex Square Covering (TVSC) Algorithm, Circle Covering Algorithm and the BIP algorithm, to place minimum number of RNs, such that for every MN MN_i, there exists at least one RN RN_j satisfying $d(MN_i, RN_j) \leq r$. The first two algorithms is based on the greedy strategy[18].

We first provide some notation utilized in this section. We let $V_{i,j}$ denote the set of four vertices of $s_{i,j}$. C_k denotes the circle with center as an RN RN_k and radius r. A spot p is said to be covered by C_k if $d(p, RN_k) \leq r$, denoted as $p \in C_k$. A polygon G is said to be covered by RN_k if $\forall$ one point p within G, $d(p, RN_k) \leq R$, denoted as $G \subset C_k$. Before introducing the algorithms, we first claim $Theorem$ 1 as the primary prerequisite for our algorithms.

$Theorem$ 1 : Assume a polygon $G = (V, E)$, where V and E denote the set of vertices and edges respectively. If $\forall$ vertex $v_i \in V$, $d(v_i, RN_k) \leq r$, then $G \subset C_k$.

$Proof$ First of all, we need to acknowledge the fact that if $d(v_i, RN_k) \leq r$, $d(v_j, RN_k) \leq r$, then $\forall\ p \in e(v_i, v_j)$ ($e(v_i, v_j)$ denotes the edge connecting v_i and v_j), $d(p, RN_k) \leq r$ (It is obviously true since the edge is fully contained in one circle if the two terminals is within the same circle). $\forall\ p \in G$, we have $p \in e(p_1, p_2)$, where $p_1 \in e(v_{m1}, v_{n1})$ and $p_2 \in e(v_{m2}, v_{n2})$. Since $\forall\ v_i \in V$, $d(v_i, RN_k) \leq r$, then $d(p_1, RN_k) \leq r$ and $d(p_2, RN_k) \leq r$. As a result, $d(p, RN_k) \leq r$, and $G \subset C_k$. □

We now claim that the SDC problem is computationally NP-complete. Apparently, the task of deploying the minimum number of RNs to cover the target squares can be decomposed into two steps: Acquiring the set containing all possible positions of RNs; choosing the minimum number of RNs from the set obtained in step 1 to cover the target squares. Step 2 can be more formally restated as: Given a universe

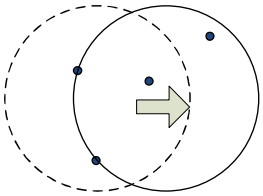

Figure 4.2: Circles with two points on border potentially cover more nodes

$\mathcal{U}$ containing all the squares, a family $\mathcal{S}$ of subsets of $\mathcal{U}$, find a subfamily $\mathcal{C} \subset \mathcal{S}$, such that the union of $\mathcal{C}$ is $\mathcal{U}$ and the cardinality of $\mathcal{C}$ is minimized. The restatement of step 2 is equal to the set covering problem in computer science and complexity theory, which was one of Karp's 21 problems shown to be NP-complete[**?**].

4.3.1 TVSC Algorithm

In this section, we will introduce the TVSC algorithm for the SDC problem. We first give the intuition behind the algorithm. Then we will present the TVSC algorithm in details, followed by the analysis of the algorithm.

Intuition

We first provide the intuition behind the proposed Two-Vertices Square Covering (TVSC) algorithm. Considering that all the MNs are moving randomly within each square, it is impossible to predict the exact position of each MN at specified time. Thus we need to cover all the busy squares using the minimum number of "disks" with a radius of r. According to Theorem 1, if the four vertices of one square are able to connect to the same RN, then all the MNs within that square are able to communicate with that RN. In other words, to guarantee that $s_{i,j} \subset C_k$, we just need to make sure that $V_{i,j}$ are covered by RN_k. Therefore, we disregard $s_{i,j}$ being covered if $V_{i,j}$ can not be covered by one RN RN_k.

Hochbaum and Maass introduced a method of covering a set of nodes with

Table 4.3: TVSC algorithm for SDC problem

TVSC($\mathcal{U}$)
1 $\mathcal{A} \leftarrow \emptyset$;
2 $\mathcal{S} \leftarrow \emptyset$;
3 $\forall v_i \in V_{r_p,c_p}$ and $v_j \in V_{r_q,c_q}$ $1 \leq p, q \leq |\mathcal{U}|$
4 **if** $d(v_i, v_j) \leq 2r$
5 $\mathcal{A} \leftarrow \mathcal{A} \bigcup C_{v_i,v_j}$;
6 **while** $\mathcal{U} \neq \emptyset$
7 do select $\mathcal{C} \in \mathcal{A}$ that maximizes $|\mathcal{S}_\mathcal{C} \bigcap \mathcal{U}|$
8 $\mathcal{U} \leftarrow \mathcal{U} - \mathcal{S}_\mathcal{C}$
9 $\mathcal{S} \leftarrow \mathcal{S} \bigcup \mathcal{C}$
10 **return** $\mathcal{S}$

minimum number of disks[38]. Their method is based on the idea that each disk deployed should have at least two nodes on its border. This intuition is justified by the fact that 2 points on the border can determine the position of a disk (there should be 2 disks determined, one can choose the disk that better serve his interests) given a fixed radius, while having the most probability to cover other nodes. As shown in Fig. 4.2, the circle with dashed line can move right and do not lose any node until two left-most points are on its border, as the circle with the solid line displays. The solid-line circle clearly covers one more node than the dashed line circle does. Inspired by this intuition, we propose the TVSC algorithm below.

Two-Vertex Square Covering Algorithm

The Two-Vertices Squaring Covering (TVSC) algorithm aims to solve the SDC problem through two steps: acquiring the set of all the possible positions for placing RNs $\mathcal{A}$ and choosing a subset $\mathcal{S} \subset \mathcal{A}$ to place RNs such that all the busy squares $\mathcal{U}$ are covered. The TVSC algorithm is presented in Table 4.3. We denote the center of the two circles with radius r and nodes v_i and v_j on its border as C_{v_i,v_j}. $|\mathcal{U}|$ denotes the cardinality of the set $\mathcal{U}$.

The algorithm works as follows. The set $\mathcal{U}$ contains, at each stage, the set of

remaining uncovered busy squares. The set $\mathcal{S}$ contains the already selected positions for placing RNs. Line 7 is the greedy decision-making step. A position $\mathcal{C}$ is chosen as the placement for one RN that covers as many uncovered squares as possible. $\mathcal{U}_\mathcal{C}$ denotes the set of squares that are covered by the RN placed at $\mathcal{C}$. After $\mathcal{C}$ is selected, the corresponding covered squares are removed from $\mathcal{U}$, and $\mathcal{C}$ is added into the subset $\mathcal{S}$. When the algorithm terminates, each of the busy squares is covered by at least one RN.

4.3.2 Circle Covering Algorithm

Intuition

To begin with, we give the intuition behind the proposed Circle Covering algorithm. According to Theorem 1, to cover a square with a disk, one ought to place an RN that is within the transmission range of its four vertices. Then we try to figure out the feasible area to place the RN so that it can cover the target square. As can be seen from Fig. 4.3, such a feasible area of one busy square is demarcated by 4 arcs as part of transmission circles of the four vertices, which approximates to a circle with radius $r - \frac{\sqrt{2}}{2}$ (Let's name it as the feasible circle for one square). There are four approximate regions between the feasible area and the feasible circle. We then approximately use the feasible circle as the area for placing the RN to cover the square for simplicity concern. Therefore, to satisfy the requirement imposed by the SDC problem, it is necessary to deploy at least one RN in the feasible circle of each busy square (Note that there are cases when one RN can be deployed in the overlap parts of feasible circles, then one RN could serve the communications for multiple busy squares). As one can picture, the feasible circles of neighboring squares would intersect, resulting in circle regions demarcated by arcs from several feasible circles

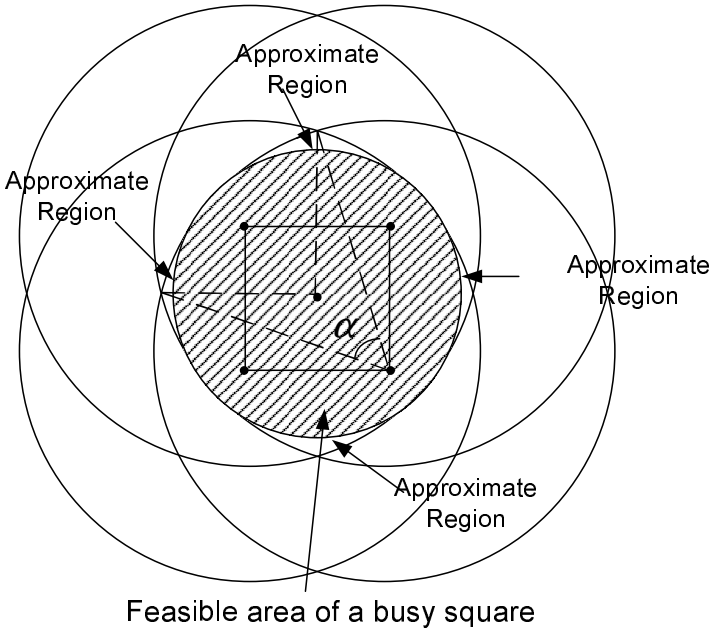

Figure 4.3: The feasible area to place the RN to cover one busy square. The 4 circles demarcate one region around the square, which can be approximated using a circle, shown as the shadow area.

corresponding to different squares. An example is shown in Fig. 4.4. Therefore, the solution for the SDC problem when using the Circle Covering algorithm is a set of such circle regions, each determined by a set of feasible circles.

Table 4.4: Circle Covering algorithm

Circle-Covering($\mathcal{U}$)
1 $\mathcal{S} \leftarrow \emptyset$;
2 Draw feasible circles for all the squares in $\mathcal{U}$;
3 Obtain the set of all circle regions CR;
4 **while** $\mathcal{U} \neq \emptyset$;
5 Do select CR_i from CR that maximize $|S_{CR} \bigcap \mathcal{U}|$;
6 $\mathcal{U} \leftarrow \mathcal{U} - S_{CR_i}$;
7 $\mathcal{S} \leftarrow R \bigcup CR_i$;
8 **return** $\mathcal{S}$;

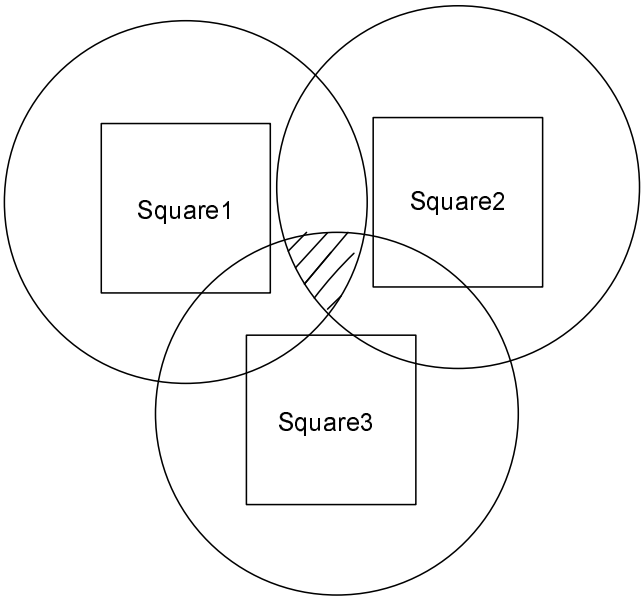

Figure 4.4: An example of three feasible circles mutually intersected. Each square has a feasible circle such that an RN placed anywhere within this circle is able to cover the entire square. An RN placed in the intersection area of all three circles can cover all three squares.

Circle covering algorithm

With all the feasible circles established, the algorithm to provide the circle covering algorithm is presented in Table 4.4.

The Circle Covering algorithm works based on a greedy strategy as well. The set $\mathcal{U}$ contains, at each stage, the set of remaining uncovered busy squares. The set $\mathcal{S}$ contains the already selected circle regions for placing RNs. Line 5 is the greedy decision-making step. A circle region CR_i is chosen for placing one RN that covers as many uncovered squares as possible. After CR_i is selected, the corresponding covered squares are removed from $\mathcal{U}$, and CR_i is added into the subset $\mathcal{S}$. When the algorithm terminates, each of the busy squares is covered by at least one RN.

4.3.3 BIP algorithm

The BIP algorithm is designed for obtaining the optimal solution to the SDC problem. Firstly, it is required that all possible positions for placing RNs should be obtained, which means no approximation method is allowed. To this end, we follow the first step of TVSC algorithm instead of the Circle Covering algorithm to obtain all the possible solutions. Then we reformulate the SDC problem as a binary integer programming problem as follows. Let $\mathcal{P} = p_1, p_2, ..., p_N$ denote the set of all possible positions obtained through executing step 1 of the TVSC algorithm. Let x_n denote the binary assignment variable with $x_n = 1$ indicating that the selection of the nth position as the placement for one RN and 0 otherwise. Let $\mathcal{S} = s_1, s_2, ..., s_M$ denote the set of all the busy squares. Construct a M by N binary coefficient matrix $\mathcal{C}$ with its element $c_{m,n} = 1$ if the RN placed at p_n can cover the square s_m and 0 otherwise. Then the SDC problem is restated as (4.5) to minimize the number of positions selected while keeping all the busy squares covered.

$$\begin{aligned} min \quad & \Sigma_{n=1}^{N} x_n \\ s.t. \quad & x_n \in \{0,1\}, 1 \leq n \leq N \\ & \Sigma_{n=1}^{M} c_{m,n} \cdot x_n \geq 1 \end{aligned} \tag{4.5}$$

The second constraint is to guarantee that each square is covered by at least one RN in the optimal solution.

For the second step, we use a linear programming (LP)-based branch-and-bound algorithm to solve the SDC problem. The algorithm searches for an optimal solution to the binary integer programming problem as stated in Eq. (4.5) by solving a series of LP-relaxation problems, in which the binary integer requirement on the variables is replaced by the weaker constraint $0 \leq x \leq 1$. More details can be referred to [83].

4.4 Complexity Analysis

We first discuss the complexity as well as the worst case performance ratios of the TVSC algorithm. Assume N denotes the number of busy squares. Since the number of iterations of the loop on lines 3-5 in Table 4.3 is at most $\frac{4N(4N-1)}{2}$. And the iterations of the loop on lines 6-9 in Table 4.3 would be run N times. Thus the total computational complexity is $8N^2 - N$. Since step 2 of TVSC algorithm is basically a greedy methodology, the TVSC algorithm yields a solution with number of RNs mostly $H(max|\mathcal{S}_\mathcal{C}| : \mathcal{S}_\mathcal{C} \in \mathcal{A})$ times larger than the optimal one[18], where $H(d)$ denotes the dth harmonic number $H_d = \Sigma_{i=1}^{d} 1/i$.

Secondly, we will analyze the Circle Covering algorithm in terms of computational complexity as well as its worst case performance ratios. Assume N denotes the number of busy squares. Since drawing the feasible circle for each busy square should be done N times, and the iterations of the loop on lines 4-7 in Table 4.4 would be run at most N times, the total computational complexity is $2N$. When the circle covering algorithm is employed, we lose 4 approximate regions for placing RNs since the area of the feasible circle is less than that of the feasible area. Then we use β to denote the approximate ratio, which is defined as the ratio of the area of feasible regions plus the area of feasible circle to the area of feasible circle, shown as (4.6).

$$\beta = \frac{\pi(r-\frac{\sqrt{2}}{2})^2+4(\frac{\alpha}{2\pi}\pi r^2-\frac{\pi(r-\frac{\sqrt{2}}{2})^2}{4}-\frac{1}{2}\frac{\sqrt{2}}{2}r\sin\frac{\alpha}{2}\times 2)}{\pi(r-\frac{\sqrt{2}}{2})^2} = \frac{2\alpha r^2-2\sqrt{2}r\sin\frac{\alpha}{2}}{\pi(r-\frac{\sqrt{2}}{2})^2} \tag{4.6}$$

where $\alpha = \arccos\frac{2\sqrt{2}r-1}{2r^2}$ represents the radian of the arc, which is served as one part out of four of the boundary of the corresponding feasible area of a busy square. r is the transmission range of MNs. Since the Circle Covering algorithm is a greedy strategy-based algorithm, which has an upper ratio bound $H(max|CR_i|, 1 \leq i \leq$

$|CR|$)[18], the Circle Covering algorithm yields a solution with number of RNs that is at most $\beta H(max|CR_i|, 1 \leq i \leq |CR|)$ times larger than the optimal, where β is defined as the approximate ratio in (4.6).

In the end, the analysis of the BIP algorithm is presented as follows. For the SDC problem, the solution space contains all the combinations of N variables, each with two values 1 and 0, showing whether the position is selected to place one RN or not. Thus the BIP algorithm could potentially search all 2^N binary integer vectors, and the running time for BIP is $O(2^N)$. N is the number of variables that need to be specified. In [53], it has been shown that such a binary integer programming problem can be solved using a graph theoretical approach by transforming it into a linear optimal distribution problem in a directed graph, which has a computational complexity of $O(N^3)$.

Although the BIP algorithm yields the least number of RNs, then is it always beneficial to resort to the BIP algorithm? According to Table 4.5, the computational complexity of the BIP algorithm is much more intense than the TVSC algorithm and Circle Covering algorithm. In contrast, the TVSC algorithm and Circle Covering algorithm yield much less computational complexity, with only a tiny disadvantage in terms of the number of RNs deployed compared with the BIP algorithm. Therefore, in real scenario when the computational resource is precious and timing is critical, the Circle Covering algorithm might be the best approach among all three, followed by the TVSC algorithm.

4.5 Simulation Results

In this section, we present our simulation results. By adopting the BIP algorithm, we first give the RN placement results in a simple 4×4 square disaster area at

Table 4.5: Comparison of complexity and approximation ratio for three relay coverage algorithms

Algorithms/Metrics	Complexity	δ-Approximation
TVSC	$O(N^2)$	$H(max\|\mathcal{S}_\mathcal{C}\| : \mathcal{C} \in \mathcal{A})$
Circle Covering	$O(N)$	$\beta H(max\|CR_i\|, 1 \leq i \leq \|CR\|)$ (4.6)
BIP	$O(N^3)$	1

all time periods when the set of busy squares changes, from the beginning until all the squares are cleared. Then in a larger 10×10 square disaster area, we compare the performance between these three algorithms, the TVSC algorithm, the Circle Covering algorithm and the BIP algorithm in terms of number of RNs deployed. All the simulation results are obtained through MATLAB 2007b [1].

4.5.1 simulation setup

We establish a large 10×10 square disaster area. There are totally 100 first responders. We propose two initial placement for first responders: all at $s_{1,1}$ and evenly distributed at four corners $s_{1,1}, s_{1,10}, s_{10,1}, s_{10,10}$. Besides, we also provide simulation results when adopting two kinds of distribution of CI values of squares in the disaster area: the CI values of all square are equal to 10; Integer CI values are randomly chosen from the interval [5, 15]. We also assume $\xi = 1$.

4.5.2 Results on mobility model

In this section, we present some simulation results on the mobility model we proposed in terms of the impact that the number of first responders and the initial placement of MNs have on the time required to clear a 10×10 disaster area and

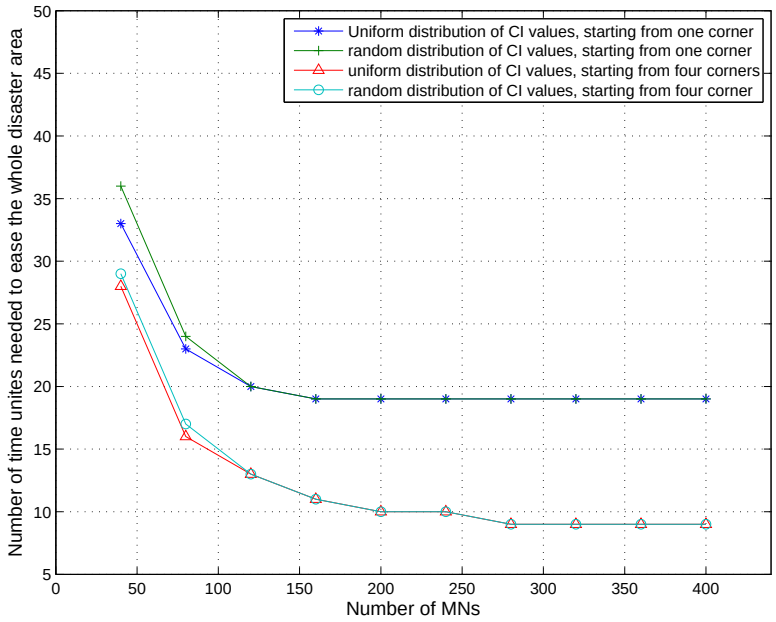

Figure 4.5: Number of time unites needed to ease a 10×10 square disaster area with the mobility model proposed, as the number of first responders changes from 40 to 400.

the average number of busy squares over the whole time period. In Fig. 4.5, we show how the number of MNs influence the length of disaster area relief period with different initial placement of MNs and distribution of CI values, based the mobility model proposed. In Fig. 4.6, we present simulation results in terms of average number of busy squares over the disaster area relief period based on the proposed mobility model, when the number of first responders change from 40 to 400.

From Fig. 4.5, it is clear that as the number of MNs increases from 40 to 280, the length of the disaster area relief period is reduced. However, the plot in Fig. 4.5 goes down more slowly as the number of MNs becomes larger, until it remains unchanged. This phenomenon is due to the mobility model, which renders many of the added first responders useless in speeding the relief process, as the number of first responders might be larger than the CI values in each square. When the number of all MNs exceeds a large value, then the added first responders would not

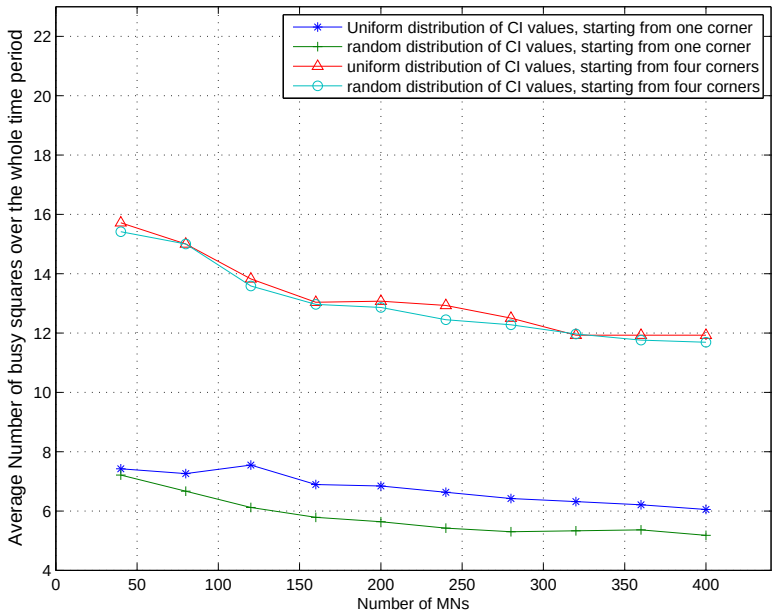

Figure 4.6: Average number of busy squares over the disaster area relief period with the mobility model proposed, as the number of first responders changes from 40 to 400.

accelerate the relief process, because they are always in busy squares that can be cleared in 1 unit of time. Besides, we can tell that the initial place of first responders have a tremendous impact on the length of disaster area relief period. When the first responders are evenly divided and assembled at four corners of the disaster area, the mobility model yields much less time than the case that first responders are assembled at one corner initially. The reason also lies in the mobility model of first responders: the wider distribution of MNs can lessen the chance that the number of MNs in each busy square is larger than its CI value, thus rendering relief efforts of first responders more efficient. At last, it should be noted that whether the CI vales are uniformly or randomly distributed does not matter much.

In Fig. 4.6, we present the simulation results in terms of average number of busy squares over the whole diaster relief period. It can be seen that the average number of busy squares is much less when the first responders are placed at the four corners

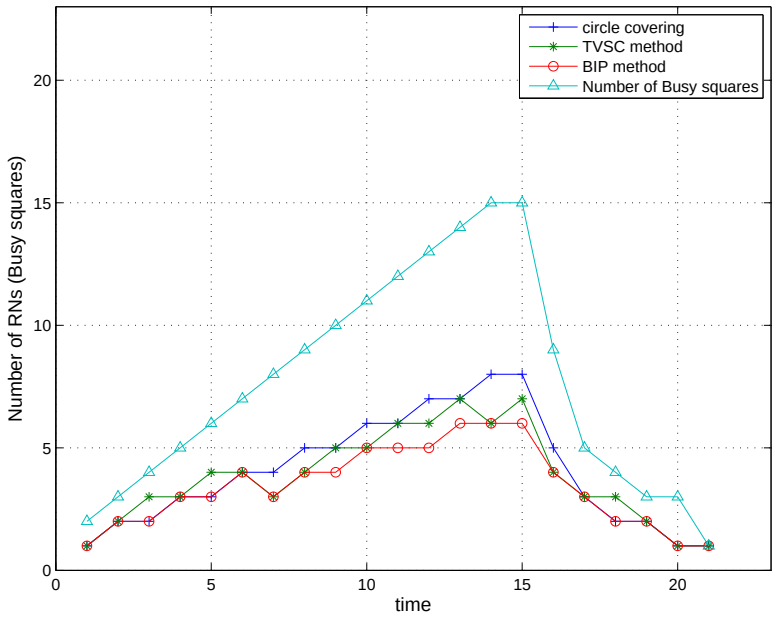

Figure 4.7: Number of RNs deployed during diaster relief. At initial stage, all MNs are in $s_{1,1}$ at time 0, and CI values of all squares are 10. r=1.7

initially compared with the case that they all start from one single square, which is very straightforward. It is also worth pointing out that the average number of busy squares mainly decreases as the number of MNs increases. This is because when the first responders are widely distributed in the middle of disaster relief period, causing a small number of MNs in each busy square, scenarios with large number of busy squares remain for a longer time with a small number of total MNs than the case with a larger number of them.

4.5.3 Deployment Results

The total number of first responders is 100. When first responders are assembled at $s_{1,1}$ at initial stage, and the CI values of all squares are equal to 10, simulation results are presented in Fig. 4.7 in terms of the number of RNs deployed with the TVSC algorithm, the Circle Covering algorithm and the BIP algorithm at each

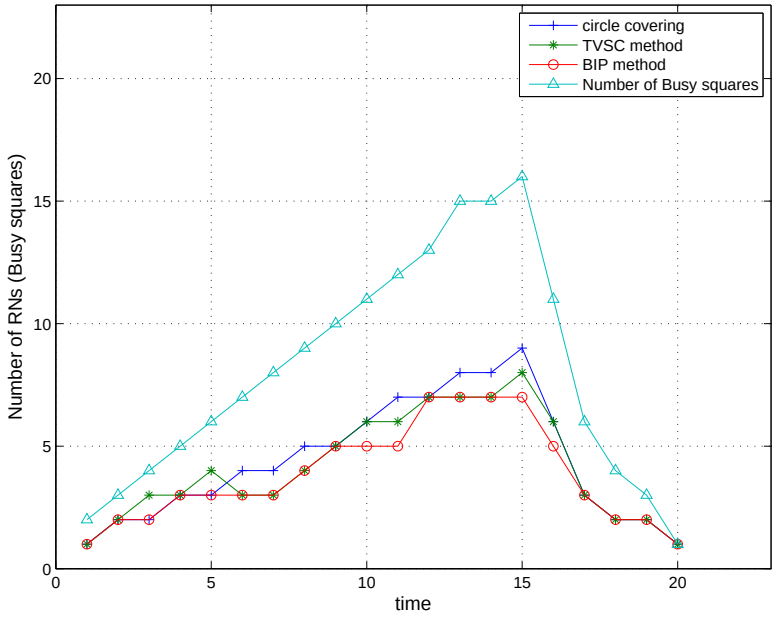

Figure 4.8: Number of RNs deployed during diaster relief. At initial stage, all MNs are in $s_{1,1}$ at time 0, and CI values of all squares are randomly chosen between 5 and 15. r=1.7

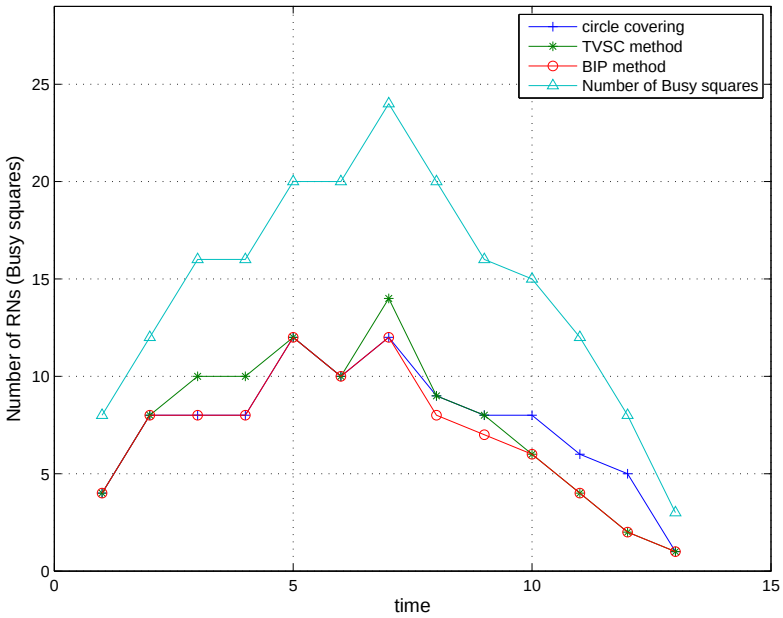

Figure 4.9: Number of RNs deployed during diaster relief. At initial stage, all MNs are evenly deployed in $s_{1,1}, s_{1,10}, s_{10,1}, s_{10,10}$ at time 0, and CI values of all squares are 10. r=1.7

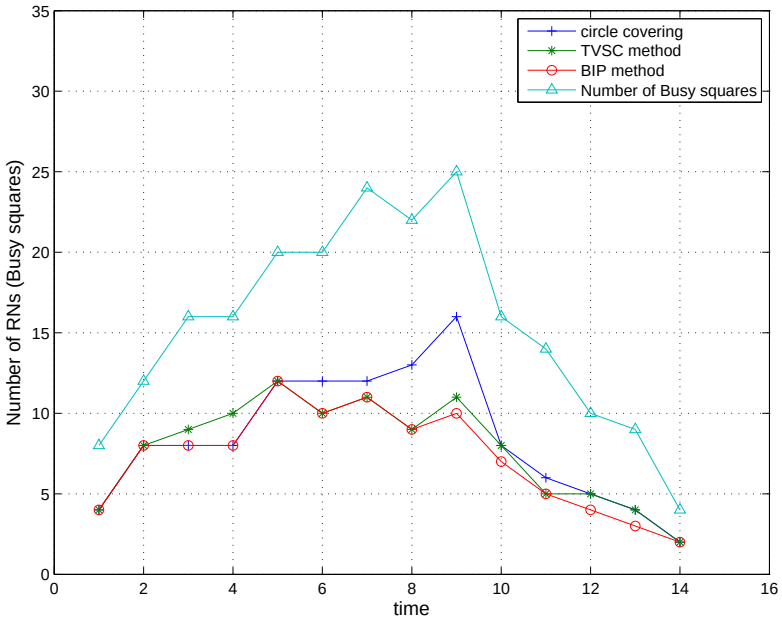

Figure 4.10: Number of RNs deployed during diaster relief. At initial stage, 100 MNs are evenly deployed in $s_{1,1}, s_{1,10}, s_{10,1}, s_{10,10}$ at time 0. CI values of all squares are randomly chosen between 5 and 15. r=1.7

time from the start to the end, when $r = 1.7$; another set of results under the same scenario is presented in Fig. 4.11 in terms of the average number of RNs deployed over the whole disaster relief period with respect to different transmission range of MNs changing from 1.5 to 2.5. Similarly, when first responders are assembled at $s_{1,1}$ at initial stage, and the CI values of all squares are randomly chosen between 5 and 15, simulation results are presented in Fig. 4.8 and Fig. 4.12; When the 100 first responders are initially evenly divided and distributed in $s_{1,1}, s_{1,10}, s_{10,1}, s_{10,10}$, the CI values of all squares are firstly set to 10, simulation results are presented in Fig. 4.9 and Fig. 4.13; At last when the 100 first responders are firstly evenly divided and assembled in $s_{1,1}, s_{1,10}, s_{10,1}, s_{10,10}$, and the CI values of all squares are randomly chosen between 5 and 15, simulation results are presented in Fig. 4.10 and Fig. 4.14.

From Fig. 4.7, Fig. 4.8, Fig. 4.9 and Fig. 4.10, with all the 4 initializations, we

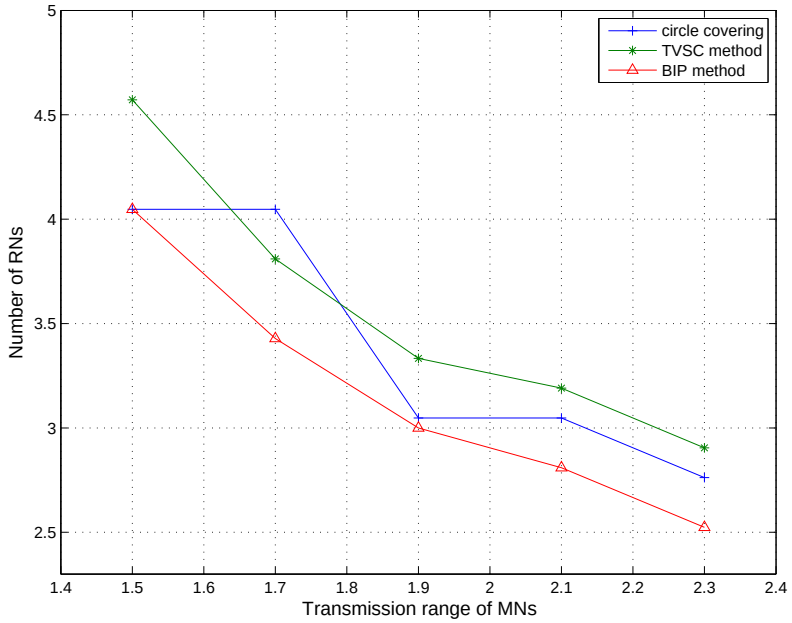

Figure 4.11: Number of RNs deployed as the transmission range changes. At initial stage, all MNs are in $s_{1,1}$ at time 0, and CI values of all squares are 10.

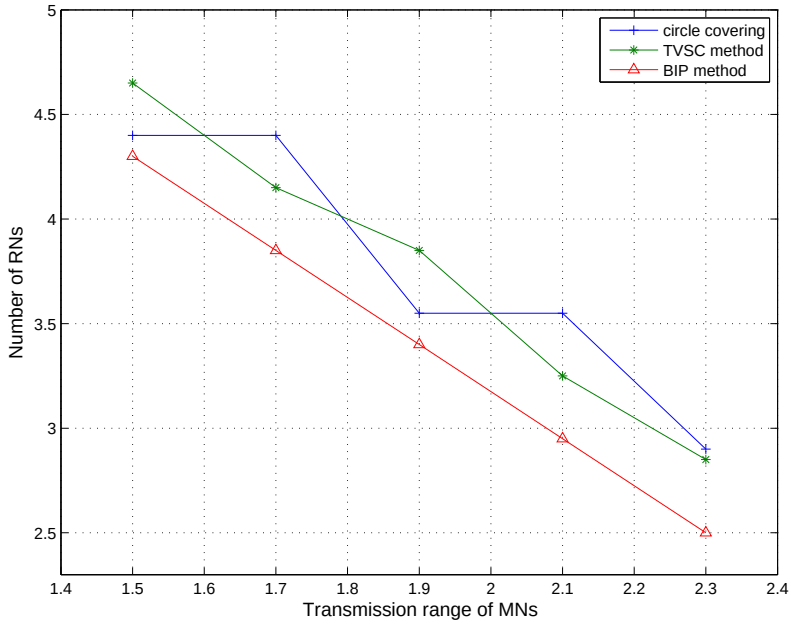

Figure 4.12: Number of RNs deployed as the transmission range changes. At initial stage, all MNs are in $s_{1,1}$ at time 0, and CI values of all squares are randomly chosen between 5 and 15.

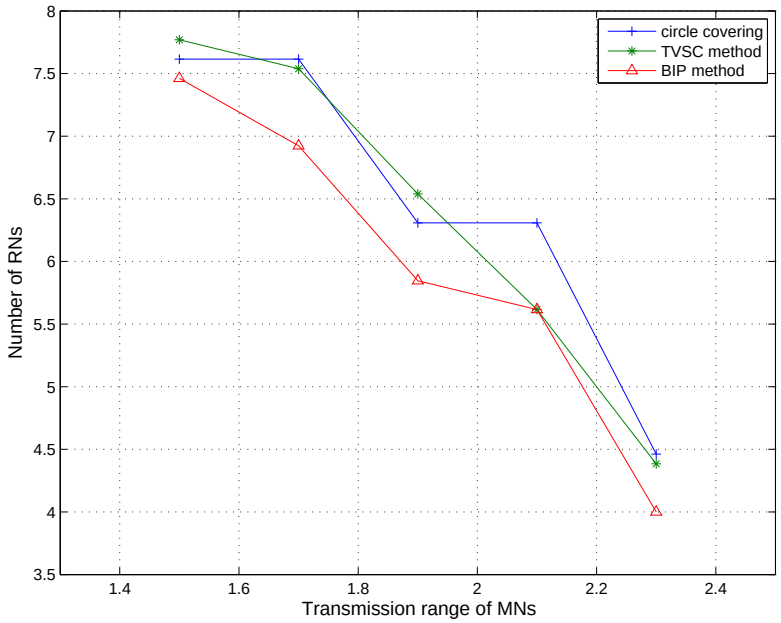

Figure 4.13: Number of RNs deployed as the transmission range changes. At initial stage, all MNs are evenly deployed in $s_{1,1}, s_{1,10}, s_{10,1}, s_{10,10}$ at time 0, and CI values of all squares are 10.

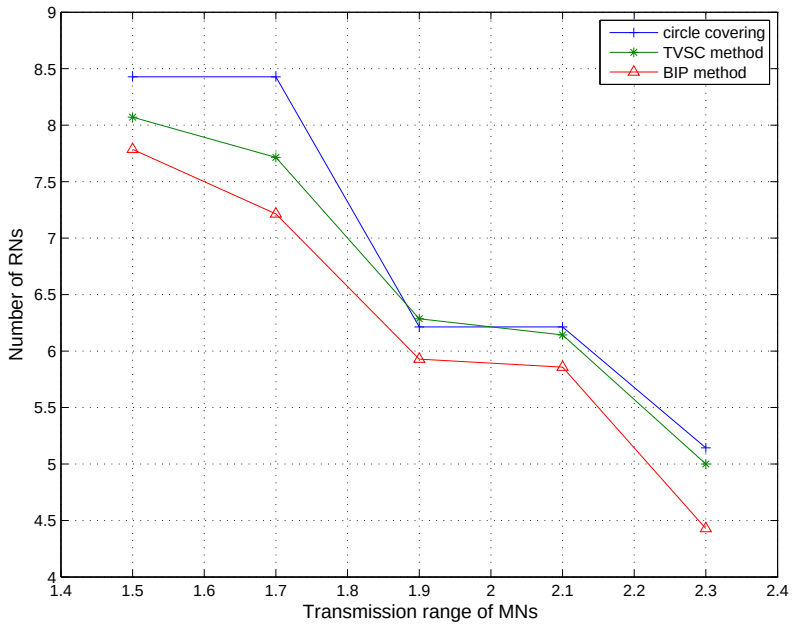

Figure 4.14: Number of RNs deployed as the transmission range changes. At initial stage, 100 MNs are evenly deployed in $s_{1,1}, s_{1,10}, s_{10,1}, s_{10,10}$ at time 0. CI values of all squares are randomly chosen between 5 and 15.

can see that the number of busy squares increases during initial periods, then it decreases after reaching its peak value. It is very straightforward in explaining this trend since during the preliminary periods, first responders expand into adjacent raw squares, and thus the number of busy squares can increase. However, during posterior periods, when first responders have cleared approximately half of the squares in disaster area, at each time, they keep entering a small number of adjacent raw squares from a larger set of cleared squares, because all the busy squares are next to each other, and the movement of MNs from one cleared square can turn only one or less than one raw square into a busy square. Therefore, it is obvious that the number of busy squares tends to be decreased within posterior periods. At each time, the number of RNs deployed to cover the busy squares follows the same trend. But it can be seen clearly at each time, the BIP algorithm, yields the least number of RNs to be deployed, coinciding with the fact that it is the optimal approach; the TVSC algorithm yields more number of RNs to be deployed than the BIP algorithm, as it utilizes the greedy strategy; Furthermore, the Circle Covering algorithm also yields more number of RNs than the optimal solution, because it employs both the greedy strategy and approximation methods.

In Fig. 4.11, Fig. 4.12, Fig. 4.13 and Fig. 4.14, we show how the number of RNs changes as the transmission range of MNs increases with respect to different algorithms and different initialization conditions utilized. It is very clear that for all the 3 algorithms, the number of RNs deployed decreases as r increases. Such a result is straightforward in that the enlarged transmission range of MNs will probably render more squares covered by one RN. Thus to cover the same set of busy squares, one surely needs a smaller number of RNs with a larger r. Again, the BIP algorithm is the best among the three in terms of the number of RNs deployed when the transmission range of MNs varies, followed by the TVSC algorithm and

the Circle Covering algorithm.

4.6 Conclusion

In this chapter, we study the topology control of DAWN to facilitate MNs' communication by deploying a minimum number of RNs dynamically. We first put forward a novel mobility model that describes the movement of first responders within a large disaster area. Secondly, we formulate the SDC problem and propose three algorithms to solve it, including the TVSC algorithm, the Circle Covering algorithm and the BIP algorithm. Simulation results demonstrate that based on our proposed mobility model, first responders can eventually clear the disaster area within a period of time, and at each time, RNs only have to cover a small number of busy squares. We also investigate carefully into the performance comparison between the TVSC algorithm, the Circle Covering algorithm, and the BIP algorithm. As the optimal approach, the BIP algorithm yields the deployment of the least number of RNs, while having the largest computational complexity $O(N^3)$; the TVSC algorithm yields the deployment of the second least number of RNs, and consuming much less computational resources in $O(N^2)$; the Circle Covering algorithm yields the deployment of the most number of RNs, but consuming the least computation resources only in $O(N)$. In practice, the TVSC algorithm and Circle Covering algorithm might be more preferable because they require much less computational complexity, but yield only a small number of the RNs deployed more than the BIP algorithm does. Future work would be dedicated to the state-of-art configuration of RNs to better facilitate communication between MNs and the backbone network in terms of scheduling, resource allocation, modulation schemes and even MAC and network layer protocols, especially in disaster area scenarios.

Chapter 5

Distributed Optimization for Cognitive Radio Networks

Over the past decade, the demand for wireless spectrum use has been growing rapidly due to the dramatic development of the mobile telecommunication industry. According to the traditional access approach, the spectrum are divided into fixed portions and assigned to license holders for exclusive use. As a result, while many licensed portions of spectrum remain under-utilized, a lot of unlicensed wireless users are prevented to access the wireless media. Therefore, the traditional spectrum allocation can be very inefficient.

In order to fully utilize the scarce spectrum resources, emerging cognitive radio technology becomes a promising approach to exploit the under-utilized spectrum [3]. In a cognitive radio network, unlicensed wireless users (secondary users) are allowed to dynamically access the licensed bands, as long as the licensed wireless users (primary users) in those particular bands are not interfered. Wireless devices equipped with cognitive radios are implemented with flexibility, including frequency agility, transmit power control, access coordination etc., which render more efficient

use of available spectrum.

In this chapter, we consider a cognitive radio network (CRN) based on Wireless Regional Area Networks (WRAN)[16], that consists of several secondary base stations (BSs) and secondary users (SUs). A primary network, consisting of several primary BSs and primary users (PUs), coexists within the same area. The spectrum of interest is divided into a set of multiple orthogonal channels using frequency division multiple access (FDMA), which are licensed to PUs. We assume that the channel usage pattern for PUs is fairly static over time so that CRN have ample time to implement primary-user detection and thereby avoid interfering with PUs' communications. We consider downlink scenario in the CRN. Each WRAN BS employs exactly one channel to support an SU. An SU can be active or idle indicating whether it is supported or not.

In this chapter, we study the joint problem of power control and channel assignment to maximize cognitive radio network throughput. Channel assignment exerts a great role in cognitive radio network throughput performance. After assigning channels to all PUs, channel assignment for SUs should be carefully designed to avoid interfering all other users. In addition, transmit power control of CRN, constrained by channel assignment of primary network, influences the interference noise powers from transmissions of SUs, thus affects the channel assignment of SUs and thereby the cognitive network throughput. Besides, transmit powers of BSs in CRN greatly impacts the rates of channels supporting SUs. Therefore, channel assignment and power control in CRN are both of great importance to cognitive radio network throughput.

The rest of this chapter is organized as follows. In Section 5.1, we describe the network and interference models and formulate the CRN maximizing throughput problem. Section 5.2 describes the distributed scheme as a near-optimal low-

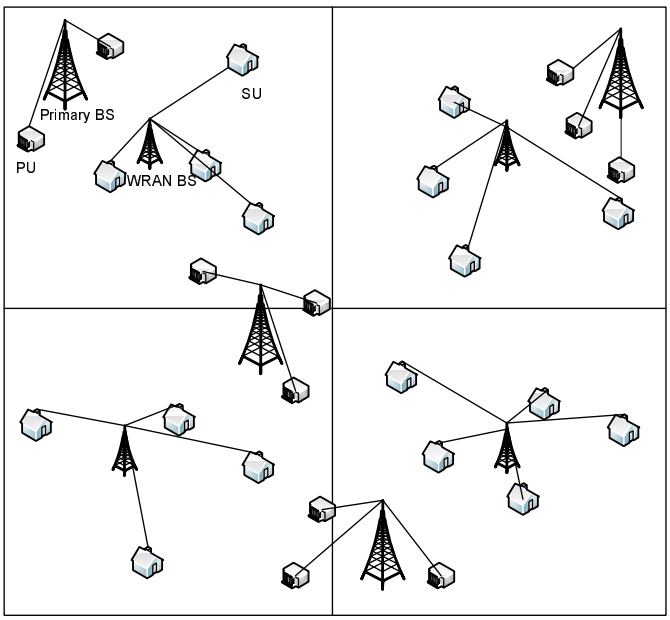

Figure 5.1: An example of WRAN-based cognitive radio networks.

complexity algorithm. In Section 5.3, we present some other related algorithms. In Section 5.4, simulation results are provided to compare the performance between the distributed and the optimal algorithm, followed by some discussion in Section 5.5 and conclusion in Section 5.6.

5.1 Network Model and Problem Formulation

We consider a WRAN scenario depicted in Fig. 5.1. The spectrum of interest is divided into K orthogonal channels through multiple access techniques, such as FDMA. There is one WRAN BS at the center of each cell, which can access all K channels. We consider the downlink scenario in which data are transmitted from WRAN BSs to SUs. We assume that a BS needs exactly one channel to support an SU. The primary network consists of several primary BSs and many PUs who are licensed to use the K orthogonal channels. Each primary BS transmits signals to nearby PUs on an arbitrary channel. Each PU receives signals on a single channel

from the nearest primary BS. In the same area, a CRN is deployed which consists of SUs and a group of WRAN BSs. Note that in the CRN, SUs can not introduce noise signals that violate interference constraints for primary network.

We first need to provide some notation. Let the number of SUs be N, the number of WRAN BSs be B, the number of PUs be J and the number of primary BSs be C. Denote the set of SUs as $\mathcal{S} = \{s_1, s_2, ..., s_N\}$, the set of WRAN BSs as $\mathcal{B} = \{b_1, b_2, ..., b_B\}$, the set of PUs as $\mathcal{P}_u = \{p_{u_1}, p_{u_2}, ..., p_{u_J}\}$, the set of primary BSs as $\mathcal{P}_b = \{p_{b_1}, p_{b_2}, ..., p_{b_C}\}$. Denote the maximum transmit power as P_{max}. We then introduce an integer parameter Q that represents the total number of power levels to which a transmitter can be adjusted, i.e. $\frac{1}{Q}P_{max}, \frac{2}{Q}P_{max}, ..., P_{max}$.

5.1.1 Network Model

Path Loss Model

For transmission from b_i to PU p_{u_j} and SU s_j, a widely used model for propagation gain are shown in (5.1) and (5.2) respectively.

$$g_{ij}^* = {d_{ij}^*}^{-n} \tag{5.1}$$

$$g_{ij} = {d_{ij}}^{-n} \tag{5.2}$$

g_{ij}^* and g_{ij} denote the propagation gain from b_i to p_{u_j} and s_j respectively, d_{ij}^* is the physical distance between b_i and p_{u_j}, d_{ij} is the physical distance between b_i and s_j, n is the path loss index.

Channel Assignment

A WRAN BS needs exactly one channel to support an SU. For CRN, each SU can be assigned at most one channel associated with a BS, as shown in (5.3).

$$\sum_{i=1}^{B}\sum_{k=1}^{K}\sum_{q=1}^{Q} x_{ij}^{kq} \leq 1 \quad j \in \{1, 2, ..., N\} \tag{5.3}$$

x_{ij}^{kq} is a binary assignment variable indicating b_i transmits data to s_j on channel k at the qth transmit power level when $x_{ij}^{kq} = 1$ and 0 otherwise.

Regarding scheduling in the frequency domain, one WRAN BS needs exactly one channel to support an SU, as shown in (5.4).

$$\sum_{j=1}^{N}\sum_{q=1}^{Q} x_{ij}^{kq} \leq 1 \quad i \in \{1, 2, ..., B\} \quad k \in \{1, 2, ...K\} \tag{5.4}$$

Transmission Throughput

Receiving constraint is considered regarding a successful transmission. Suppose there is a transmission from b_i to s_j on channel k using transmit power $\frac{qP_{max}}{Q}$. The received power Pr_{ij}^{kq} can be calculated as (5.5).

$$Pr_{ij}^{kq} = \frac{qg_{ij}Pmax}{Q} \tag{5.5}$$

$$i \in \{1, 2, ..., B\} \quad j \in \{1, 2, ...N\} \tag{5.6}$$

$$k \in \{1, 2, ..., K\} \quad q \in \{1, 2, ...Q\} \tag{5.7}$$

The received power at s_j should be no less than a preset transmit threshold power, denoted as t_t. Then we can define a channel capacity matrix $\mathcal{A}$ as (5.10).

$$\mathcal{A}_{ij}^{kq} = \begin{cases} W \times log_2(1 + \frac{Pr_{ij}^{kq}}{N_o}) & : \quad if \ \ \frac{qP_{max}g_{ij}}{Q} \geq t_t; \\ 0 & : \quad otherwise; \end{cases} \tag{5.8}$$

$$i \in \{1, 2, ..., B\} \quad j \in \{1, 2, ...N\} \tag{5.9}$$

$$k \in \{1, 2, ..., K\} \quad q \in \{1, 2, ...Q\} \tag{5.10}$$

N_o denotes the ambient noise power and W represents the bandwidth of one channel.

Interference Constraint

For a link to be interference free from another transmitter, it is required that the received interference power from any transmitter working on that channel should be no greater than a preset threshold value, denoted as t_i. Thus, for s_j to be able to receive signals on channel k, we derive the following constraint (5.11).

$$\sum_{Pr_{ij}^{kq} \geq t_i} x_{il}^{kq} + (I_j^k + \sum_{a=1}^{C} y_{a*j}^k) \times \sum_{i=1}^{B} \sum_{q=1}^{Q} x_{ij}^{kq} \leq I_j^k \tag{5.11}$$

$$i \in \{1, 2, ..., B\} \quad j \in \{1, 2, ...N\} \quad l \in \{1, 2, ...N\} \tag{5.12}$$

$$k \in \{1, 2, ..., K\} \quad q \in \{1, 2, ...Q\} \tag{5.13}$$

I_j^k denotes the cardinality of the set $\{x_{il}^{kq} | Pr_{ij}^{kq} \geq t_i, l \neq j, 1 \leq l \leq N, 1 \leq i \leq B, 1 \leq q \leq Q\}$. We introduce another binary constant y_{a*j}^k indicating the primary BS p_{b_a} is transmitting on channel k and interfering with s_j (the received power from p_{b_a} at s_j is no less than t_i on channel k) when $y_{a*j}^k = 1$ and 0 otherwise.

Protecting Primary Users

To protect primary users from interference, it is required that the received power from secondary links on the same channel that the primary user is operating should all be less than t_i, as shown in (5.14).

$$\sum_{c_{j*k}Pr^{kq}_{ie*}>=t_i} \sum_{l=1}^{N} x^{kq}_{il} = 0 \tag{5.14}$$

$$i \in \{1, 2, ..., B\} \quad j \in \{1, 2, ...N\} \quad e^* \in \{1, 2, ..., J\} \tag{5.15}$$

$$k \in \{1, 2, ..., K\} \quad q \in \{1, 2, ...Q\} \quad j^* \in \{1, 2, ..., J\} \tag{5.16}$$

Pr^{kq}_{ie*} denotes the received power from b_i to p_{u_e} on channel k when the transmit power is $\frac{qP_{max}}{Q}$. In addition, c_{j*k} is a binary variable indicating p_{u_j} is operating on channel k when $c_{j*k} = 1$ and 0 otherwise.

Objective

The objective of our problem is to maximize the total throughput of cognitive radio networks, which can be stated as (5.17).

$$Maximize \sum_{i=1}^{B} \sum_{j=1}^{N} \sum_{k=1}^{K} \sum_{q=1}^{Q} x^{kq}_{ij} \mathcal{A}^{kq}_{ij} \tag{5.17}$$

$$i \in \{1, 2, ..., B\} \quad j \in \{1, 2, ...N\} \tag{5.18}$$

$$k \in \{1, 2, ..., K\} \quad q \in \{1, 2, ...Q\} \tag{5.19}$$

5.1.2 Problem Formulation

Putting together all the constraints described in Section 5.1.1, we have the following formulation (5.1.2). The optimization problem is in the form of binary integer

programming, which is NP-hard in general.

$$Maximize \sum_{i=1}^{B}\sum_{j=1}^{N}\sum_{k=1}^{K}\sum_{q=1}^{Q} x_{ij}^{kq}\mathcal{A}_{ij}^{kq} \tag{5.20}$$

$$s.t. \sum_{i=1}^{B}\sum_{k=1}^{K}\sum_{q=1}^{Q} x_{ij}^{kq} \leq 1 \tag{5.21}$$

$$\sum_{j=1}^{N}\sum_{q=1}^{Q} x_{ij}^{kq} \leq 1 \tag{5.22}$$

$$\sum_{Pr_{ij}^{kq} \geq t_i} x_{il}^{kq} + (I_j^k + \sum_{a=1}^{C} y_{a*j}^{k}) \times \sum_{i=1}^{B}\sum_{q=1}^{Q} x_{ij}^{kq} \leq I_j^k \tag{5.23}$$

$$\sum_{c_{j*k} Pr_{ie*}^{kq} >= t_i} \sum_{l=1}^{N} x_{il}^{kq} = 0 \tag{5.24}$$

$$x_{ij}^{kq} \in \{0,1\} \quad i \in \{1,2,...M\} \quad j \in \{1,2,...N\} \tag{5.25}$$

$$k \in \{1,2,...,K\} \quad q \in \{1,2,...,Q\} \quad l \in \{1,2,...,N\} \tag{5.26}$$

$$a \in \{1,2,...,C\} \quad e \in \{1,2,...,J\} \tag{5.27}$$

5.1.3 Fairness Considerations

In this chapter, we focus on throughput maximization for the cognitive radio network. Since the cognitive radio network is bandwidth limited and space constrained, it comes down that some secondary users may suffer from zero rates. Therefore, when the number of secondary users is large, we need to frequently reassign the channels to satisfy fairness requirement. In particular, we can divide the set of secondary users into multiple subsets, and consider these subsets in a round-robin manner. Given a particular subset of secondary users, we can then apply the distributed algorithm to maximize the network throughput.

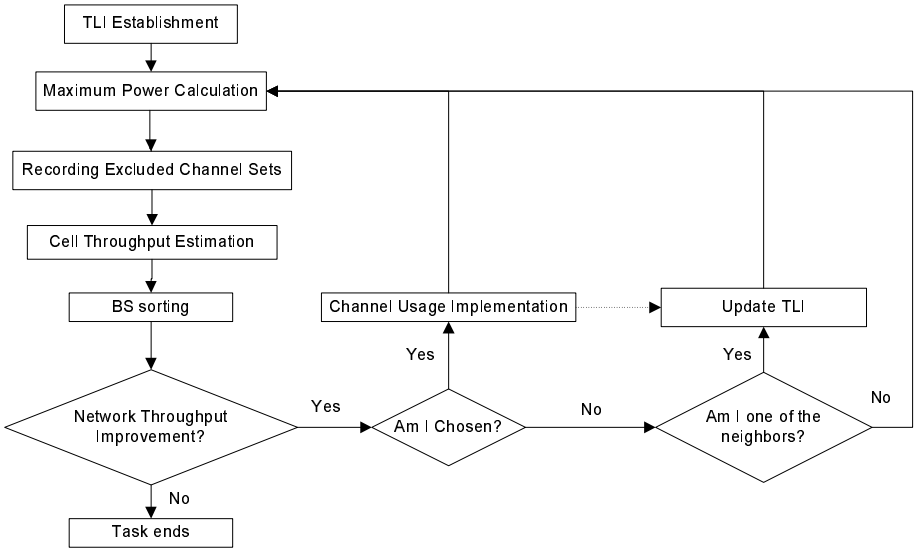

Figure 5.2: The flow chart showing how our distributed algorithm works. Arrows with solid line denotes the calling sequence of each module. Arrows with dashed line denotes the information flow.

5.2 A Distributed Optimization Algorithm

In this section, we present a distributed optimization algorithm. This algorithm increases the cognitive radio network throughput iteratively until it can not be increased. The main idea is presented in Section 5.2.1, which includes maximum power calculation, potential throughput gain estimation, BS sorting and channel usage implementation. The details of each module is described in Section 5.2.2, followed by complexity analysis in Section 5.2.3 and convergence proof in Section 5.2.4.

5.2.1 Overview

Our distributed algorithm increases the overall cognitive radio network throughput iteratively and terminates until the overall network throughput can not be further increased. Our distributed algorithm consists of the following steps.

- In the CRN, each WRAN BS maintains the sum of capacity of all links connected with itself. We assume that each WRAN BS also maintains a table of local information (TLI) of PUs and SUs. In particular, each WRAN BS first obtains the knowledge of positions of local SUs and PUs. We assume each SU acquires its position through GPS (Global Positioning System) and sends it to the WRAN BS. It is also assumed that PUs subscribe to primary network service providers and register their positions at primary BSs. Therefore, each WRAN BS can obtain the positions of PUs by communicating with primary BSs. For those PUs and SUs that have already been assigned channels, the WRAN BS also understands their associated transmit power settings as well as channel usage pattern.

- After TLI establishment, each WRAN BS estimates the maximum throughput it can produce, which includes power control calculation and potential throughput gain estimation. Before estimating potential maximum throughput gain, each BS pretends that all existing assigned links connected to itself are annihilated. Each WRAN BS calculates its possible maximum transmit power on each channel to avoid interfering with other existing links. Then each WRAN BS proceed calculating the maximum throughput produced by itself under the interference constraints imposed by both the primary network and CRN.

- After estimating the maximum throughput, each WRAN BS exchanges its result with neighboring WRAN BSs and finally the largest is identified associated with one WRAN BS. When there are multiple WRAN BSs with the same largest cell throughput, we break the tie deterministically based on their cell IDs. The benefit of the deterministic approach is that a unique WRAN

BS is always picked in our distributed algorithm. Then the chosen WRAN BS is required to implement its channel assignment and transmit power setting to best increase the overall network throughput.

- During the last step of each iteration, the changes of channel assignment and power control information should be updated in the TLIs of neighboring WRAN BSs.

The basic diagram of the distributed algorithm is shown in Fig. 5.2.

5.2.2 Details of Each Module

Before we present the details of the distributed algorithm, we first introduce the following notation. Let l_{ij}^k denote the link between b_i and the s_j on channel k. We assume UB_q^k denotes the maximum allowed transmit power that b_q can utilize on channel k without interfering all existing links in neighboring cells that operate on the same channel. Recall that P_{max} is the maximum transmit power. During an iteration, we may find that, under the interference constraint, UB_q^k is usually smaller than P_{max}. We use UB_q^k for this purpose, where the acronyms UB indicates the current upper bound on the transmit power.

We define the *excluded channel set* as the set of channels that can not be assigned to one SU, i.e. s_{q_j}, denoted as Ω_j. $\mathcal{N}(b_q)$ denotes the set of neighboring BSs of b_q. n_r denotes the current set of unconnected SUs. q_i denotes the ith SU within the cell of b_q. r_{jk} denotes the throughput gain of the channel k when assigned to the jth element of the current set of unconnected SUs. y_{jk} is a binary assignment variable indicating the kth channel is assigned to the jth element of the current set of unconnected SUs when $y_{ij}^k = 1$ and 0 otherwise.

TLI Establishment

We first present the method of TLI establishment. For each WRAN BS, the TLI only records the positions of PUs and SUs, channel usage pattern and associated transmit power settings within the cell as well as neighboring cells. When one WRAN BS tends to assign one channel, it also entails information of already existing local links, in terms of positions of user nodes and associated transmit powers, to carefully avoid causing interference.

Maximum Power Calculation

We now present the method in the module of maximum power calculation. The maximum transmit power for any assigned link is always bounded by P_{max}. The effort to achieve the maximum transmit power agrees perfectly well with the objective to produce the maximum cell throughput. In particular, for each cell, the WRAN BS operates at certain levels of transmit powers on each channel. In order to produce the largest cell throughput, the WRAN BS would boost its transmit power on all channels to the point that existing links are about to be interfered.

The procedure of maximum power calculation algorithm is to browse all links in both CRN and primary network in neighboring cells that operates on the same channel and chooses the smallest upper link power. The Implementation of the module should follow the algorithm presented in Table 5.1. $\lfloor z \rfloor$ represents the maximum power level that is less than the value of z.

Recording Excluded Channel Sets

Subsequently, we present the method of recording excluded channel set. This module is necessary because it is possible that some SUs in the cell can not be supported due to already too much interference noise on certain channels. In other words, even the

Table 5.1: Maximum power calculation

```
1 for each channel k,
2  UB_q^k = inf
3  for each existing link l_ij^k
4   if UB_q^k > t_i / g_qj
5    UB_q^k = ⌊t_i / g_qj⌋
6   end if
7  end for
8  for each PU p_uj
9   if UB_q^k > t_i / g_qj* and c_j*k = 1
10    UB_q^k = ⌊t_i / g_qj*⌋
11   end if
12  end for
13 if UB_q^k > P_max
14   UB_q^k = P_max;
15  end if
16 end for
17 return UB
```

transmit power is set as P_{max}, the link still can not conduct successful transmission because the SINR requirement is not satisfied.

As mentioned in Section 5.2.1, after calculating the upper bound power for each channel, each WRAN BS should also be aware that some channels can not be assigned to certain SUs within the cell because of two much interference noise. Thus we assume each WRAN BS records excluded channel sets associated with SUs following the algorithm presented in Table 5.2. Pr_{i*j} denotes the received power from p_{b_i} to s_j.

Maximum Cell Throughput Estimation

We then present the method for each WRAN BS to estimate the maximum cell throughput. Being aware that some channels can not be assigned to certain SUs, the WRAN BS sets out to assign each channel to the SUs within the cell after

Table 5.2: Recording Excluded Channel Sets

```
1  for each SU s_j
2   for each channel k
3    for each existing link l_il^kq
4    if Pr_il^kq ≥ t_i
5     Add the channel k to list of Ω_j, break;
6    end if
7   end for
8   for each primary BS p_{b_i} that operates on channel k
9    if Pr_{i*j} ≥ t_i
10     Add the channel k to list of Ω_j, break;
11    end if
12   end for
13  end for
14 end for
15 return Ω
```

calculating the maximum transmit powers. This problem can be formulated as the Assignment Problem, which is one of the fundamental combinatorial optimization problems in the branch of optimization or operations research in mathematics. It consists of finding a maximum weight matching in a weighted bipartite graph. The assignment problem can be solved by the famous Hungarian Algorithm.

Being aware that some channels can not be assigned to certain SUs, the WRAN BS sets out to assign each channel to the SUs within the cell after calculating the maximum transmit powers. Then the WRAN BS can calculate the rates of each link associating with all channel-SU pairs. When one channel can not be assigned to one SU, then the rate associating with this channel-SU pair is set as 0. We now can generate a gain matrix shown as (5.28).

$$\mathbf{r} = \left\{ \begin{array}{cccc} r_{11} & r_{12} & ... & r_{1K} \\ r_{21} & r_{22} & ... & r_{2K} \\ : & : & & : \\ : & : & & : \\ r_{n_r} & r_{n_r 2} & ... & r_{n_r K} \end{array} \right\}. \tag{5.28}$$

Now the problem of maximum cell throughput estimation can be formulated as (5.29).

$$\begin{array}{l} max \sum_{j=1}^{n_r} \sum_{k=1}^{K} r_{jk} v_{jk} \\ \\ s.t. \quad \sum_{j=1}^{n_r} y_{jk} \leq 1 \quad k \in \{1, 2, ..., K\} \\ \\ \sum_{k=1}^{K} y_{jk} \leq 1 \quad j \in \{1, 2, ..., n_r\} \end{array} \tag{5.29}$$

This problem can be formulated as the Assignment Problem, which can be solved by the famous Hungarian Algorithm. We now present the Hungarian algorithm [49] to assign channels within each cell, independent to what happens in the rest, as follows.

- Step 1: If **r** is not a square matrix (there are more channels than local SUs or conversely), we have to augment **r** into a square matrix by adding zero rows or columns.
- Step 2: Multiply the matrix **r** by -1.
- Step 3: Subtract the minimum value of each row from row entries.
- Step 4: Subtract the minimum value of each column from column entries.

- Step 5: Select rows and columns across which you draw lines, such that all zeros are covered and that no more lines have been drawn than necessary.

- Step 6: If the number of the lines equals the number of rows, choose a combination of zero elements from the modified gain matrix such that the position of each chosen element is incident on a unique row and column. Then the optimal assignment result consists of the channel-SU pairs as represented by the chosen elements in the modified gain matrix. If the number of the lines is less than the number of rows, go to Step 7.

- Step 7: Find the smallest element which is not covered by any of the lines. Then subtract it from each entry which is not covered by the lines and add it to each entry which is at the intersection of a vertical and horizontal line. Go back to Step 5.

BS sorting

Subsequently, we discuss the method of BS sorting. This module is aimed to calculate the maximum cell throughput and hence the network throughput can be increased greedily. The implementation of this module entails a certain amount of information exchange. After each WRAN BS is associated with a maximum cell throughput, they can exchange their results with neighboring WRAN BSs in a distributed fashion. At the end of this process, each WRAN BS should keep the maximum cell throughput along with the ID of the cell that produces this amount.

This module is aimed to find the maximum cell throughput and hence the network throughput can be increased greedily. The implementation of this module entails a certain amount of information exchange. After each WRAN BS is associated with a maximum cell throughput, they can exchange their results with

neighboring WRAN BSs in a distributed fashion. Once a WRAN BS receives its knowingly best cell throughput, it propagates this datum to its neighboring WRAN BSs exactly once. In particular, each WRAN BS is only concerned if its maximum cell throughput is larger than any other WRAN BS in this iteration. Thus they would discard their own maximum cell throughput along with the associated channel usage information once they realizes some other WRAN BSs produces larger cell throughput. For the case of equal cell throughput, the WRAN BS would also discard its own results if the WRAN BS that produces the same amount of cell throughput is indexed smaller. This sorting procedure terminates when any WRAN BS has not been notified of any larger cell throughput for a preset amount of time.

Channel Usage Implementation

Finally, we discuss the method of channel usage implementation. This module is only applied at the WRAN BS whose maximum cell throughput is the largest among all WRAN BSs in each iteration. The WRAN BS implements the calculated channel assignment and transmit power settings. This WRAN BS also has to inform its neighboring BSs to update their TLIs for calculating the maximum transmit powers in the next iteration.

5.2.3 Complexity Analysis

As for the distributed scheme, the modules that do the majority computation include maximum transmit power estimation, recording excluded channel sets and calculating the cell throughput. For the module of maximum transmit power estimation, we mainly investigate the number of loops in Table 5.1. We suggest the main complexity factor is the number of SUs N, while B, C and J are all of $O(1)$. Since the procedure between line 2 to line 15 can be iterated at most $(BN + J)$, the computation for

the module can be as much as $O((BN + J) \times C)$=$O(N)$. Consider the module of recording excluded channel sets, the procedure is iterated $O(n_r(N - n_r))$ according to Table 5.2. Thus the computation complexity can be $O(N^2)$. Then we look at the module of calculating the cell throughput. Based on [49], the assignment problem proposed by the module can be solved within running time $O(max\{C, n_r\}^4)$. It can be inferred that the computation for one BS during one iteration can be calculated as $O(N^4)$. As only one BS is required to implement its channel assignment and power control in one iteration, the total number of iterations is measured as $O(B)$. Therefore, the overall computation complexity for the distributed scheme at one BS is $O(B \times (N + N^2 + N^4)) = O(BN^4) = O(N^4)$, which is much less than the optimal algorithm.

5.2.4 Convergence Behavior

We now show that the algorithm must converge. We show that each iteration the algorithm increases the throughput performance of CRN. Since the overall throughput is upper bounded, this implies that the algorithm must converge.

We first denote the sum rates of the links connected to b_i as T_i. Then we obtain (5.30).

$$T_i = \sum_{j=1}^{N} \sum_{k=1}^{K} \sum_{q=1}^{Q} x_{ij}^{kq} \mathcal{A}_{ij}^{kq} \quad i \in \{1, 2, ..., B\} \tag{5.30}$$

Thus the objective of our throughput maximization problem is $\sum_{i=1}^{B} T_i$. At the beginning of each iteration, each WRAN BS's configuration represents a feasible solution to the maximum throughput problem as shown in (5.1.2). After solving the maximum throughput estimation problem as shown in (5.29), b_i obtains the optimal

T_i. As a result, the new value of T_i must be no less than the previous iteration. Subsequently, one WRAN BS b_i is chosen to implement its result while keeping links to other WRAN BSs protected, which means the value of $T_j(j \neq i)$ remain the same. Therefore, no matter which BS is chosen to implement new settings for channel assignment and power control, the network throughput is expected to grow larger than the lower bound at the beginning of the iteration. Since the network throughput performance monotonically increases after every iteration, convergence of the greedy algorithm is guaranteed.

5.3 Other Related Algorithms

5.3.1 Optimal Algorithm

Since the problem formulation (5.1.2) falls into the binary integer programs, it can be solved by the branch and bound algorithm [83], which yields the optimal solution.

The complexity analysis of the optimal algorithm is presented as follows. For the channel assignment and power control problem, the solution space contains all combinations of $BNKQ$ binary variables. Thus the optimal algorithm could potentially search all 2^{BNKQ} binary integer vectors, and the running time is $O(2^{BNKQ})$.

5.3.2 Two-phased Algorithm

In [37], a problem of maximizing network throughput for cognitive radio network is studied. A two-phased scheme is proposed to control transmit power of BSs and assign channels. In the first phase, a distributed power updating process is employed to maximize the coverage of the network. In particular, the maximum transmit powers of BSs on all channels are sought to avoid interfering with PUs. In

the second phase, centralized channel assignment is carried out within the cognitive network to maximize its throughput. To specify, given the maximum transmit powers of BS on all channels, the channel assignment problem can be transformed into finding a maximum weighted matching from a weighted bipartite graph. The two-phased scheme has a complexity of $O(N^4)$.

5.3.3 Dynamic Interference Graph Allocation

In [36], Hoang and Liang propose the *Dynamic Interference Graph Allocation (DIGA)* that implements power control and channel assignment to maximize coverage for cognitive radio networks. In the DIGA scheme, a channel is allocated to one SU at a time, until either all SUs are served, or there is no more feasible assignment. At each iteration, channel assignment and power control should be carefully implemented so that any prior established links and all PUs are protected. According to DIGA, to establish a link between one WRAN BS and an SU on channel k with a certain power level, a penalty value is defined as the total number of unserved SUs that can not be assigned the same channel anymore. Thus, the smallest penalty value is sought in each iteration to iteratively implement channel assignment and power control. As for our work, since the objective is to maximize the capacity of the CRN, we redefine the definition of penalty value to be the total capacity loss associated with unserved SUs on the specific channel. After this minor adaptation, we compare the performance of our distributed algorithm with DIGA in Section 5.4. The complexity of DIGA is $O(CN^5 + CN^2J) = O(CN^5) = O(N^5)$ [36].

5.3.4 Power-based Algorithm

In [50], the problem of allocating channels is studied to satisfy the rate requirements of the application while the total transmit power is minimized. The proposed power-

based scheme is also an iterative approach, similar as DIGA[37]. The difference lies in the definition of the penalty value which is defined as the increase in the total transmit power of links associated with channel k if this channel is assigned with a certain transmit power. This scheme is termed as *Minimum Incremental Power Allocation (MIPA)*. The complexity of the MIPA scheme is $O(CN^5 + CN^2J) = O(CN^5) = O(N^5)$, i.e. at the same order as the complexity of DIGA scheme [50].

5.4 Performance Evaluation

In this section, we evaluate the performance of our distributed algorithm through simulations. We compute optimal solutions using CPLEX9.0 [43]. We compare the results of distributed algorithm with the globally optimal method.

5.4.1 Simulation Setup

We consider a square service area of size 100 km by 100 km in which a cognitive radio network is deployed. 4 WRAN BSs are deployed at the centers of 4 square sub-areas, as shown in Fig. 5.1. We consider one random scenario of primary network, with coordinates of primary BSs shown in Table 5.3 and PUs shown in Table 5.4. SUs are randomly deployed across the entire service area with uniform distribution. A sample network is shown in Fig. 5.1. The ambient noise power at each each PU and SU is $N_o = 5 \times 10^{-11}$ watt. The number of channels $K = 4$. We establish the primary network as follows. Each of the 4 primary BSs choose different channels to serve the PUs. The transmit power for all primary BSs is set as $20mW$. According to the physical distance to each primary BS, each PU is covered by the nearest primary BS.

Table 5.3: Node Coordinates of 4 Primary BSs

p_{b_i}	(x_i, y_i) (in meters)	p_{b_i}	(x_i, y_i) (in meters)
1	(95970, 75130)	3	(34040, 25510)
2	(58530, 50600)	4	(22380, 69910)

Table 5.4: Node Coordinates of 10 PUs

p_{u_i}	(x_i, y_i) (in meters)	p_{u_i}	(x_i, y_i) (in meters)
1	(65570, 50600)	6	(85770, 82350)
2	(13570, 63180)	7	(94310, 69480)
3	(84910, 67690)	8	(39220, 31710)
4	(33400, 74620)	9	(65550, 55020)
5	(57870, 49710)	10	(27120, 23440)

5.4.2 Simulation Results

In this section, we provide simulation results by comparing the distributed algorithm with other algorithms. In particular, we look into the impacts of 4 different system parameters, the number of SUs N, the transmit threshold power t_t, the interference threshold power t_i, the number of power levels Q. We vary each of 4 system parameters while keeping the others unchanged to produce different parameter settings. For each set of system parameters, we generated 100 instances of different deployments of SUs to obtain the average performance. Totally five schemes are considered, i.e. the global optimal scheme, our proposed distributed scheme, the two-phase algorithm, the DIGA and MIPA scheme. The simulation results are discussed next.

The Impact of Transmit Threshold Power

In Fig. 5.3, we look at the impact of transmit threshold power t_t on the throughput of CRN. We compare the performance of the optimal algorithm, the distributed algorithm, the two-phase algorithm the DIGA scheme and the MIPA scheme. As can be observed from Fig. 5.3, Global Optimal scheme gives the best performance while

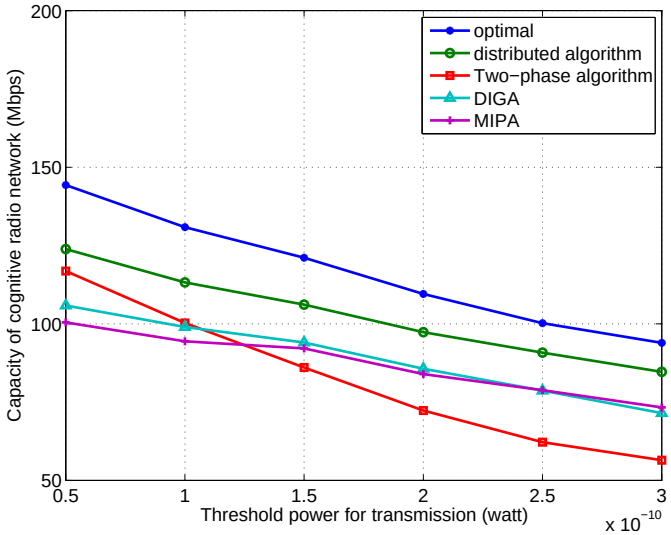

Figure 5.3: The Impact of Transmit Threshold Power. $N = 20$, $n = 2$, $Pmax = 50mW$, $t_i = 10^{-11}W$, $Q = 5$

our proposed distributed scheme consistently outperforms the two-phase algorithm, the DIGA scheme and the MIPA scheme. The performance gain for our distributed algorithm over other schemes is mainly due to three reasons. First, our distributed scheme directly addresses the objective of maximizing throughput in each iteration. The two-phase algorithm tries to maximize transmit powers of BSs on all channels in the first phase, which might not best serve the interest of maximizing the network throughput. The DIGA and MIPA schemes introduce the penalty value of potential throughput loss and transmit power increase for each channel assignment with a power level, and seeks to minimize the value in each iteration. They ignore the fact that the newly added link probably will not bring the maximal incremental throughput, which does not agree with the objective from a greedy perspective. Secondly, our distributed algorithm uses transmit power more efficiently. Under the distributed algorithm, each BS boosts its transmit power to provide higher rates for SUs. While for the two-phase algorithm, after WRAN BSs set their high transmit power the first phase, SUs may not be able access downlink channels due to high

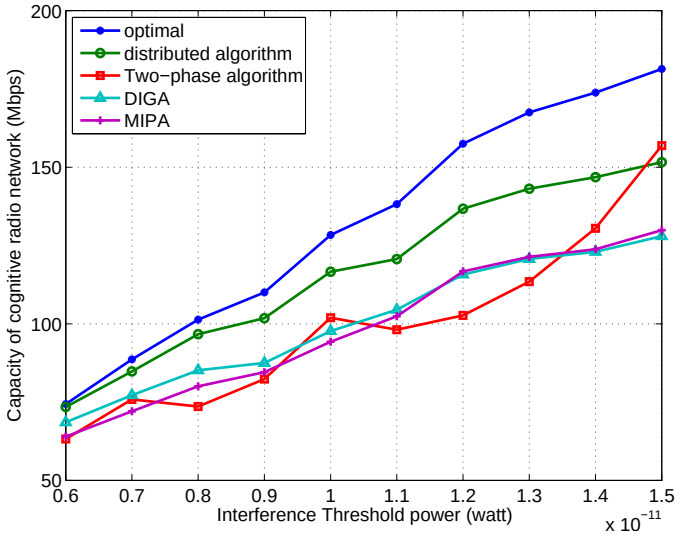

Figure 5.4: The Impact of Interference Threshold Power. $N = 20$, $n = 2$, $t_t = 1 \times 10^{-10}W$,$P_{max} = 50mW$, $Q = 5$

interference. Thirdly, our distributed algorithm is implemented by each BS, bringing the maximal incremental throughput by establishing links with multiple SUs at the same time. The DIGA and MIPA schemes only establish one link at each step, which probably generates less benefits in terms of maximizing overall throughput.

It can be observed that the overall throughput monotonically decreases as t_t is enlarged. The reason behind is very simple: higher threshold power decreases the number of feasible links.

The Impact of Interference Threshold Power

Fig. 5.4 investigates the impact of interference threshold power on the throughput of CRN. The main trend is that the overall throughput increases as the interference threshold power is enlarged. This can be explained by the fact that larger interference threshold power generates more opportunities for more links to be active simultaneously, thus brings throughput increase to the overall performance. It can also be noted that our distributed algorithm outperforms the two-phase algorithm,

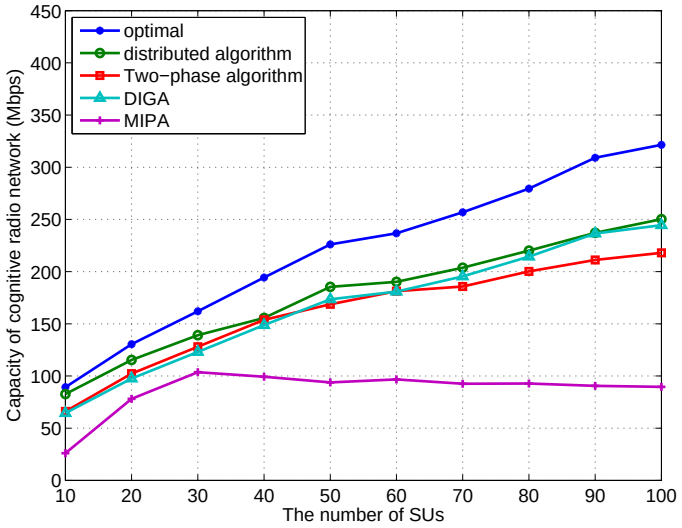

Figure 5.5: The Impact of Number of SUs. $n = 2$, $t_t = 1 \times 10^{-10}W$,$t_i = 10^{-11}W$, $Q = 5$, $P_{max} = 50mW$

the DIGA scheme and the MIPA scheme consistently.

The Impact of Number of SUs

Fig. 5.5 shows the impact of number of SUs on the throughput of CRN. The main trend is that the total throughput is increased as the number of SUs increases. The rationale behind is that more SUs tend to render more opportunities to establish links with higher capacity, i.e. the WRAN BSs are closer to their associated SUs. It should also be noted that the our proposed distributed scheme yields better performance than the other 3 schemes.

The Impact of Number of Power Levels

Fig. 5.6 depicts the impact of number of power levels on the throughput of CRN. It is obvious that the number of power levels will increase the throughput performance of CRN. With larger number of power levels, the transmit power can be more finely controlled, thus it is probable that multiple links on the same channel can be

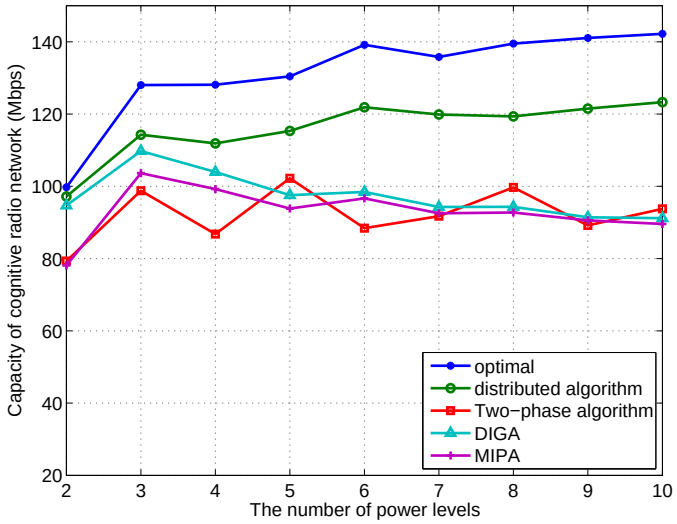

Figure 5.6: The Impact of Number of Powre Levels. $N = 20$, $n = 2$, $t_t = 1 \times 10^{-10}W$,$t_i = 10^{-11}W$, $P_{max} = 50mW$

active simultaneously. However, when Q is large enough, the plots do not obviously increase because at this point larger Q will have little impact on the assignment result, i.e. increase the number of assigned channels. Furthermore, it can be also observed that our distributed scheme produce better solutions in terms of total throughput of CRN than other three schemes.

5.5 Discussion

The reason that the distributed algorithm demonstrates good performance is due to the optimization of large set of variables. A detailed investigation at (5.29) and (5.1.2) would reveal the truth. During each iteration, the distributed algorithm performs optimization on a set of variables which share the same attributes, i.e. associated with the same WRAN BS. After each iteration, many variables can be determined. Let's consider the extreme case. If only one WRAN BS is available, the distributed algorithm yields the optimal solution. In contrast, the two-phase scheme

over boosts the transmit powers of WRAN BSs during the first phase, which harms the overall performance by causing too much interference. The DIGA and MIPA scheme only determines one variable using greedy strategy during each iteration, which is probably not in the interest of the overall performance of the CRN. Besides, although some variables associated with one user node can be set to 0 at each step, many more variables are still unspecified than the distributed algorithm. From the foregoing, the advantage of the distributed algorithm should be attributed to the manipulation of large set of variables at each step.

The distributed algorithm performs satisfyingly close to the optimal solution as shown in Section 5.4. The algorithm "divides the conquer" by taking advantage of the computing ability of WRAN BSs, and assigns a considerably smaller computing task to each WRAN BS. Fortunately, each computing task also involves a very large set of variables. All the facts above support the advantage of the distributed algorithm.

5.6 Conclusion

In this chapter, we investigate the cross-layer design and distributed optimization algorithm for a cognitive radio network. We first developed a mathematical model for such problem with joint consideration of power control and channel assignment. The main contribution of this chapter is the development of a distributed optimization algorithm that iteratively increases the overall CRN network throughput. This algorithm consists of several modules, including maximum power calculation, cell throughput estimation, BS sorting and channel usage implementation. Through simulation results, we compared the performance of the distributed optimization algorithm with other algorithms and validated its efficacy.

Chapter 6

Interference Alignment for Multi-hop Wireless Networks

Multi-hop wireless networks, such as mobile ad hoc networks, wireless sensor networks, and wireless mesh networks, have gained a lot of research attentions in the past decade. Probable explanation to this trend might be that one-hop networks are seriously constrained by limited coverage, poor quality-of-service (QoS) performance, restricted applications, etc. In contrast, due to easy deployment and significant reachability, multi-hop wireless networks can be employed in many practical scenarios, i.e. tactical communication within a battlefield, disaster rescue after an earthquake, greenhouse temperature monitor, and last-mile network access.

The QoS performance of a multi-hop wireless network is largely measured by end-to-end throughput. Recent research on maximizing the throughput of multi-hop wireless network focus on power control, spectrum access schemes, link scheduling techniques and routing algorithms. However, the throughput performance is fundamentally limited by the available spectrum resources and constrained transmission power. Consequently, some ground-breaking new techniques should be introduced

to better exploit the network resources.

The emergence of the idea of interference alignment provides a new perspective to achieve higher throughput: allowing multiple transmitter-receiver pairs to achieve interference-free transmission simultaneously. Initially introduced in [14], interference alignment allows a transmitter to align its interference to unused directions of other links, generating no harmful interference at the receiver ends. Consequently, the implementation of interference alignment transmitter nodes can greatly improve the network throughput. The canonical example of interference alignment is a communication scenario where every user is able to achieve one half of the capacity that could be achieved in the absence of all interference. Therefore, interference alignment stands as a promising technique to improve throughput of multi-hop wireless networks.

In this chapter, we study the network throughput optimization problem for a multi-hop wireless network by considering interference alignment at physical layer. We first transform the problem of dividing the set of links into multiple maximal concurrent link sets into finding all maximal cliques of a graph. Then each concurrent link set is further divided into one or several multi-access interference networks, on which interference alignment is implemented to guarantee simultaneous interference-free transmission. The network throughput optimization problem is then formulated as a non-convex nonlinear programming (NLP) problem, which is NP-hard generally. Thus we resort to developing a branch-and-bound framework, which guarantees an achievable performance bound. We use numerical results to validate the efficacy of the algorithm and to offer insights on the throughput enhancement brought by interference alignment.

The rest of this chapter is organized as follows. In Section 6.2, we describe the network model and formulate the NLP problem. In Section 6.3, we propose a branch-

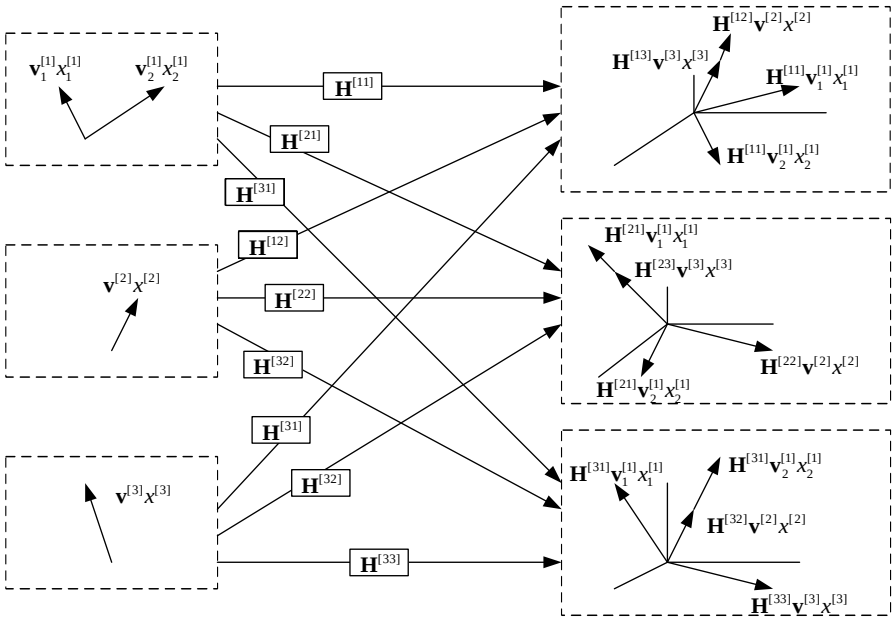

Figure 6.1: Interference Alignment on the three-user interference channel to achieve $\frac{4}{3}$ degrees of freedom.

and-bound algorithm to solve the optimization problem. In Section 6.4, simulation results are presented to demonstrate the efficacy of the proposed algorithm. Section 6.5 concludes this chapter.

6.1 Background: Interference Alignment Applied to Constant Interference Channel

The fundamental idea of interference alignment, rather than nulling all interference at the receivers like zero forcing, the transmitters can align the interfering signals in a direction that is different from the desired signal. Specifically, "interference alignment refers to a construction of signals in such a manner that they cast overlapping shadows at the receivers where they constitute interference while they remain distinguishable at the receivers where they are desired" [14].

A simple example will be illustrated by applying interference alignment to constant interference channel. Consider the 3 user interference channel, comprised of 3 transmitters and 3 receivers. Each node is equipped with only one antenna. The interference alignment schemes are based on beamforming over multiple symbol extensions of the interference channel. As shown in Fig. 6.1, User 1 achieves 2 degrees of freedom by transmitting two independently coded streams along the beamforming vectors $\mathbf{v}_1^{[1]}$, $\mathbf{v}_2^{[1]}$ while users 2 and 3 achieve one degree of freedom by sending their data streams along the beamforming vectors $\mathbf{v}^{[2]}$, $\mathbf{v}^{[3]}$, respectively. we are able to achieve 4 DoF over 3 symbol extension of the channel with $K = 3$ single antenna users, so that a total of $\frac{4}{3}$ DoF are achieved per channel use.

To determine the beamforming vectors, let us pick $\mathbf{v}^{[2]}$ be the 3×1 vector of all ones.

$$\mathbf{v}^{[2]} = \mathbf{1}_{3\times 1} \tag{6.1}$$

The remaining beamforming vectors are chosen as follows.

- At receiver 1, the interference from transmitters 2 and 3 are perfectly aligned.

$$\mathbf{H}^{[12]}\mathbf{v}^{[2]} = \mathbf{H}^{[13]}\mathbf{v}^{[3]} \Rightarrow \mathbf{v}^{[3]} = (\mathbf{H}^{[13]})^{-1}\mathbf{H}^{[12]}\mathbf{1}_{3\times 1} \tag{6.2}$$

- At receiver 2, the interference from transmitter 3 aligns itself along one of the dimensions of the two-dimensional interference signal from transmitter 1.

$$\begin{aligned} &\mathbf{H}^{[23]}\mathbf{v}^{[3]} = \mathbf{H}^{[21]}\mathbf{v}_1^{[1]} \Rightarrow \\ &\mathbf{v}_1^{[1]} = (\mathbf{H}^{[21]})^{-1}\mathbf{H}^{[23]}(\mathbf{H}^{13})^{-1}\mathbf{H}^{[12]}\mathbf{1}_{3\times 1} \end{aligned} \tag{6.3}$$

- At receiver 3, transmitter 2 aligns its interference along one of the dimensions

of interference from transmitter 1.

$$\mathbf{H}^{[32]}\mathbf{v}^{[2]} = \mathbf{H}^{[31]}\mathbf{v}_2^{[1]} \Rightarrow \mathbf{v}_2^{[1]} = (\mathbf{H}^{[31]})^{-1}\mathbf{H}^{[32]}\mathbf{1}_{3\times 1} \tag{6.4}$$

Remark : for any $\varepsilon > 0$ it is possible to align interference within a multi-user interference channel network to achieve ε fraction of 1/2 DoF (per user). The tradeoff is that the larger the number of symbols (time slots), the smaller the value of ε. The proof can be found in [14].

6.2 Problem Formulation

We consider a multi-hop wireless network with N single-antenna nodes arbitrarily located in a 2D space. We assume that there is a single wireless channel and each active link can cause interference to any other link. Let n_i, $1 \leq i \leq N$ denote the nodes, and d_{ij} denote the distance between nodes n_i and n_j. Let d_{ij} denote the physical distance between n_i and n_j. ρ denotes the path loss index. l_{ij} denotes the link between n_i and n_j. P denotes the same power level that all transmitters employ. The received power from n_i to n_j is denoted as p_{ij}, which can be calculated using (6.5). Then the capacity of l_{ij}, denoted as c_{ij}, can be calculated using (6.6), where p_n denotes the noise power and B denotes the bandwidth of the channel.

$$p_{ij} = \frac{P}{d_{ij}^{\rho}} \tag{6.5}$$

$$c_{ij} = B \times log_2(1 + \frac{p_{ij}}{p_n}) \tag{6.6}$$

Each node has a radio transceiver with interference threshold power th_i and transmission threshold power th_t ($th_t \geq th_i$). We consider a transmission from n_i

to n_j is successful if $p_{ij} \geq th_t$. Similarly, n_i can cause interference to n_j if $p_{ij} \geq th_i$. Note that a node may not send and receive at the same time (half-duplex) nor transmit to more than one node simultaneously (unicast only). Then we will define the concept of **concurrent link set** (**CLS**) as follows. A CLS is defined as a set of links that can be active simultaneously. Then the **maximum concurrent link set** (**MCLS**) is defined as a CLS that can not grow larger. Suppose there are a total of K MCLSs within the wireless network. Let $I_1, I_2, ..., I_K$ denote these MCLSs and $\lambda_i, 0 \leq \lambda_i \leq 1$ denote the fraction of time allocated to I_i (i.e., the time during which the links in I_i can be active).

Recent studies show that interference alignment has potential to improve network throughput [14]. Thus we make the following observation. We view links belonging to the same MCLS as pairs of transmitters and receivers. Within the same multi-access interference network, each transmitter can cause interference to all receivers . With interference alignment, the links within the same interference network can be active simultaneously. Therefore, each MCLS consists of one or multiple multi-access interference network(s) between which no interference is generated. M_{ij} denotes the jth multi-access interference network in I_i. L_{ij} denotes the number of links in M_{ij}. Then the summation of DoF assigned to each link in M_{ij} is upper bounded by $\frac{L_{ij}}{2}$ at perfect interference alignment[14].

We consider communication of multiple sessions between pairs of sources and destinations. We try to *schedule MCLSs and assign DoF at each time fraction to maximize the overall end-to-end throughput*. We assume that packet transmissions at individual nodes can be finely controlled and carefully scheduled by an omniscient and omnipotent central entity. We then formulate the maximum achievable throughput problem between the sources and destinations as a *maximum-flow problem* as

shown below.

$$Max \sum_{w=1}^{W} \sum_{l_{swj} \in \mathbf{E}} f_{swj}^{w} \tag{6.7}$$

$$s.t.: \sum_{l_{ij} \in \mathbf{E}} f_{ij}^{w} = \sum_{l_{ji} \in \mathbf{E}} f_{ji}^{w}, \forall n_i \in \mathbf{V} - \{n_{s_w}, n_{d_w}\}, 1 \leq w \leq W \tag{6.8}$$

$$\sum_{l_{isw} \in \mathbf{E}} f_{is_w}^{w} = 0, 1 \leq w \leq W \tag{6.9}$$

$$\sum_{l_{dwi} \in \mathbf{E}} f_{d_w i}^{w} = 0, 1 \leq w \leq W \tag{6.10}$$

$$f_{ij}^{w} \geq 0 \forall l_{ij} \in \mathbf{E}, 1 \leq w \leq W \tag{6.11}$$

$$\sum_{i=1}^{M} \lambda_i = 1 \tag{6.12}$$

$$\lambda_i \geq 0, 1 \leq i \leq M \tag{6.13}$$

$$\sum_{w=1}^{W} f_{ij}^{w} \leq c_{ij} \times \sum_{l_{ij} \in I_k}^{K} \lambda_k \beta_{ij}^{k}, \forall l_{ij} \in \mathbf{E}, 1 \leq k \leq K \tag{6.14}$$

$$\sum_{l_{ij} \in M_{km}} \beta_{ij}^{k} = \frac{L_{km}}{2}, 1 \leq m \leq |I_k| \tag{6.15}$$

f_{ij}^{w} denotes the amount of flow on wireless link l_{ij} which belongs to the wth session. $\mathbf{E}$ represents the set of all links in the network, and $\mathbf{V}$ represents the set of all nodes. W represents the number of sessions. s_w and d_w denote the source and destination node of the wth session, respectively. β_{ij}^{k} denotes the assigned DoF of l_{ij} when $l_{ij} \in I_k$. The objective is to maximize the summation of data flow out of the source nodes of all sessions.

The constraint of (6.8) represents flow-conservation, i.e., at each node, except the source and destination, the amount of incoming flow is equal to the amount of outgoing flow. In (6.9), it is required that the incoming flow to the source is 0, while in (6.10) it is indicated that the outgoing flow from the destination node is 0. As required by (6.11), the flow on each link to be non-negative. The constraint

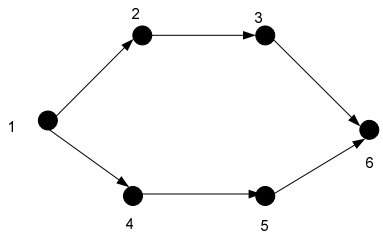

Figure 6.2: An example to show that interference alignment can achieve higher throughput.

of (6.12) says that at most one MCLS will be scheduled to transmit at any time, followed by (6.13) saying that the time fraction should be non-negative. Based on (6.14), the actual flow delivered on each link is limited by the active period of the MCLSs that contain this link and its correspondingly assigned DoF. From (6.15), the summation of DoF assigned to each link in M_{km} should be equal to $\frac{L_k m}{2}$.

We now use a simple example to illustrate that interference alignment has potential to achieve higher throughput. As shown in Fig. 6.2 , n_1 and n_6 are the source and destination nodes respectively. There are 6 links with unit capacity corresponding with the edges in Fig 6.2. We compare the throughput performance of the example network with and without interference alignment implementation. When no interference alignment is implemented, each link is interfered by each other. Thus at any time, only one link is scheduled to be active (each MCLS contains one link). It can be drawn easily that the optimal throughput is 1/3 with l_{12}, l_{23}, l_{36} each being active for 1/3 of time period. However, using interference alignment, each MCLS can achieve 3/2 DoF as each MCLS consists of 3 disconnected links. We can easily figure out that the network throughput can achieve 1/2 when each of the two MCLS, $\{l_{12}, l_{45}, l_{36}\}$ and $\{l_{14}, l_{23}, l_{56}\}$, is scheduled for 1/2 of the time period and each link assigned 1/2 DoF.

6.3 Technical Approach

6.3.1 Finding the MCLSs

We first present the method to find all MCLSs within a multi-hop wireless network. We introduce a graph $G = (V, E)$, where $\forall v_i \in V$ represents a link from the multi-hop wireless network. Let t_i and r_i denote the transmitter and receiver of v_i respectively. e_{ij} denotes the edge connecting v_i and v_j. e_{ij} exists when v_i and v_j can be active at the same time, which means they are either within the same multi-access interference network or far away from each other that no interference is generated. We rule out the possibility that v_i and v_j can be active at the same time when either t_i can cause interference to r_j or t_j can cause interference to r_i, because the two links are not interference-free from each other in the first place. Then finding all MCLSs within the multi-hop wireless network is tantamount to finding all maximal cliques of the graph G. The Bron-Kerbosch algorithm [13] can be utilized to find maximal cliques in an undirected graph.

Recall that each MCLS contains one or multiple multi-access interference networks. Thus we introduce a graph $H = (V, E)$ for each MCLS, where $\forall v_i \in V$ represents a link in the MCLS. Let t_i and r_i denote the transmitter and receiver of v_i respectively. e_{ij} denotes the edge connecting v_i and v_j. e_{ij} exists when v_i and v_j are within the same multi-access interference network. Based on the same token, finding all maximal cliques within the MCLS is tantamount to finding all maximal cliques of the graph H. The Bron-Kerbosch algorithm [13] can be utilized again to find maximal cliques in an undirected graph.

6.3.2 Overview of the Solution Procedure

Branch-and-bound is a general algorithm of finding solutions for various optimization problems [83]. In this chapter, we present a branch-and-bound based algorithm that guarantees $(1-\epsilon)$ optimal solution, where ϵ is a small positive constant. This algorithm is very similar to the one presented in [73] except the part of local search algorithm. To begin with, by using some relaxation techniques, the NLP is transformed into a linear programming problem, whose solution provides the upper bound UB to the objective function. Starting from the relaxation solution, a local search algorithm is employed to find a feasible solution to the original NLP problem, which provides a lower bound LB to the objective function. The LB could be far away from the UB, which calls for a tighter relaxation. Note that the gap between LB and UB is mainly caused by the linear approximation of the variables in nonlinear terms (denoted as division variables). Therefore, it is intuitive to achieve tighter relaxation by narrowing down the value intervals of division variables. The detailed branch-and-bound algorithm is shown in Table 6.1.

6.3.3 Linear Relaxation

During each iteration of the branch-and-bound procedure, we need a linear relaxation to obtain an upper bound of the objective function. The only nonlinear term is the polynomial term $\lambda_k \beta_{ij}^k$. Reformulation-Linearization Technique [72] enables us to use new variables to replace those polynomial terms and add linear constraints for these new variables, thus relaxing a nonlinear constraint into a linear constraint. Specifically, we introduce a new variable w_{ij}^k for $\lambda_k \beta_{ij}^k$. Let $(\lambda_k)_L \leq \lambda_k \leq (\lambda_k)_U$ and $(\beta_{ij}^k)_L \leq \beta_{ij}^k \leq (\beta_{ij}^k)_U$. Then we can obtain the following linear constraints for w_{ij}^k [72].

Table 6.1: Branch-and-bound Algorithm

1 Initialization:
2 Let the initial solution $\psi_\epsilon = \emptyset$.
3 Let the initial lower bound $LB = -\infty$.
4 Relax the original problem and obtain upper bound UB_1 and solution $\hat{\psi}_1$.
5 Add the linear relaxation to the problem list along with UB_1 and $\hat{\psi}_1$.
8 Iteration:
9 Select the problem z with the maximum UB_z in the problem list.
10 Find a feasible solution ψ_z from $\hat{\psi}_z$ via local search algorithm.
11 Denote the objective value as LB_z
12 **If**$(LB_z > LB)$ $\psi_\epsilon = \psi_z$ and $LB = LB_z$.
13 **If**$(LB_z \geq (1-\epsilon)UB_z))$ we stop with $(1-\epsilon)$ optimal solution ψ_z.
14 **else** remove any problem x with $(1-\epsilon)UB_x \leq LB$.
15 Define the relaxation error for a division variable as the difference between the values in ψ_z and $\hat{\psi}_z$.
16 Select a division variable with the maximum relaxation error and divide its value interval into two new intervals by its value in $\hat{\psi}_z$.
17 Define two new problems z_1 and z_2 based on these two intervals.
18 Remove problem z from problem list.
19 **If**$((1-\epsilon)UB_{z_1} > LB)$ add problem z_1 to the problem list.
20 **If**$((1-\epsilon)UB_{z_2} > LB)$ add problem z_2 to the problem list.

$$
\begin{aligned}
&(\lambda_k)_L \times \beta_{ij}^k + (\beta_{ij}^k)_L \times \lambda_k - w_{ij}^k \leq (\lambda_k)_L \times (\beta_{ij}^k)_L \\
&(\lambda_k)_U \times \beta_{ij}^k + (\beta_{ij}^k)_L \times \lambda_k - w_{ij}^k \geq (\lambda_k)_U \times (\beta_{ij}^k)_L \\
&(\lambda_k)_L \times \beta_{ij}^k + (\beta_{ij}^k)_U \times \lambda_k - w_{ij}^k \geq (\lambda_k)_L \times (\beta_{ij}^k)_U \\
&(\lambda_k)_U \times \beta_{ij}^k + (\beta_{ij}^k)_U \times \lambda_k - w_{ij}^k \leq (\lambda_k)_U \times (\beta_{ij}^k)_U
\end{aligned}
\tag{6.16}
$$

Through the relaxation, we can substitute the nonlinear term $\lambda_k \beta_{ij}^k$ with w_{ij}^k in (6.14) and add the constraints above for w_{ij}^k.

6.3.4 Local Search Algorithm

An linear relaxation, the original problem now can be solved in polynomial time. Denote the relaxation solution as $\hat{\psi}_z$, which provides an upper bound to problem z but may not be feasible. We now show how to derive a feasible ψ_z based on $\hat{\psi}_z$. We propose a greedy algorithm to iteratively increase the throughput performance near the infeasible solution $\hat{\psi}_z$ until the solution converges. Let $\mathbf{T}$ denote the current scheduling vector, representing the active time fraction for all MCLSs. $\mathbf{D}$ denotes the current assignment of DoF within each MCLS. $\mathbf{F}$ denotes the function to calculate the solution to the liner programming problem given either $\mathbf{T}$ or $\mathbf{D}$. During each iteration, we first obtain $\mathbf{T}$ from $\hat{\psi}_z$. Then the solution ψ_z given $\mathbf{T}$ can be computed with polynomial time using linear programming. $\mathbf{D}$ can be obtained from ψ_z. Using $\mathbf{D}$, we can update ψ_z. Because the upper bounded objective value is increased iteratively, the local search algorithm is guaranteed convergent. The detailed local search algorithm to determine a feasible solution is shown in Table 6.2.

LB_{old}^z denotes the objective value of ψ_z after the last iteration, while LB_{new}^z denotes the objective value of ψ_z in the current iteration. ϵ denotes a small constant positive value.

Table 6.2: Local Search Algorithm

1	$LB^z_{old} = 0$;
2	Derive $\mathbf{D}$ from $\hat{\psi}_z$;
3	$(LB_{new}, \psi_z) = \mathbf{F}(\mathbf{D})$;
4	**While** $\lvert LB^z_{old} - LB^z_{new} \rvert <= \epsilon$;
5	$LB^z_{old} = LB^z_{new}$;
6	Derive $\mathbf{T}$ from ψ_z ;
7	$(LB^z_{new}, \psi_z) = \mathbf{F}(\mathbf{T})$;
8	Derive $\mathbf{D}$ from ψ_z;
9	$(LB^z_{new}, \psi_z) = \mathbf{F}(\mathbf{D})$;

Table 6.3: Cartesian coordinates for the line topology

node	$Coordinate(x)$	*node*	$Coordinate(x)$
n_1	230	n_2	460
n_3	190	n_4	50
n_5	810	n_6	420
n_7	390		

6.4 Numerical Results

6.4.1 Simulation Setup

In this section, we present numerical results to validate the efficacy of the branch-and-bound algorithm. We consider both line and square scenarios, where the nodes are randomly deployed on a line and over $1000 \times 1000\ m^2$ square area. The coordinates of network nodes for the two scenarios are shown in Table 6.3 and 6.4 respectively. The sessions for the line scenario consists of flows from n_1 to n_5 and from n_6 to n_4. For the square scenario, the source-destination pairs includes $(n_1, n_9), (n_2, n_8)$ and (n_4, n_6). The noise power $p_n = 10^{-6} watt$. The path loss exponent $\rho = 2$. The bandwidth $B = 1MHz$.

Table 6.4: Cartesian coordinates for the square topology

$node$	$Coordinate(x, y)$	$node$	$Coordinate(x, y)$
n_1	(120, 420)	n_2	(220, 310)
n_3	(450, 310)	n_4	(650, 720)
n_5	(450, 700)	n_6	(620, 280)
n_7	(380, 490)	n_8	(210, 670)
n_9	(550, 510)	n_{10}	(200, 500)

6.4.2 No Interference Alignment

To validate the advantage of interference alignment regarding the throughput performance, we compare the results with the case in which interference alignment is not implemented. Under such circumstances, each MCLS consists of links that are mutually interference-free. Then, finding all maximal cliques within the multi-hop network is tantamount to finding all maximal cliques of the graph H. The Bron-Kerbosch algorithm can be utilized again to find maximal cliques in an undirected graph. Then the maximum throughput optimization problem for a multi-session multi-hop wireless network can be formulated similar as in Section 6.2, with minor modifications: within each MCLS, one DoF is assigned for each link, no matter how many links the MCLS contains.

6.4.3 Greedy Algorithm

For the purpose of demonstrating the efficacy of the branch-and-bound algorithm, we compare it with a simple greedy algorithm, which is very similar to the local search algorithm introduced in Section 6.3. The difference lies in that the scheduling vector $\mathbf{T}$ is set as $\{\frac{1}{M}, \frac{1}{M}, ..., \frac{1}{M}, \}$ before the first iteration. During each iteration, the DoF vector $\mathbf{D}$ is updated by the computed optimal solution under the current $\mathbf{T}$. Based on the newly derived $\mathbf{D}$, we can update $\mathbf{T}$ by computing the optimal result. Therefore, the throughput performance is iteratively increased until convergence.

6.4.4 Impact of P

We first look at the impact of the transmit power P on the throughput performance of the branch-and-bound algorithm, the greedy algorithm and the case when no interference alignment is implemented. From Fig. 6.3 and Fig.6.4, it can be seen that as P increases, the overall throughput performance of the 3 cases are all enhanced, which agrees with (6.6). Moreover, with interference alignment, it is obvious that the branch-and-bound algorithm achieves better performance than the case when no interference alignment is employed. In addition, as P is enlarged, the benefits brought by interference alignment seems to grow more apparent. The explanation for this phenomenon can be two-fold: first, when P grows larger, more links could be mutually interfered, giving rise to more multi-access interference networks. Therefore, more opportunities for simultaneous transmissions are generated by larger value of P. On the contrary, larger P means less MCLSs as well as reduced number of links of each MCLS. It is also worth mentioning that the branch-and-bound algorithm achieves much better performance than the greedy algorithm.

6.4.5 Impact of th_t

Next, we investigate the impact of the transmission threshold th_t. From Figure 6.5 and 6.6, it can be drawn that the main trend for both scenario is that the throughput performance is degraded as th_t increases. The reason behind is that the number of possibly successful links are reduced as the received power constraint is set tighter. Besides, the advantage of interference alignment is illustrated by the fact that the branch-and-bound algorithm achieves better performance than the case that no interference alignment is involved. Compared with the greedy algorithm, the branch-and-bound algorithm stands as a better approach in terms of the overall

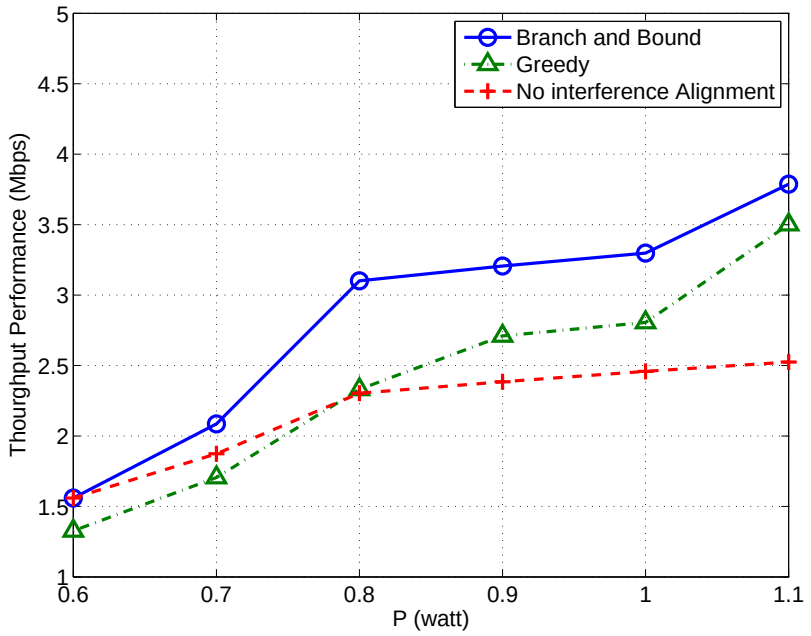

Figure 6.3: Throughput Performance when P varies. $th_t = 2 \times 10^{-5}$ watts. $th_i = 5 \times 10^{-6}$ watts. Line Scenario.

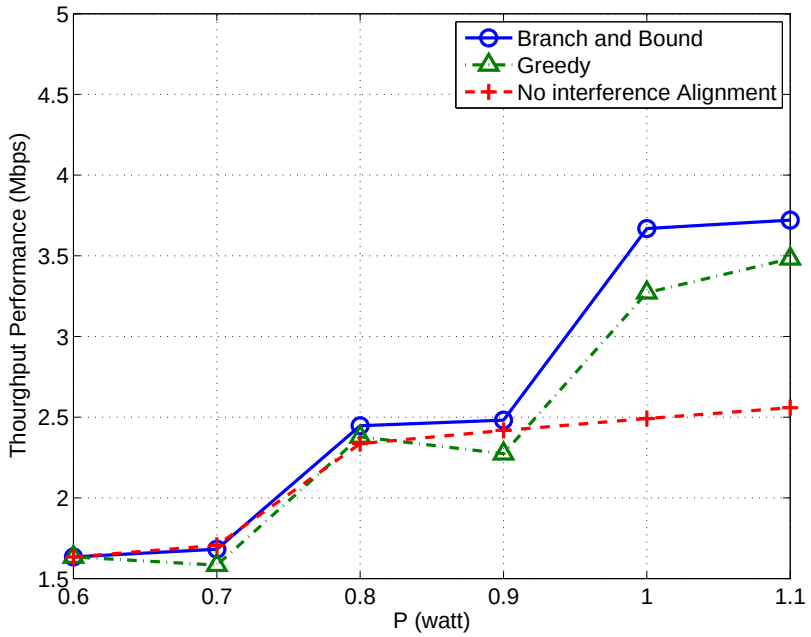

Figure 6.4: Throughput Performance when P varies. $th_t = 2 \times 10^{-5}$ watts. $th_i = 5 \times 10^{-6}$ watts. Square Scenario.

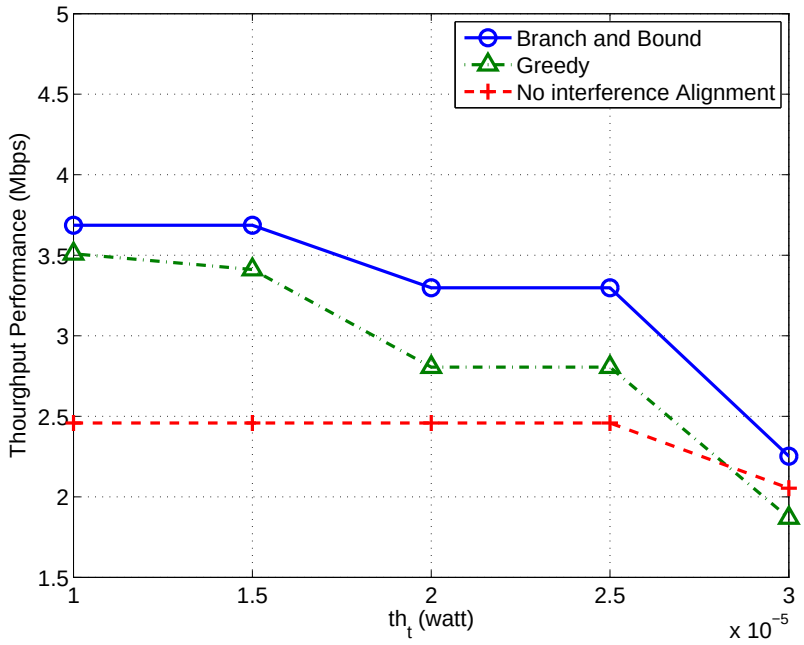

Figure 6.5: Throughput Performance when th_t varies. $P = 1$ watts. $th_i = 5 \times 10^{-6}$ watts. Line Scenario.

end-to-end throughput.

6.4.6 Impact of th_i

At last, we look at the impact of the interference threshold th_i on the performance results in Fig. 6.7 and 6.8. The first impression is that the performance for both the branch-and-bound algorithm and greedy algorithm decreases as the value th_i increases. To explain this, one needs to see that larger th_i induces less mutually interfered links, causing less multi-access interference networks. As a result, less opportunities for simultaneous transmission are generated by interference alignment. Again, the branch-and-bound algorithm achieves better performance than both the greedy algorithm and the optimal throughput when no interference alignment is employed. Therefore, it is demonstrated that the branch-and-bound algorithm is effective and the multi-hop networks with interference alignment result larger throughput.

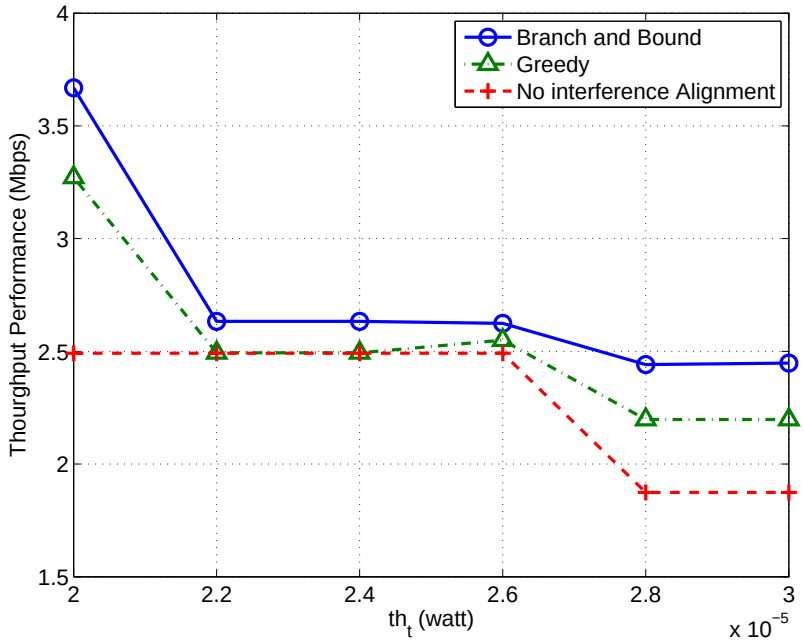

Figure 6.6: Throughput Performance when th_t varies. $P = 1$ watts. $th_i = 5 \times 10^{-6}$ watts. Square Scenario.

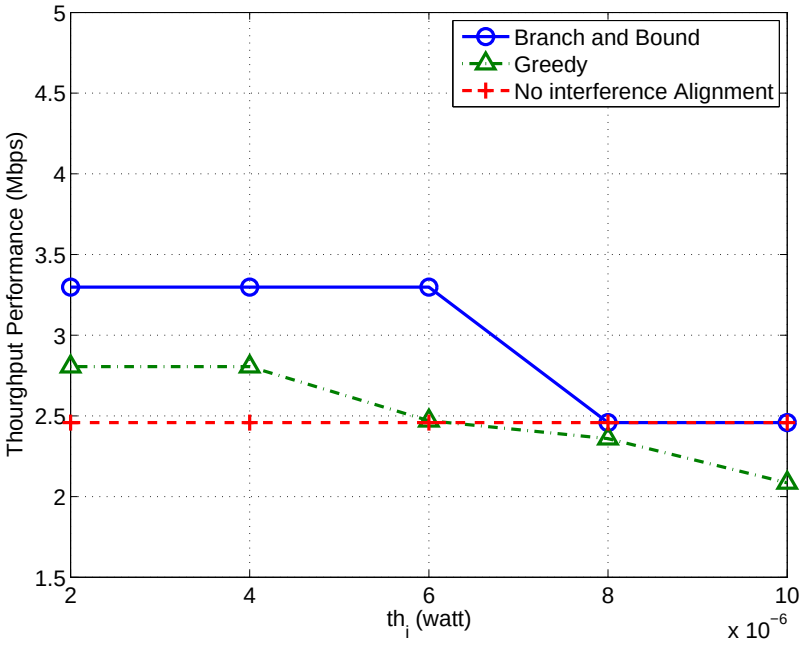

Figure 6.7: Throughput Performance when th_i varies. $P = 1$ watts. $th_t = 2 \times 10^{-5}$ watts. Line Scenario.

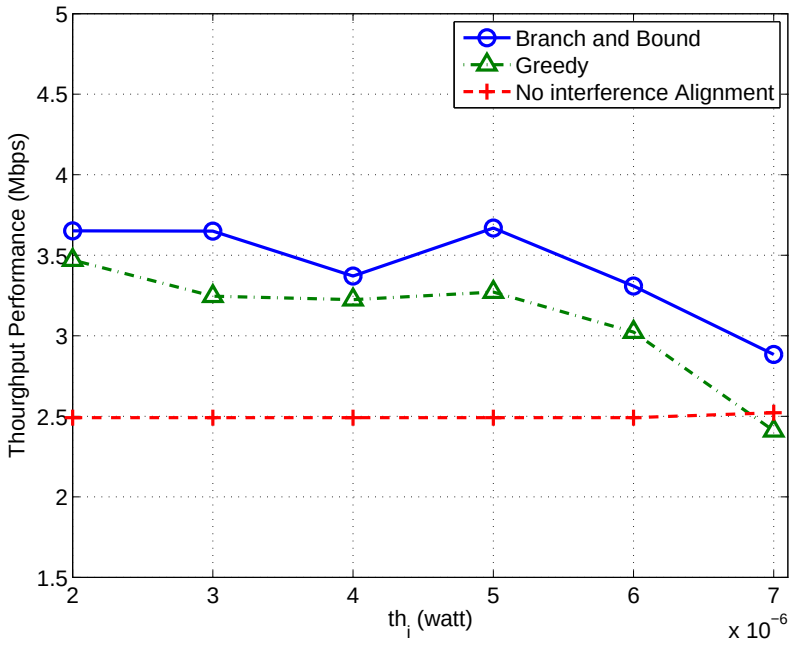

Figure 6.8: Throughput Performance when th_i varies. $P = 1$ watts. $th_t = 2 \times 10^{-5}$ watts. Square Scenario.

6.5 Conclusion

In this chapter, we study throughput enhancement for multi-hop wireless networks using interference alignment. First of all, the set of links within a multihop wireless network is divided into multiple MCLSs. Then the throughput optimization problem is formulated as a NLP problem. A branch-and-bound algorithm is proposed to yield $(1 - \epsilon)$ optimal performance. Numerical results show that interference alignment does bring throughput enhancement for multi-hop wireless networks and the branch-and-bound algorithm can solve the throughput optimization problem efficiently.

Chapter 7

Conclusions and Future Work

7.1 Conclusions

As for wireless networks, resource allocation is the process of deciding how to implement spectrum management, link scheduling as well as power and topology control. In this dissertation, we address resource allocation and performance optimization for different kinds of wireless networks. In particular, we incorporate time scheduling, spectrum management, power and topology control into problem formulation to allocate different kinds of resources. Subsequently, we employ linear and nonlinear optimization techniques to render optimal and heuristic solutions. Results are presented mainly by comparing the performance of heuristic approach with the optimal algorithm. In addition, we also investigate the cost and impacts of the system parameters. We summarize our results by each chapter below.

In Chapter 2, we study an optimization problem to maximize the total number of information packets received at the base station during the network lifetime, which is defined as the time period from start to all the relay nodes die. we demonstrate a solution to obtain the optimal transmit power for a relay node such that it can send

the maximum number of packets to the base station during the network lifetime. The proposed weighted clustering algorithm is a heuristic approach to find the best placement locations for relay nodes that can assist edge nodes to send packets to the base station. The proposed scheme demonstrates better performance than the existing methods in literature.

In Chapter 3, we solve a joint problem of power control and channel assignment within a wireless mesh network such that the minimal capacity of all links is maximized. The key obstacle lies in the nonlinearity of the objective function. We successfully transform the max-min objective to more solvable linear objective with additional constraints in compromise of optimality. In particular, we propose a heuristic approach to iteratively increase the minimal throughput of all links tightening the constraint that the capacity of each link is larger than a threshold value. We prove that when the sum rate of all links are maximized and each link share the same capacity, it is guaranteed that max-min performance is optimized. Then the upper bound of max-min fairness problem can be easily acquired by solving a linear programming problem. The upper bound offers a benchmark to measure the quality of the feasible solution obtained from the heuristic approach. Simulation results show that solutions obtained by this algorithm are very close to the upper bounds obtained via relaxation, thus suggesting that the solution produced by the algorithm is near-optimal.

In Chapter 4, we first propose a novel and practical mobility model for mobile nodes in a disaster area. Based on the typical movement pattern of first responders in disaster relief operation. Subsequently, we strive to use minimum number of relay nodes such that each mobile node can connect to at least one relay node. We formulate the square disk cover problem and propose three algorithms to solve it, including the Two-Vertex Square Covering algorithm, the Circle Covering algorithm

and the binary integer programming algorithm. We also investigate carefully into the performance comparison between the TVSC algorithm, the Circle Covering algorithm, and the binary integer programming algorithm. As the optimal approach, the binary integer programming algorithm yields the deployment of the least number of relay nodes, while having the largest computational complexity $O(N^3)$; the TVSC algorithm yields the deployment of the second least number of relay nodes, and consuming much less computational resources in $O(N^2)$; the Circle Covering algorithm yields the deployment of the most number of relay nodes, but consuming the least computation resources only in $O(N)$. In practice, the TVSC algorithm and Circle Covering algorithm might be more preferable because they require much less computational complexity, but yield only a small number of the relay nodes deployed more than the binary integer programming algorithm does.

In Chapter 5, we explore the joint problem of power control and channel assignment to maximize cognitive radio network throughput. It is assumed that an overlaid cognitive radio network coexists with a primary network. We model the opportunistic spectrum access for cognitive radio network and formulate the cross-layer optimization problem under the interference constraint imposed by the existing primary network. Subsequently, a distributed greedy algorithm is proposed to approximate the optimal network throughput. Cross-layer optimization for cognitive radio network is often implemented in centralized manner to avoid co-channel interference. The distributed algorithm coordinates the channel assignment with local channel usage information. Thus the computation complexity is greatly reduced. In particular, we compare the distributed algorithm with 4 other algorithms, the optimal algorithm, two-phased algorithm and dynamic interference graph allocation and power-based algorithm. The computation complexity of the distributed algorithm is $O(N^4)$ and the optimal algorithm is of $O(2^N)$. Simulation results show that

the distributed algorithm outperforms 3 other algorithms and perform close to the optimal.

In Chapter 6, we study the network throughput optimization problem for a multi-hop wireless network by considering interference alignment at physical layer. We first transform the problem of dividing the set of links into multiple maximal concurrent link sets into the problem of finding all maximal cliques of a graph. Each concurrent link set is further divided into one or several multi-access interference networks, on which interference alignment can be implemented to guarantee simultaneous interference-free transmission. The network throughput optimization problem is then formulated as a non-convex nonlinear programming problem, which is NP-hard generally. We resort to developing a branch-and-bound framework, which guarantees an achievable performance bound. We use numerical results to validate the efficacy of the algorithm and to offer insights on the throughput enhancement brought by interference alignment technique.

7.2 Suggested Future Work

From our extensive study in wireless network resource allocation and performance optimization techniques presented in this dissertation, we suggest the directions for future work in this area as below.

First and foremost, it is always of much interest in investigating algorithms with less complexity. Some schemes proposed in this dissertation are of very high computing complexity. For instance, in Chapter 2, the binary integer programming algorithm could potentially search all 2^n binary integer vectors, where n is the number of variables. However, it has been proved that such a binary integer programming problem could be transformed into a linear optimal distribution problem [53] by

generating a directed graph, to reduce the computation complexity to only $O(n^3)$. It is worth of the effort of transforming the binary integer programming algorithm to the graph-based scheme.

Another promising research direction is to incorporate other kinds of resources into the formulation of optimization problem. For instance, in Chapter 5, it is also meaningful to consider link scheduling during time slots. Since primary users can access the spectrum any time, considering link scheduling would approximate the network model more closely to real world applications. In addition, it would be promising to use directional antennas to limit interference such that little interference can be generated towards primary users. Besides, the primary network can be cooperative with the cognitive radio network.

Finally, there are additional performance objectives that can be explored for different application scenarios. For example, it is more desirable under certain circumstances to investigate the fairness among secondary users instead of the overall performance of cognitive radio networks. In Chapter 3, proportional fairness might be more convincing than max-min fairness. In Chapter 4, the maximization of sum rate would be more meaningful as the optimization objective for data-oriented applications.

Bibliography

[1] "www.mathworks.com."

[2] S. Agarwal, S. V. Krishnamurthy, R. H. Katz, and S. K. Dao, "Distributed power control in ad-hoc wireless networks," in *Personal Indoor Mobile Radio Conf.*, 2001.

[3] I. F. Akyildiz, W. Lee, M. C. Vuran, and S. Mohanty, "Next generation/dynamic spectrum access/cognitive radio wireless networks: A survey," *Computer Networks*, vol. 50, no. 13, pp. 2127–2159, Sep. 2006.

[4] M. Alicherry, R. Bhatia, and L. Li, "Joint channel assignment and routing for throughput optimization in multi-radio wireless mesh networks," in *Mobicom*, 2005.

[5] G. Anastasi, E. Borgia, M. Conti, and A. Passarella, "Understanding the real behavior of mote and 802.11 ad hoc networks: an experimental approach," *Pervasive and Mobile Computing*, no. 1, pp. 237–256, 2005.

[6] N. Aschenbruck, E. Gerhards-Padilla, M. Gerharz, M. Frank, and P. Martini, "Modelling mobility in disaster area scenarios," in *MSWIM'07*, Oct. 2007.

[7] K. Balachandran, K. Budka, T. Chu, T. Doumi, and J. Kang, "Mobile responder communication networks for public safety," *IEEE Communications magazine*, vol. 44, no. 1, pp. 56–64, 2006.

[8] C. A. Balanis, *Advanced Engineering Electromagnetics*. John Wiley and Sons, Inc., 1989.

[9] J. Bazerque and G. Giannakis, "Distributed scheduling and resource allocation for cognitive ofdma radios," *Mobile Network Applications*, vol. 13, no. 5, pp. 452–462, 2008.

[10] A. Behzad and I. Rubin, "Impact of power control on the performance of ad hoc wireless networks," in *Infocom'05*, April 2005.

[11] C. Bettstetter and C. Wagner, "The spatial node distribution of the random waypoint mobility model," in *WMAN?2*, 2002.

[12] S. Bittner, W. Raffel, and M. Scholz, "The area graph-based mobility model and its impact on data dissemination," in *IEEE PerCom'05*, 2005.

[13] C. Bron and J. Kerbosch, "Algorithm 457: Finding all cliques of an undirected graph," *ACM Commun.*, vol. 16, no. 9, pp. 575–577, 1973.

[14] V. Cadambe and S. Jafar, "Interference alignment and the degrees of freedom for k user interference channel," *IEEE Transactions on Information Theory*, vol. 54, no. 10, pp. 4010–4018, 2008.

[15] L. Cao and H. Zheng, "Understanding the power of distributed coordination for dynamic spectrum management," *Mobile Network Applications*, vol. 13, no. 5, pp. 477–497, 2008.

[16] K. Challapali, C. Corderiro, and D. Birru, "Ieee 802.22: the first worldwide wireless standard based on cognitive radios," in *First IEEE International Symposium on New Frontiers in Dynamic Spectrum Access Networks*, 2005.

[17] C. Chin, M. Sim, and S. Olafssont, "A dynamic channel assignment strategy via power control for ad-hoc network systems," in *Vehicular Technology Conference*, 2007.

[18] T. Cormen, C. Leiserson, and R. Rivest, *Introduction to Algorithms*, 1st ed. The MIT Press, 1986.

[19] B. Das, R. Sivakumar, and V. Bharghavan, "Routing in ad hoc networks using a virtual backbone," in *IEEE ICCCN?7*, Sep. 1997.

[20] L. DaSilva, G. Morgan, C. Bostian, D. Sweeney, S. Midkiff, J. Reed, C. Thompson, W. Newhall, and B. Woerner, "The resurgence of push-to-talk technologies," *IEEE Communications magazine*, vol. 44, no. 1, pp. 48–55, 2006.

[21] F. Digham, "Joint power and channel allocation for cognitive radios," in *IEEE Wireless Communications and Networking Conference (WCNC'08)*, March 2008.

[22] T. Doumi, "Spectrum considerations for public safety in the United States," *IEEE Communications magazine*, vol. 44, no. 1, pp. 30–37, 2006.

[23] J. Gao, L. Guibas, J. Hershberger, L. Zhang, and A. Zhu, "Discrete mobile centers," *Discrete Computing Geometry*, vol. 30, no. 1, pp. 45–63, 2003.

[24] S. Gollakota, S. D. Perli, and D. Katabi, "Interference alignment and cancellation," in *ACM SIGCOMM*, 2009.

[25] K. Gomadam, V. Cadambe, and S. Jafar, "Approaching the capacity of wireless networks through distributed interference alignment," in *IEEE Globecom08*, 2008.

[26] M. Gunes and J. Siekermann, "CosMos: Communication scenario and mobility scenario generator for mobile ad-hoc networks," in *the 2nd Int.Worfkshop on MANETs and Interoperability Issues (MANET'05)*, 2005.

[27] W. Guo and X. Huang, "Relaying packets in a two-tiered wireless network using binary integer programming," in *WASA*, 2007.

[28] ——, "Relay management for mobile users in disaster area wireless network," in *WASA*, 2008.

[29] ——, "achieving capacity fairness for wireless mesh networks," *Wireless Communication and Mobile Computing*, 2009.

[30] ——, "On throughput enhancement of multi-hop wireless networks using interference alignment," in *WOCC*, 2011.

[31] H. Gupta, S. Das, and Q. Gu, "Connected sensor cover: self organization of sensor networks for efficient query execution," in *ACM MOBIHOC'03*, June 2003.

[32] Z. Han, Z. Ji, and K. J. R. Liu, "Non-cooperative resource competition game by virtual referee in multi-cell ofdma networks," *IEEE J. Select. Areas Commun.*, pp. 1079–1090, 2007.

[33] J. Hershberger, "Smooth kinetic maintenance of clusters," in *ACM SoCG'03*, June 2003.

[34] T. Himson, W. Pam, Z. Han, and K. Liu, "Lifetime maximization via cooperative nodes and relay depolyment in wireless networks," *IEEE Journal on Selected Areas of in Communication*, vol. 25, no. 2, 2007.

[35] I. W. Ho and S. C. Liew, "Impact of power control on performance of ieee 802.11 wireless networks," *IEEE Transactions on mobile computing*, vol. 6, no. 11, pp. 1245–1258, Nov. 2007.

[36] A. Hoang and Y. Liang, "Downlink channel assignment and power control for cognitive radio networks," *IEEE Transactions on Wireless Communications*, vol. 7, no. 8, pp. 3106–3117, 2008.

[37] A. Hoang, Y. Liang, and M. Islam, "Power control and channel allocation in cognitive radio networks with primary users' cooperation," *IEEE Transactions on Mobile Computing*, vol. 9, no. 3, pp. 348–360, 2010.

[38] D. Hochbaum and W. Maass, "Approximation schemes for coveirng and packing problems in image processing and VLSI," *Journal of the ACM*, vol. 32, no. 1, pp. 130–136, 1985.

[39] X. Hong, M. Gerla, G. Pei, and C. Chiang, "A group mobility model for ad hoc wireless networks," in *ACM Int. Workshop on Modelling a. Simulation of Wireless Mobile Systems*, 1999.

[40] Y. Hou, Y. Shi, and H. Sherali, "Spectrum sharing for multi-hop networking with cognitive radios," *IEEE Journal on Selected Areas of Communications*, vol. 26, no. 1, pp. 146–155, 2008.

[41] Y. T. Hou, Y. Shi, and H. D. Sherali, "Rate allocation in wireless sensor networks with network lifetime requirement," in *ACM MobiHoc*, 2004, pp. 67–77.

[42] Y. Hou, Y. Shi, H. Sherali, and S.F.Midkiff, "On energy provisioning and relay node placement for wireless sensor networks," *IEEE Transactions on Wireless Communications*, vol. 4, pp. 2579–2590, 2005.

[43] http://www-01.ibm.com/software/integration/optimization/cplex optimizer.

[44] H. Huang, A. Richa, and M. Segal, "Approximation algorithms for the mobile piercing set problem with applications to clustering in ad hoc networks," *ACM/Kluwer MONET*, vol. 9, no. 2, pp. 151–161, 2004.

[45] D. Johnson and D. Maltz, *Dynamic Source Routing in Ad Hoc Wireless Networks, Mobile Computing.* Kluwer Academic Publishers, 1996.

[46] V. Kawadia and P. R. Kumar, "Power control and clustering in ad hoc networks," in *Infocom*, 2003.

[47] K.Jain, J.Padhye, V. Padmanabhan, and L.Qiu, "Impact of interference on multi-hop wireless network performance," in *MobiCom'03*, 2003.

[48] J. Kraaier and U. Killat, "Calculating mobility parameters for a predefined stationary user distribution," in *IEEE Int. Conf. on Networks*, 2004.

[49] H. W. Kuhn, "The hungarian method for the assignment problem," *Naval Research Logistics Quarterly*, 1955.

[50] G. Kulkarni, S. Adlakha, and M. Srivastava, "Subcarrier allocation and bit loading algorithms for ofdma-based wireless networks,," *IEEE Transactions on Mobile Computing*, vol. 4, no. 6, pp. 652–662, 2005.

[51] J. C. Lagarias, J. A. Reeds, M. H. Wright, and P. E. Wright, "Convergence properties of the nelder-mead simplex method in low dimensions," *SIAM Journal of Optimization*, vol. 9, no. 1, pp. 112–147, 1998.

[52] C. Li and W. Hsu, "A local metric for geographic routing with power control in wireless networks," in *Infocom*, 2006.

[53] G. Li and H. Liu, "Resource allocation for ofdma relay networks with fairness constraints," *IEEE Journal on Selected Areas of Communication*, vol. 24, no. 11, pp. 2061–2069, 2005.

[54] ——, "Resource allocation for ofdma relay networks with fairness constraints," *IEEE Journal on selected areas in communications*, vol. 24, no. 11, Nov. 2006.

[55] B. Liang and Z. Haas, "Predictive distance-based mobility management for PCS networks," in *IEEE Infocom'99*, 1999.

[56] Y. Liang, V. V. Veeravalli, and H. V. Poor, "Resource allocation for wireless fading relay channels: Max-min solution," *IEEE Transactions on Information Theory*, vol. 53, no. 10, pp. 3432–3453, Oct. 2007.

[57] H. Liu, P. Wang, and X. Jia, "On optimal placement of relay nodes for reliable connectivity in wireless sensor networks," *Journal of Combinatorial Optimization*, vol. 11, pp. 249–260, 2006.

[58] E. L. Lloyd and G. Xue, "Relay node placement in wireless sensor networks," *IEEE Transactions on Computers*, vol. 56, no. 1, pp. 134–138, 2007.

[59] W. Lu, W. Seah, E. Peh, and Y. Ge, "Communications support for disaster recovery operations using hybrid mobile ad hoc networks," in *LCN'07*, Oct. 2007.

[60] A. M. M. Maddah-Ali and A. Khandani, "Signaling over mimo multi-base systems-combination of multi-access and broadcast schemes," in *ISIT*, 2006.

[61] S. Narayanaswamy, V. Kawadia, R. S. Sreenivas, and P. R. Kumar, "Power control in ad-hoc networks: Theory, archtecture, algorithm and implementation of the compow protocol," in *Eurapean Wireless Conference*, 2002.

[62] A. Naveed, S. S. Kanhere, and S. K. Jha, "Topology control and channel assignment in multi-radio multi-channel wireless mesh networks," in *IEEE International Conference on Mobile Adhoc and Sensor Systems (MASS)*, Oct. 2007.

[63] S. Nelson, A. Harris, and R. Kravets, "Eventdriven, rolebased mobility in disaster recovery networks," in *CHANTS'07*, Sep. 2007.

[64] N. Pogkas, G. Karastergios, C. Antonopoulos, S. Koubias, and G. papadopoulos, "Architecture design and implementation of an ad-hoc network for disaster relief operations," *IEEE Transactions on Industrial Informatics*, vol. 3, no. 1, pp. 63–72, Feb. 2007.

[65] J. Proakis, *Digital Communications*. McGraw Hill, New York, 1995.

[66] D. Qiao, S. Choi, and K. G. Shin, "Interference analysis and transmit power control in ieee 802.11a/h wireless lans," *IEEE Transactions on Networking*, vol. 15, no. 5, pp. 1007–1020, Oct. 2007.

[67] K. N. Ramachandran, E. M. Belding, K. C. Almeroth, and M. M. Buddhikot, "Interference-aware channel assignment in multiradio wireless mesh networks," in *Infocom*, 2006.

[68] A. Raniwala, K. Gopalan, and T. Chiueh, "Centralized channel assignment and routing algorithms for multi-channel wireless mesh networks," *SIGMOBILE Mobile Computer Communications*, vol. 8, no. 2, pp. 50–65, April 2004.

[69] A. K. Sadek, Z. Han, and K. Liu, "A distributed relay-assignment algorithm for cooperative communications in wireless networks," in *IEEE Conference on Communications*, vol. 4, 2006, pp. 1592–1597.

[70] A. Salkintzis, "Evolving public safety communication systems by integrating WLAN and TETRA networks," *IEEE Communications magazine*, vol. 44, no. 1, pp. 38–46, 2006.

[71] C. E. Shannon, "Communication in the presence of noise," *Proceedings of the IRE*, vol. 37, no. 1, 1949.

[72] H. Sherali and W. Adams, *A Reformulation-Linearization Technique for Solving Discrete and Continuous Nonconvex Problems*. Kluwer Academic Publishers, 1999.

[73] Y. Shi, T. Hou, and H. Sherali, "Cross-layer optimization for date rate utility problem in uwb-based ad hoc networks," *IEEE Transactions on Mobile Computing*, vol. 7, no. 8, pp. 764–777, 2008.

[74] A. So and B. Liang, "Enhancing wlan capacity by strategic placement of tetherless relay points," *IEEE Transactions on Mobile Computing*, vol. 6, no. 5, pp. 474–487, May 2007.

[75] A. Srinivas, G. Zussman, and E. Modiano, "Mobile backbone networks-construction and maintenance," in *MobiHoc'06*, May 2006.

[76] Q. Sun, X. Zeng, R. Rasool, Z. Ke, and N. Chen, "The capacity of wireless ad hoc networks with power control," in *International workshop on Cross Layer Design(IWCLD'07)*, June 2007.

[77] H. Suzuki, Y. Kaneko, K. Mase, S. Yamazaki, and H. Makino, "An ad hoc network in the sky, SKYMESH, for large-scale disaster recovery," in *IEEE VTC*, Feb. 2006.

[78] C. S. Tang, "A max-min allocation problem: its solutions and applications," *Operations Research*, vol. 36, no. 2, pp. 359–367, 1988.

[79] J. Tang, B. Hao, and A. Sen, "Relay node placement in large scale wireless sensor networks," *Computer Communications (Elsevier)*, vol. 29, no. 4, pp. 490–501, 2006.

[80] J. Tang, S. Misra, and G. Xue, "Joint spectrum allocation and scheduling for fair spectrum sharing in cognitive radio wireless networks," *Journal of Computer Networks*, vol. 52, pp. 2148–2158, 2008.

[81] H. Wang, B. Crilly, C. Autry, and S. Swank, "Implementing mobile ad hoc networking (MANET) over legacy tactical radio links," in *IEEE MILCOM*, Oct. 2007.

[82] Q. Wang, K. Xu, G. Takahara, and H. Hassanein, "Locally optimal relay node placement in heterogeneous wireless sensor networks," in *IEEE Globecom*, 2005.

[83] L. Wolsey, *Integer Programming*. John Wiley and Sons, 1998.

[84] J. Wong, A. J. Mason, M. J. Neve, and K. W. Sowerby, "Base station placement in indoor wireless systems using binary integer programming," *IEE Proceedings of Communications*, vol. 153, no. 5, pp. 771–778, 2006.

[85] H. Wu, C. Qiao, S. De, and O. Tonguz, "Integrated cellular and ad hoc relaying systems: iCAR," *IEEE Journal on Selected Areas in Communications*, vol. 19, pp. 2105–2115, 2001.

[86] Q. Xin and J. Xiang, "Joint qos-aware admission control, channel assignment, and power allocation for cognitive radio cellular networks," in *IEEE 6th Internation Conference on Mobile Adhoc Sensor Systems, 2009, MASS'09*, Oct. 2009.

[87] T. G. Y. Xin and M. Shayman, "Relay deployment and power control for lifetime elongation in sensor networks," in *Proceedings of IEEE ICC*, 2006.

[88] K. Zeng, W. Lou, and H. Zhai, "On end-to-end throughput of opportunistic routing in multirate and multihop wireless networks," in *IEEE Infocom'08*, April 2008.

[89] H. Zhai and Y. Fang, "Impact of routing metrics on path capacity in multirate and multihop wireless ad hoc networks," in *IEEE ICNP*, 2006.